THE UNIVERSITY OF MICHIGAN

INDUSTRY PROGRAM OF THE COLLEGE OF ENGINEERING

THE EFFECT OF TEMPERATURE ON THE DETONATION CHARACTERISTICS OF HYDROGEN-OXYGEN MIXTURES

Morton P. Moyle

A dissertation submitted in partial fulfillment of the requirements for the degree of Doctor of Philosophy in the University of Michigan.

December, 1956

IP-195

ACKNOWLEDGEMENTS

I would like to express my appreciation for the advice and encouragement given me by the doctoral committee during the course of this investigation. I appreciate Dr. Stuart W. Churchill's efforts as chairman of the doctoral committee and his advice and support during the course of the investigation. I am indebted to Dr. Richard B. Morrison, who suggested the problem, for stimulating my interest in detonation phenomena.

I would also like to thank Mr. Bruce Arden of the Statistical Research Laboratory for his aid in programing the analytical solution on the IBM 650 digital computor and for instruction in machine operation.

Finally I would like to express appreciation to the Industry Program of the University of Michigan for the reproduction of this thesis.

TABLE OF CONTENTS

TABLE OF CONTENTS (Cont'd)

LIST OF TABLES

LIST OF FIGURES

LIST OF FIGURES (Cont'd)

NOMENCLATURE

a	Speed of sound ft/sec.
c_1	Constant in Equation 4
c_2	Constant in Equation 5
c_3	Constant In Equation 6
$\overline{C}_p$	Average specific heat at constant pressure -Btu/lb°F
$\overline{C}_v$	Average specific heat at constant volume - Btu/lb°F
D	Diameter of Tube - inches
E	Energy in consistent units
g_c	Conversion factor (lbs mass) ft/lb force) sec^2
J	Mechanical equivalent of heat - ft.lbs/Btu
^oK	Temperature - degrees Kelvin
K_c	Equilibrium constant - mols per gram
K_p	Equilibrium constant - mols per atm.
k	Thermal conductivity - Btu/hr°F/ft.
M	Mach number
n	Moles
Pr	Prandtl number $= \frac{C_p k}{\mu}$
q_w	Heat transfer to the wall - Btu/hr ft^2
ΔE_c	Heat of combustion - Btu/lb
R	R-gas constant in consistent units
S	Entropy
t	Time
T	Temperature
T_r	Recovery temperature
T_w	Wall temperature

NOMENCLATURE (Cont'd)

U	Velocity outside the boundary layer
u	Velocity - ft/sec.
V	Specific volume in consistent units
w	Particle velocity - ft/sec.
x	Distance - ft.
X	Mol fraction
γ	Ratio of specific heat at constant pressure to specific heat at constant volume
Δ	Increment
τ	Shear stress - lbs/ft sec^2.
ρ	Density - lbs/ft^3.
μ	Viscosity - lbs/ft sec.

Subscripts:

1	Initial value of the variable
2	Final value of the variable
C	Concentration
D	Detonation
p	Pressure
r	Recovery
rw	Reflected wave
w	Wall
∞	Outside boundary layer

I. INTRODUCTION

A flame front advancing into a combustible mixture may, under certain conditions, accelerate rapidly to a velocity considerably in excess of the speed of sound in the unburned mixture. When such a phenomen occurs, it is known as detonation, it may be further described as a shock wave followed by combustion. The spark schlieren photographs shown in Figure 1 represent a time sequence in the initiation of detonation in a 50 percent acetylene-oxygen mixture. Each photograph is for a different detonation with the delay after ignition increased. In Figures 1a, 1b, and 1c, the flame front with the preceeding shock wave can be seen propagating along the tube. In Figures 1d, and 1e the shock front has initiated combustion directly behind it and is finally propagating as a detonation through the mixture. The basic difference between a pure shock wave and the detonation wave is the energy release in the detonation front. As a result of this energy release, the velocity of the detonation wave is maintained indefinitely whereas in the pure shock wave, the velocity decays due to energy degradation by viscous action and heat conduction.

In general, the study of detonation waves parallels the study of shock waves. The experimental equipment used to study detonations

(a)

(b)

(c)

(d)

(e)

Figure 1. Spark Ignition of Acetylene-Oxygen Detonation
(in five sections)

for example, may be the open or closed flame tube or the shock tube (36). Furthermore, many of the existing relations describing shock phenomena may be extended to apply to the detonation.

Detonation phenomena have been studied for seventy-five years; even so, many aspects of the problem remain essentially unexplored. The structure of the detonation wave, for example, remains analytically intractable unless the very elementary model of a first order reaction is assumed. Even then the numerical solution is at best uncertain (21). The effects of initial temperature and initial pressure on the detonation velocity are also uncertain. A search of the literature reveals that detonation velocities have not previously been measured below ten degrees centigrade and that experimental investigations of the effect of sub-atmospheric pressures on the detonation velocity in hydrogen-oxygen mixtures have been confined to stoichiometric mixtures. The limits of detonability of gaseous mixtures are also uncertain. The limits are affected by tube diameter, initial pressure and temperature, method of ignition and intensity of the ignition source. Thus, existing tables of data on detonation limits must be considered tentative with the real ization that the actual limits may be greater than those given.

The main objective of the present study is the determination of the effect of initial temperature on the detonation velocity in hydrogen-oxygen mixtures and the evaluation of existing theories of detonation over the experimental range from 160 to 480 degrees Kelvin.

CHAPTER II

HISTORY OF THE DEVELOPMENT OF THE THEORY OF DETONATION

The literature on the subject of detonation has been reviewed extensively by many writers (3,8,9,10,21,24,33,56). Rather than repeat these reviews, a history of the development of the hydrodynamic-thermodynamic theory will be given here.

The discovery of the detonation phenomena was made independently by Berthelot and Vielle (6,7) and Mallard and Le Chatelier (34,35) while studying flame propagation in tubes. They found that the detonation velocity was a physical constant of the mixture and was essentially independent of (a) tube diameter, (b) initial pressure and temperature, (c) method of ignition and (d), whether ignition took place in a closed end or open end tube.

During the next twenty-five years, the theory of the detonation velocity was developed in terms of thermodynamic and hydrodynamic properties of the system. Many investigators took part in the development of the theory which is based upon the formulation of the adiabatic pressure-volume relation for non-isentropic systems, the Rankine-Hugoniot relation, and the assumption that the detonation wave travels at the speed of sound with respect to the burned gases behind the front-the Chapman-Jouguet condition.

Riemann (45) began the theoretical development with this classic work on the theory of sound waves in 1860. His work was not entirely applicable to strong shock waves, however, since he incorrectly assumed the relation $PV^{\gamma} = C$ for the shock wave. Rankine (43) arrived at the correct relation in 1870 and Hugoniot (23) also obtained it in 1887.

The relation is now generally known as the Rankine-Hugoniot relation.

Thus the pressure-volume relation for a non-isentropic system (the shock wave) had been developed even before the discovery of the detonation phenomena. It was a simple extension to include the detonation in the analysis.

The explanation of the detonation velocity was attempted by may investigators. Berthelot and Vielle found that the magnitude of the velocity of detonation was of the order of the molecular velocity in the reaction products and indeed showed that the Clausius equation[1] for the mean velocity of translation of molecules at the moment of reaction approximated the detonation velocity.

As early as 1883, Dixon (14) suggested that the detonation wave traveled at the speed of sound in the hot gases and formulated an empirical expression for the detonation velocity. In 1889, Chapman (12) approached the problem from the point of view of thermodynamic reasoning including the compressible flow of fluids and was able to compute detonation velocities in good agreement with experimental data. Chapman's work was the first attempt to formulate the problem in hydrodynamic and thermodynamic terms. Chapman's theory was not complete since he had incorrectly applied the formulas of Riemann to the shock wave.

It was Jouguet (25,26,27) who completed the formulation of the theory in 1905. He postulated that the detonation wave advanced at the speed of sound relative to the burned gases (following Chapman)

---

1 The Clausius equation is given by Bolle (8) as $u = 29.35\ (T/\rho)^{1/2}$ where T is the explosion temperature and ρ is the density of the burned gases.

but he used the Rankine-Hugoniot relation for the pressure-volume relation. The assumption of the detonation velocity to use is now generally known as the Chapman-Jouguet condition. Many investigators notably, Becker (2), Schmidt (48), Zeldovich (55,56), von Neuman (38), Scorah (49) and Doering (15), have contributed refinements to the theory of detonation in gaseous mixtures since the work of Jouguet.

Lewis and Friauf (32) made the first critical evaluation of the theory in 1930. They compared experimental detonation velocities in hydrogen-oxygen mixtures with those predicted by the hydrodynamic theory (including the effects of dissociation) and found the agreement to be good. Berets, Greene and Kistiakowsky (4) repeated the experiments but used newer values for the thermodynamic properties of the system to calculate the theoretical values. Their results are not materially different from the work of Lewis and Friauf (32).

No tests of the theory have been made to date over an extended temperature or pressure range however. In fact no reliable experimental results have been obtained on the effect of initial temperature on the detonation velocity since the limited experiment of Dixon (14) and very little experimentation has been done on the effect of pressure (5,14,22). Brown (10) wrote in 1924, "A study of the literature reveals no conclusive evidence of the effect of varying conditions of initial temperature or pressure upon the characteristics of gaseous explosions or upon the development of detonation." The limited experimental work performed along these lines since that time has not clarified the situation materially.

CHAPTER III

THE HYDRODYNAMIC THEORY OF DETONATION

Detonation theory is based upon the fundamental work of Chapman and Jouquet with extensions by Becker (2), Zeldovich (56) von Neuman (38), and Doring (15) as noted in the previous section.

Consider the plane detonation wave propagating in a one dimensional system as shown in Figure 2 below.

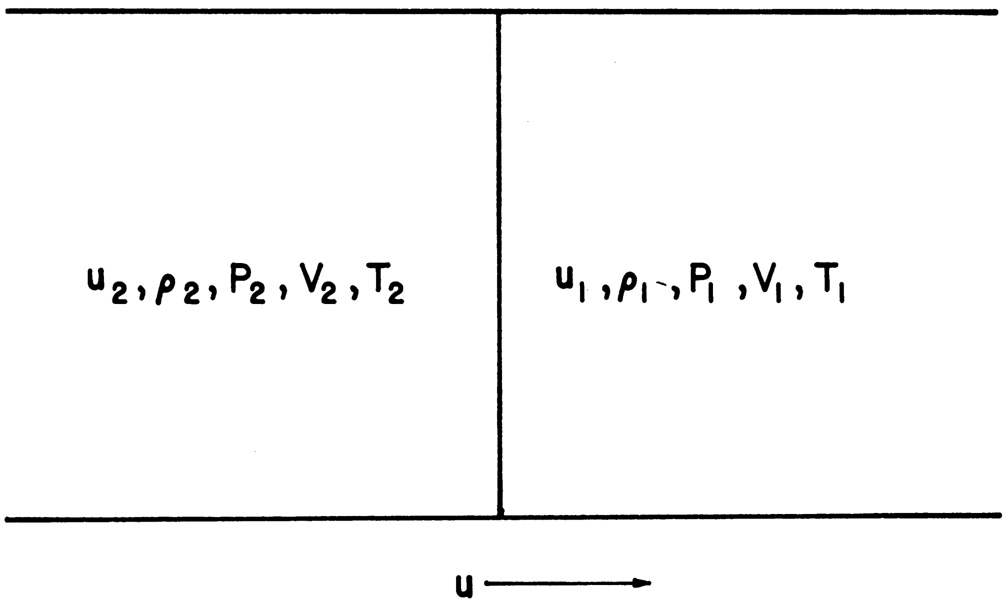

Figure 2. Schematic Representation of the Detonation Wave in a One Dimensional System

Ahead of the wave is the unburned mixture which is undisturbed by the advancing front; behind the wave are the reaction products which may or may not be changing with time. Between these two regions is the reaction zone. The detonation wave is assumed to be steady with space and time.

The derivation begins with the conservation equations for a one-dimensional system:

$$u \frac{\partial \rho}{\partial x} + \rho \frac{\partial u}{\partial x} = 0 \qquad \text{mass} \tag{1}$$

$$\rho u \frac{\partial u}{\partial x} + \frac{\partial}{\partial x}\left(P - \mu \frac{\partial u}{\partial x}\right) = 0 \qquad \text{momentum} \tag{2}$$

$$\rho u \frac{\partial E}{\partial x} = \left(P - \mu \frac{\partial u}{\partial x}\right) \frac{u}{\rho} \frac{\partial \rho}{\partial x} + \frac{\partial}{\partial x}\left(k \frac{\partial T}{\partial x}\right) \text{ energy} \tag{3}$$

These equations may be integrated to yield:

$$\rho \ u = c_1 \qquad \text{mass} \tag{4}$$

$$P + \rho u^2 - c_2 = \mu \rho u \frac{d(1/\rho)}{dx} \qquad \text{momentum} \tag{5}$$

$$E + \frac{c_2}{\rho} - \frac{u^2}{2} - c_3 = \frac{k}{c_1} \ dT/dx \qquad \text{energy} \tag{6}$$

It has not been possible to solve these three equations in closed form for general values of the parameters. For the case of a shock wave ($Q = 0$), Becker (3) expressed the temperature as a power series of the velocity and has been able to obtain a solution for the structure of the shock wave; Thomas (51) has calculated the thickness of a shock wave in air using the method of Becker. His results are shown in table I below.

TABLE I

CALCULATED SHOCK THICKNESS FOR
VARIOUS SHOCK PRESSURES IN AIR

Shock Pressure (Atm)	Shock Thickness (Mean Free Paths)
4.5	3.98
9.8	3.08
19.7	2.05
43.7	1.98

Eyring et al. (17) extended the calculation of the thickness of the shock wave to include the case with chemical reaction and found that the reaction zone is so long compared to the thickness of the shock wave that the shock wave could be analyzed on the assumption that negligible reaction had occurred. Some experimental values for the lengths of reaction zones for various explosives are given in table II.

TABLE II

EXPERIMENTALLY MEASURED LENGTHS OF REACTION ZONES FOR VARIOUS EXPLOSIVES[2]

Explosive	length (cm)
TNT	0.076
Picric Acid	0.083
Nitroguanidine	0.538
2Co + O_2 (gas)	1.1

Thus it has been shown that the thickness of the shock wave is of the order of mean free paths and that negligible chemical reaction occurs in the wave itself. Now consider the terms $\frac{d(\frac{1}{\rho})}{dx}$ and dT/dx; it is evident that they are every where zero except in a narrow zone of the order of a few free mean paths. Thus in considering the detonation wave from the macroscopic point of view it is permissible to drop these terms which automatically eliminates the effects of heat transfer and viscosity. Looking at the detonation wave from the microscopic point of view however, requires the solution to contain these terms.

By neglecting the terms $d(\frac{1}{\rho})dx$ and dT/dx it is possible to write the solution of equations 4, 5, and 6 as simple difference

[2] H. Eyring, R. Powell, G. Duffey, and R. Parlin, Chem. Revs., 45, 69 (1949).

equations:

$$\rho_1 u_1 = \rho_2 u_2 \qquad \text{mass} \qquad (7)$$

$$P_1 + \rho_1 u_1^2 = P_2 + \rho_2 u_2^2 \qquad \text{momentum} \qquad (8)$$

$$E_1 + P_1 V_1 + u_1^2/2 = E_2 + P_2 V_2 + u_2^2/2 \qquad \text{energy} \qquad (9)$$

By combining equations 7 and 8, we obtain Hugoniot's equation for velocities:

$$\rho_1 u_1 = \rho_2 u_2 = \left[\frac{P_2 - P_1}{V_1 - V_2}\right]^{1/2} \qquad (10)$$

Equation 10 may be used now to eliminate the velocity terms from the energy equation to obtain the so called Hugoniot equation:

$$E_2 - E_1 = 1/2 \left[P_1 + P_2\right]\left[V_1 - V_2\right] \qquad (11)$$

The Hugoniot relation takes the place of the reversible adiabatic law of compression $PV^\gamma = C$ for the case of extremely rapid and intense compression such as occurs in shock and detonation waves. For infinitesimal increases in ΔE and ΔV, the Hugoniot relation reduces to the adiabatic relation $dE + pdV = 0$. A comparison is made of the values obtained by using the Hugoniot relation for the pressure volume relationship and the adiabatic law $PV^\gamma = C$ in table III below.

TABLE III

COMPARISON OF THE FINAL VALUES OBTAINED USING THE HUGONIOT RELATION FOR THE PRESSURE VOLUME RELATION WITH THOSE OBTAINED FROM THE LAW $PV^\gamma = C$.

Pressure Ratio	T_2 °K (Hugoniot)	T_2 °K ($PV^\gamma = C$)
2	336	330
10	705	515
100	3860	950
2000	29000	2070

It is evident that the law $PV^\gamma = C$ is seriously in error when applied to strong shock waves.

Now if it is assumed that E = f(T) only, an additional relation is obtained:

$$E_2 - E_1 = \int_{T_1}^{T_2} c_v dT - \Delta E_c \qquad (12)$$

where ΔE_c is the energy release during constant volume combustion. The assumption that E = f(T) implies the assumption of a perfect gas which of course is very good at the high temperatures and moderate pressures attained in the detonation wave. The state equation for the perfect gas may be written:

$$PV = nRT \qquad (13)$$

Now E_2, n_2 and c_v all depend upon the progress of the combustion reactions which may be arbitrarily fixed or may be fixed by the requirement of thermodynamic equilibrium. For a given mixture, there are four equations namely 10, 11, 12, and 13, and five unknowns, E_2, P_2, n_2, T_2, and u_2. An additional relation is required for the solution.

By eliminating the energy terms in equation 11 by means of equations 12 and 13 the Hugoniot curve can be plotted in the PV plane as is shown schematically in Figure 3 below.

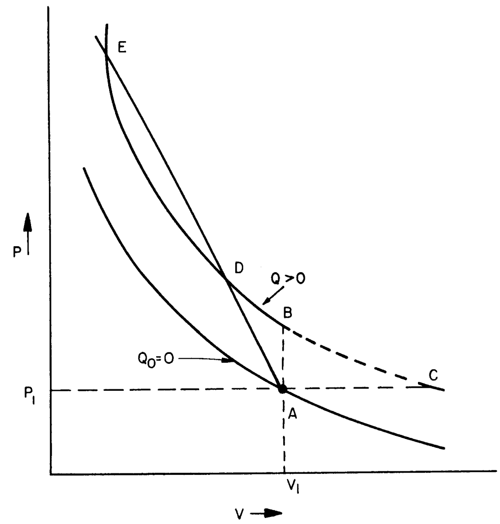

Figure 3. Qualitative Representation of the Hugoniot Curve in the Pressure-Volume Plane

The curve $Q_o = 0$ represents a pure shock wave in an inert medium whereas the curve $Q_1 > 0$ represents a shock wave with heat addition such as a detonation. For a given reaction, there will be an infinite number of curves lying between Q_o and Q_1 representing each infinitesimal degree of completion of the reaction. Gordon (19) has calculated the Hugoniot curves corresponding to successive tenths of a fraction reacted for hydrogen-air mixtures. The point A in Figure 3 corresponds to the initial values of P and V of the unburned gas. The Hugoniot curve yields the point on which P_2, V_2 must lie to be consistent with the conservation equations. When $V_2 = V_1$ corresponding to combustion at constant volume ($\Delta E = 0$) the pressure P_2 increases corresponding to point B on the "H" curve. For $P_2 = P_1$, the increase in volume equals the work done $\Delta E = P\Delta V$ represented by point C. The "H" curve passing through points B and C gives all possible values of the state P_2 , V_2 for a given P_1, V_1. Now a straight line L drawn through P_1V_1 and P_2V_2 represents the solution of equation 10 for the detonation velocity. The intersection of the two curves yields the solution or solutions for the value of the detonation velocity consistent with both equations. For a given P_1, V_1 there are two values of the detonation velocity corresponding to the intersections at D and E. At the point of tangency however, the solution is single valued.

It is possible to show algebraically that the point of tangency corresponds to the condition that $D = w + a$. In order to conclude that the point of tangency corresponds to normal detonation, it is necessary to apply thermodynamic reasoning suggested by Scorah (49).

Since the conditions ahead of the wave are constant, differentiation along the Hugoniot curve yields:

$$(V_1 - V_2)\, dP_2 - (P_1 + P_2)\, dV_2 - 2dE_2 = 0 \qquad (14)$$

Since the compostion of the burned gas is known, by assumption or by equilibrium, the entropy may be introduced by:

$$T_2 dS_2 = dE_2 + P_2 dV_2$$

so that

$$dS_2/dV_2 = \frac{(V_1 - V_2)}{2T_2} \left[\frac{P_2 - P_1}{V_1 - V_2} + \frac{dP_2}{dV_2} \right] \qquad (15)$$

The second derivative is:

$$\frac{d^2S_2}{d\,V_2^2} = \left[\frac{V_1 - V_2}{2T_2}\right] \left[\frac{d^2P}{dV_2^2}\right]_s \qquad (16)$$

at the point where $d\,S_2/dV_2 = 0$.

Now $$\frac{d^2P_2}{dV_2^2} = \frac{d}{dv_2}\left[\frac{-\gamma_2\, P_2}{V_2}\right]_s = \frac{\gamma_2(\gamma_2 + 1)(P_2)}{V_2^2}$$

which is always positive. In compression waves where $V_2 < V_1$, the second derivative $\frac{d^2S_2}{d\,V_2^2}$ is also always positive so that

$$\frac{P_2 - P_1}{V_1 - V_2} = -\left[\frac{dP_2}{dV_2}\right]_s = \frac{\gamma P_2}{V_2} \qquad (17)$$

represents a point of minimum entropy. Multiplication of both sides by V_2^2 yields

$$\frac{V_2^2(P_2 - P_1)}{V_1 - V_2} = \gamma_2 P_2 V_2 \qquad (18)$$

or that $u_2 = a_2$ where a_2 is the speed of sound in the burned gases at T_2 which completes the arguement that the point of tangency corresponds to the Chapman-Jouguet detonation velocity.

CHAPTER IV

PREDICTION OF THE DETONATION VELOCITY BY THE HYDRODYNAMIC THERMODYNAMIC THEORY OF DETONATION

The theoretical calculation of the detonation velocity was undertaken for comparison with the experimental results and to test the validity of the theory over an extended temperature range. The set of conservation equations derived in the preceeding section were rearranged to forms more suitable for machine computation. By combining equations 11 and 12 and eliminating the pressure terms by means of the equation of state, 13, equation 12 becomes:

$$\bar{C}_V(T_2-T_1) - \Delta E_c - (R/2)(V_1/V_2 - 1)(n_2T_2 + \frac{n_1T_1V_2}{V_1}) = 0 \qquad (19)$$

and equation 17 becomes:

$$\frac{2V_1^2}{V_2^2} - (\gamma_2 + 1)\frac{V_1}{V_2} + \frac{n_1 T_1}{n_2 T_2} = 0 \qquad (20)$$

To obtain a solution for the detonation velocity requires the solution of equations 19 and 20 to obtain the final state of the mixture.

An additional boundary condition is required for the determination of the reaction products. The assumption was made that thermodynamic equilibrium was attained at the Chapman-Jouguet Plane. The work of Peek and Thrap (42) and Berets, Greene and Kistiakowsky (4) indicates that the assumption is a valid one. Many equilibria are involved in the hydrogen-oxygen reaction. The ones considered were:

(1) $H_2 + 1/2\ O_2 \rightleftarrows H_2O$ (21)

(2) $1/2\ H_2 + 1/2\ O_2 \rightleftarrows OH$ (22)

(3) $1/2\ H_2 \rightleftarrows H$ (23)

(4) $1/2\ O_2 \rightleftarrows O$ (24)

The ozone reactions were neglected because the constant for ozone decomposition was so large compared with the other constants involved. The equilibrium constants for the above reactions may be written:

$$K_{p1} = \frac{(H_2O)}{(H_2)\ (O_2)^{1/2}} \qquad (25)$$

$$K_{p2} = \frac{(OH)}{(H_2)^{1/2}\ (O_2)^{1/2}} \qquad (26)$$

$$K_{p3} = \frac{(H)}{(H_2)^{1/2}} \qquad (27)$$

$$K_{p4} = \frac{(O)}{(O_2)^{1/2}} \qquad (28)$$

The equilibrium constants in this form are pressure, temperature and composition dependent so are unsuitable for this computation. As the pressure approaches zero as a limiting value K_p approaches K_f. K_f is a function of temperature only, but the final pressures involved are significantly different from zero.

By defining the equilibrium constant in terms of concentration units a method of solution can be obtained. The equilibrium constant K_c is given by:

$$K_c = \frac{(C_L)^l (C_m)^m}{(C_A)^a (C_B)^b} \qquad (29)$$

For an ideal gas:

$$C_i = \frac{Ni}{V} = \frac{XiP}{RT} \qquad (30)$$

so that:

$$Kp = K_c\ (RT)^{\Sigma n} \qquad (31)$$

The units in equation 31 are in terms of mols per liter. It is desirable to divide by V and obtain the relation:

$$K_c' = K_p\left(\frac{RT}{V}\right)^{-\Sigma n} \qquad (32)$$

where the units are in mols/gram. The equilibrium constants and the thermodynamic data were taken from the National Bureau of Standards tables (37). A four point Lagrangian interpolation method was used to obtain intermediate values.

The method of solution was by trial and error. The unknowns involved were the final specific volume, temperature, composition, heat of reaction and the ratio of specific heats. The initial computation was performed on a desk calculator. The problem was then programmed for the IBM 650 digital computor which has a 2000 word magnetic drum storage. Since there was adequate storage space for the problem, the thermodynamic data were stored on the drum and a table look up operation using the four point Lagrangian interpolation method was used in preference to curve fitting the thermodynamic data. The program was written in the Symbolic Optimal Assembly Program form and loaded on single word load cards. Data were entered through ten word-8 digit punched cards. The problem was set up on the drum as shown in table IV below:

TABLE IV

DRUM LOCATION RESERVATIONS

Location	Reservation
1950-1999	Post Mortem
1100-1949	Thermodynamic Data
0501-0510	Data
0550-0551	Data
0527-0536	Results
0000	Error

0039-0050	Square Root Subroutine
0001	Start
0401-0416	Thermodynamic Functions

The method invloved in solving the equations for a given set of initial conditions required some manual operation of the IBM machine. The program was loaded on the drum of the calculator and the data cards were entered. The machine began the computation immediately and an address stop of 0843 was used to stop the solution at the final T_2. The result appeared on the console of the machine. In order to obtain a solution, it was necessary to assume a value for the final temperature and for the ratio of the final specific volume to the initial specific volume. Fortunately the specific volume ratio is relatively constant and affects the solution only slightly. The assumed temperature was used to obtain the equilbrium constants. The equilibrium equations were then solved starting with the values of the reaction products assuming a complete reaction with no dissociation. By making a mass balance on the hydrogen, a new value was obtained for the water concentration; a mass balance on the oxygen composition was used as the criteria for convergence; the trial value of oxygen was compared with the calculated value. Several cycles were required for convergence.

These compositions were used to obtain the heat of reaction, average specific heat, and final enthalpy of the mixture. Equation 19 was then solved for V_1/V_2 and equation 20 solved for T_2 which was compared with the trial T_2. As mentioned earlier, the temperature appeared on the console. The value indicated was used as the basis for a new trial value. No satisfactory method was found for convergence other then by trial and error. The value of V_1/V_2 obtained was used as the new trial value for that parameter. In general, the final solutions obtained were within 1 degree of the trial values. The calculations were performed over an initial temperature range from 200°K to 500°K, pressure range from 0.5 to 2.0 atmosphere and composition range from 25% hydrogen to 80% hydrogen.

CHAPTER V

DESCRIPTION OF EQUIPMENT AND EXPERIMENTAL PROCEDURES

A. Equipment for Velocity Measurement

The experimental determination of the detonation velocity requires a timing system, a mixing and charging system, and a shock or detonation tube (several were used). A schematic diagram of the overall system is shown in Figure 4.

The measurement of the velocity of a detonation wave can be accomplished either photographically or electronically, a number of techniques are available. The photographic methods were considered unfeasible in this study at the low temperatures invloved; therefore an electronic method was chosen.

The electronic method chosen utilized the ionized gases behind the detonation front to ultimately trigger a time interval meter. This was accomplished by means of an ionization probe connected in a thyratron circuit. A number of ionization probes are described in the literature (30, 36, 44) but none of these were directly applicable in this work involving small diameter tubes. Therefore a probe of modified design was developed. The probe design finally adopted is shown in Figures 5 and 6. It consisted of a stainless steel sleeve containing a teflon insert. A number 76 drill was drilled into the teflon and left in to serve as the electrode. The probe worked excellently for approximately twenty to thirty runs despite the fact that the degree of ionization as calculated by the Saha equation (50) was quite low. No satisfactory method was found for restoring the activity of the probe so new ones were used frequently.

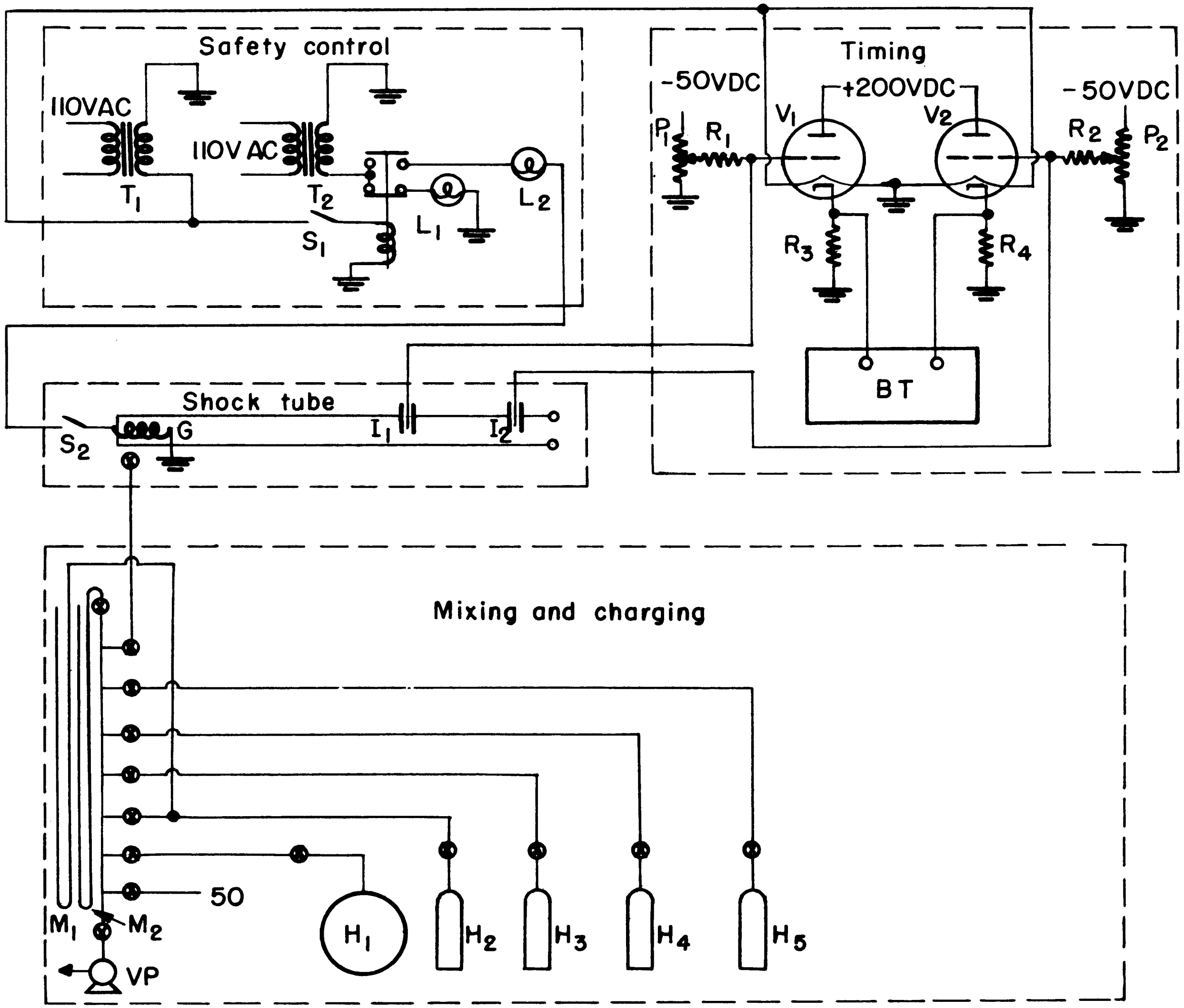

Components

T_1 – 6.3V filament transformer

T_2 – 6.3V filament transformer

S_1 – Microswitch

S_2 – Ignition switch

L_1 – Warning switch

L_2 – Ready light

P_1 – .5 meg potentiometer

P_2 – .5 meg potentiometer

V_1 – 884 thyratron

V_2 – 884 thyratron

R_1 – 1K resister, 1%

R_2 – 1K resister, 1%

$C_{1\text{-}11}$ – Needle valves

C_{12} – Master control valve actuates S_1

H_1 – 1 ft^3 Stainless steel storage vessel, fixed

H_2 – 0.5 ft^3 steel storage vessel, 6 interchangeable

H_3 – Nitrogen purge

H_4 – Hydrogen

H_5 – Oxygen

Figure 4. Schematic Diagram of the Experimental Apparatus

The ionization probe acted as a shorting switch in the grid of a number 884 thyratron tube. The grid of the thyratron was connected to a minus forty-five volt battery through a 1/2 megohm potentiometer. In order to obtain maximum sensitivity, the grid bias was adjusted almost to the firing point. When a detonation front passed over the probe, the hot ionized gases materially lowered the resistance between the probe electrode and ground. As a result the bias voltage dropped which caused the thyratron to fire and to start the time interval meter counting. The meter used in this work was a Berkley timer[3] model #5120. In any actual time interval measurement, two probe and thyratron circuits are required, one to start the timer counting and one to stop it. The time interval must be divided by the distance between the probe stations to obtain the average velocity. The probe stations varied from tube to tube as shown in table V. The minimum starting distance was seven feet in all cases however. Lafitte's (28) data on the length of path required for the initiation of stable detonation in hydrogen-oxygen mixtures shows that seven feet is many times that actually required for Chapman-Jouguet detonation in a one inch tube. Greene (20) measured the length of path required for transition of a flame into

[3] The time interval meter was on loan from the Aircraft Propulsion Lab.

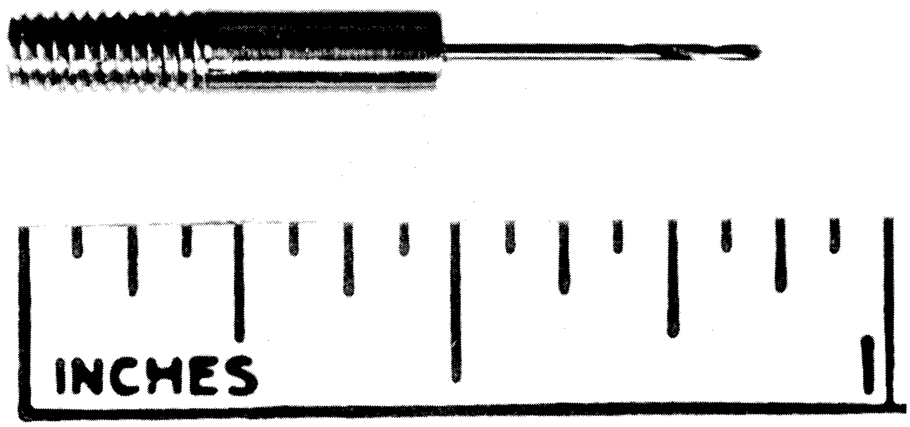

Figure 5. Photograph of the Ionization Probe

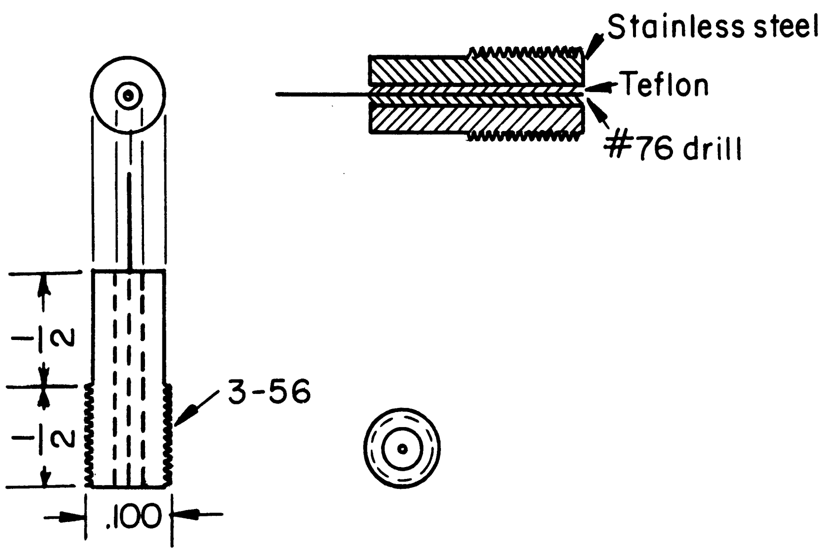

Figure 6. Diagram of the Ionization Probe

detonation in hydrogen-oxygen mixtures and found that transition occurs within 50 centimeters and the velocity is stable within 60 to 70 centimeters. Once the Chapman-Jouguet detonation is established the velocity remains constant thereafter; thus only two measuring stations are actually required.

B. The Mixing and Charging System

The mixing and charging system was used to premix the gases and to load the detonation tubes. A stand was constructed to support the detonation tubes and a panel board. A manifold (constructed from Ermeto tees, stainless steel tubing, and Hoke needle valves) was mounted behind the panel board. The manifold was connected to a mercury U tube, a vacuum pump, a storage vessel, and cylinders of hydrogen, oxygen, and nitrogen. A master control valve was connected between the manifold and the premixed gas storage vessel. The master control valve actuated a microswitch in the ignition circuit. When the valve was open the ignition circuit was dead. Two panel lights were used to indicate when the valve was open or closed. A green light indicated a closed valve. The unit is shown in several views in Figures 7, 8, and 9.

In this work, the mixing operation was done by the partial pressure method; corrections were made for changes in barometric pressure during mixing. The purity of the initial gases was checked on the mass spectrograph and found to be $99.5\%^{+}$ and the partial pressure method was checked periodically by analyzing the mixtures on the mass spectrograph. The composition obtained by the partial pressure method is plotted versus the composition obtained in the mass spectrograph in Figure 10. No significant difference is evident.

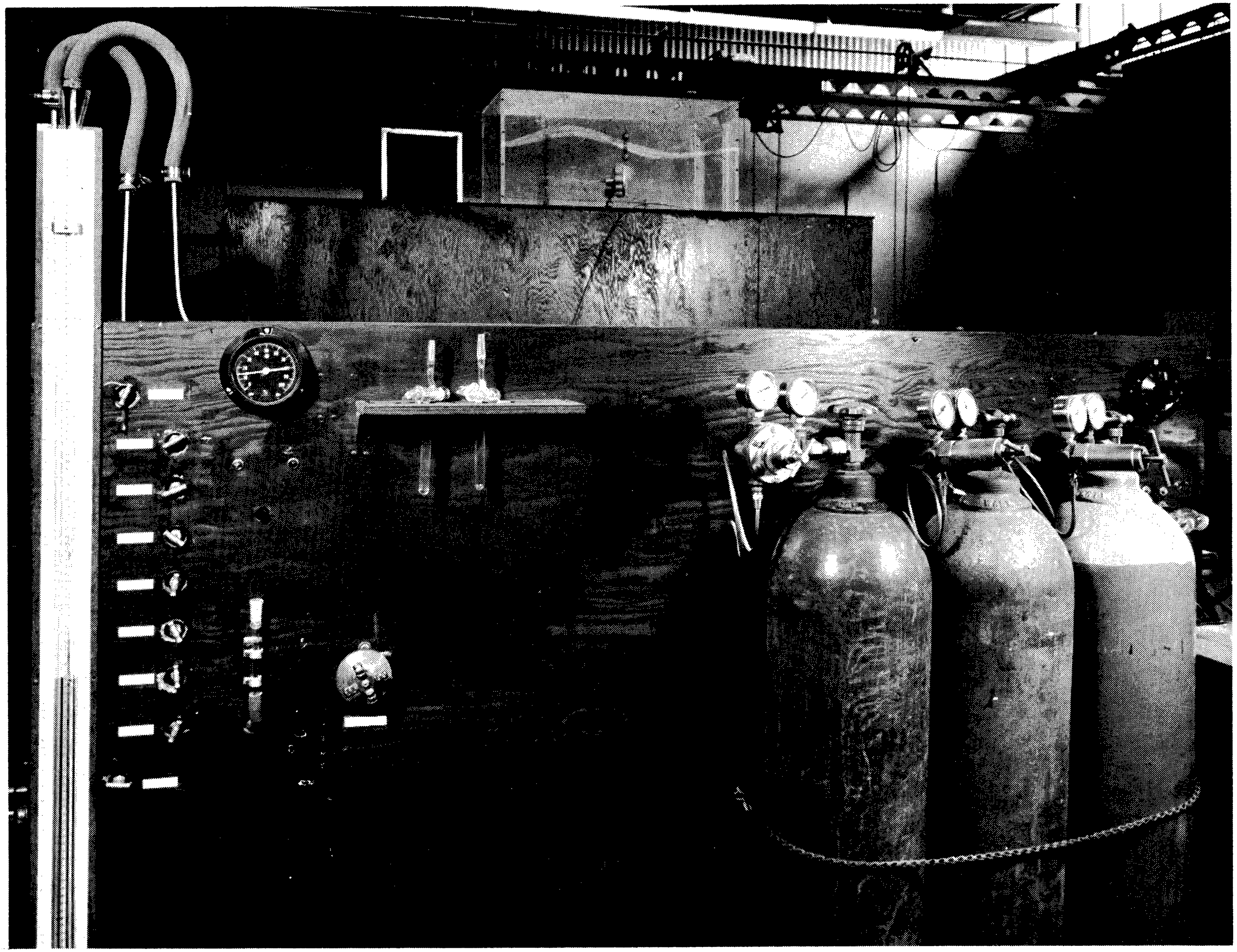

Figure 7. Photograph of the Mixing and Charging System from the Left Side

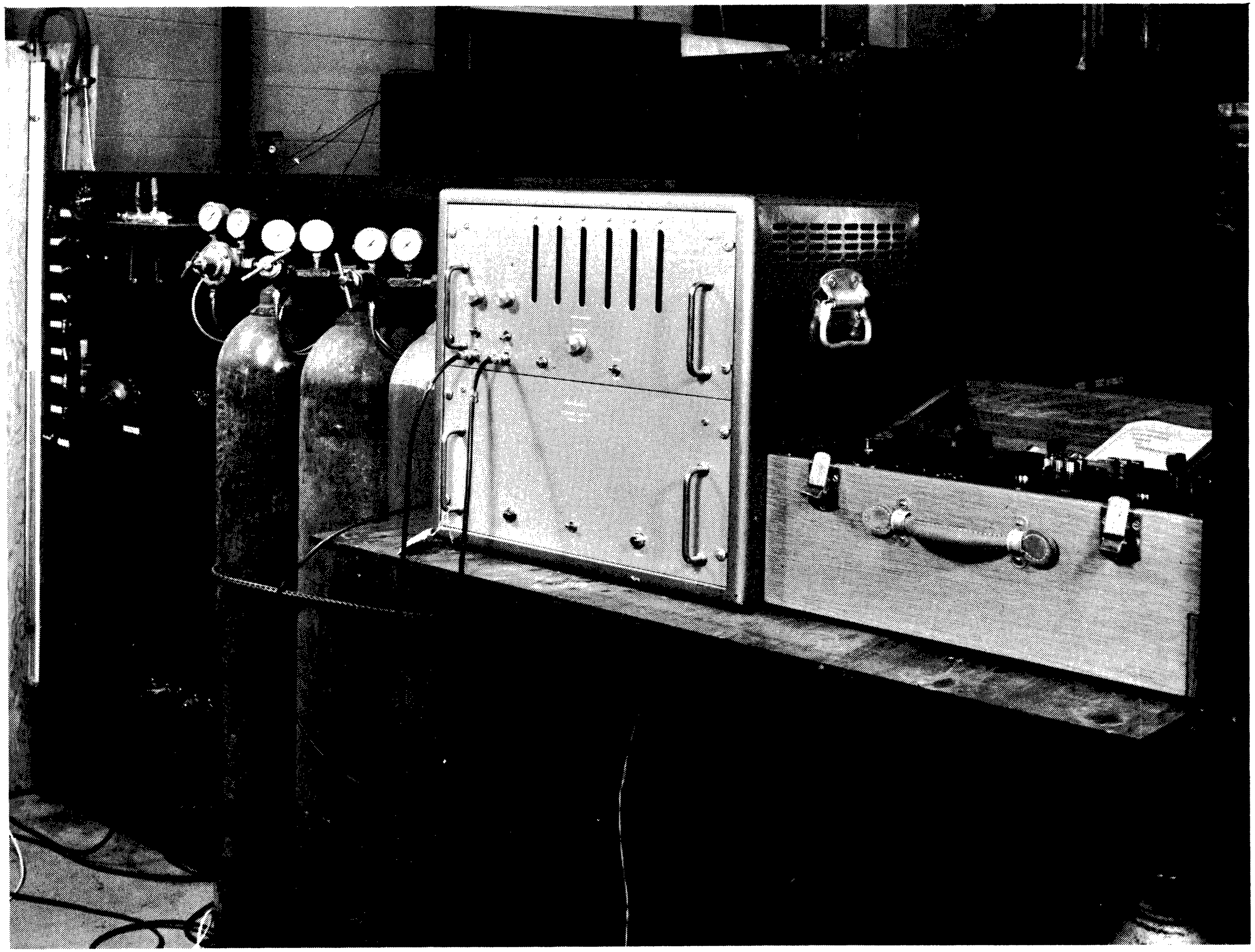

Figure 8. Photograph of the Mixing and Charging System from the Right Side

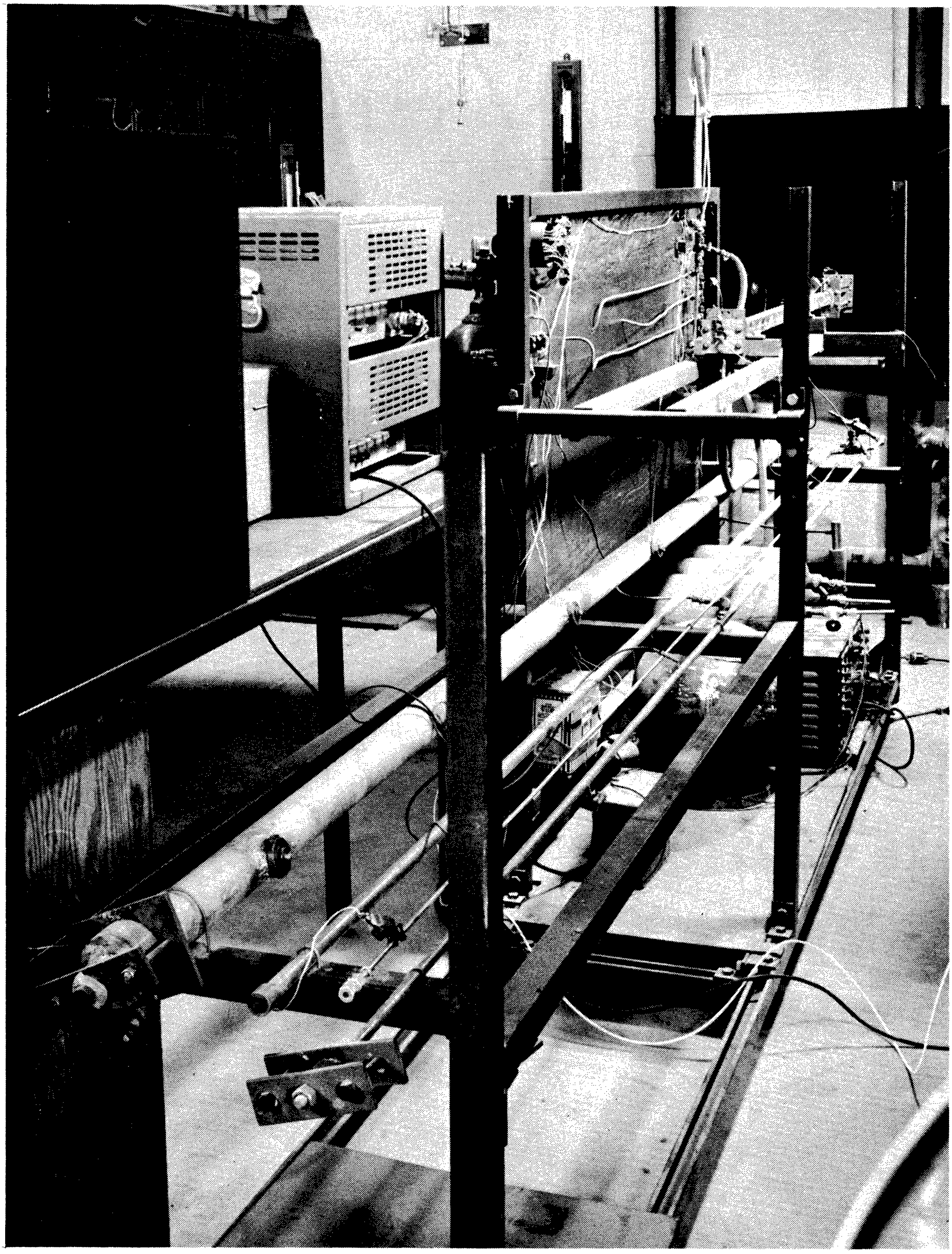

Figure 9. Photograph of the Mixing and Charging System from the Rear

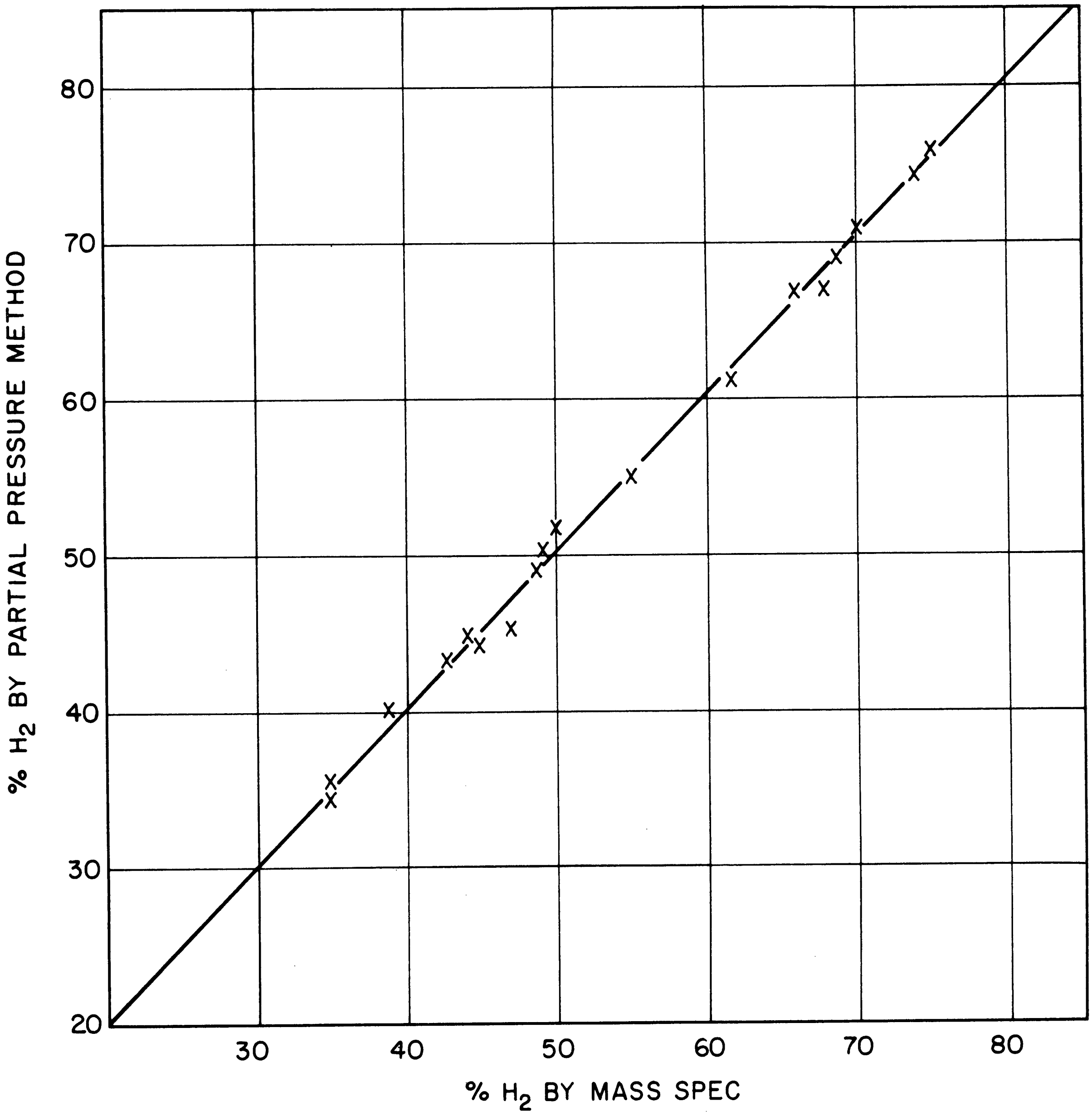

Figure 10. Comparison of Analysis by Mass Spectrograph with Partial Pressure Method

C. Schlieren Equipment

The schlieren methods of flow observation are based upon the refraction of light from its undisturbed path when it passes through a medium in which there is a component of the gradient of refractive index normal to the ray. There are many ways to set up the schlieren system using either lenses or mirrors. They are described in detail in references (1,46,54). The method used in this work is known as the Toepler method (1).

A diagram of the arrangement of the optics is shown in Figure 11 and a photograph of the experimental apparatus used is shown in Figure 12. The lenses were 5.25 inch diameter coated achromats with 24.75 inch focal lengths. In operation, parallel light entered the test section and was bent toward the regions of higher density. This caused a change in the illumination of the image of the region or point

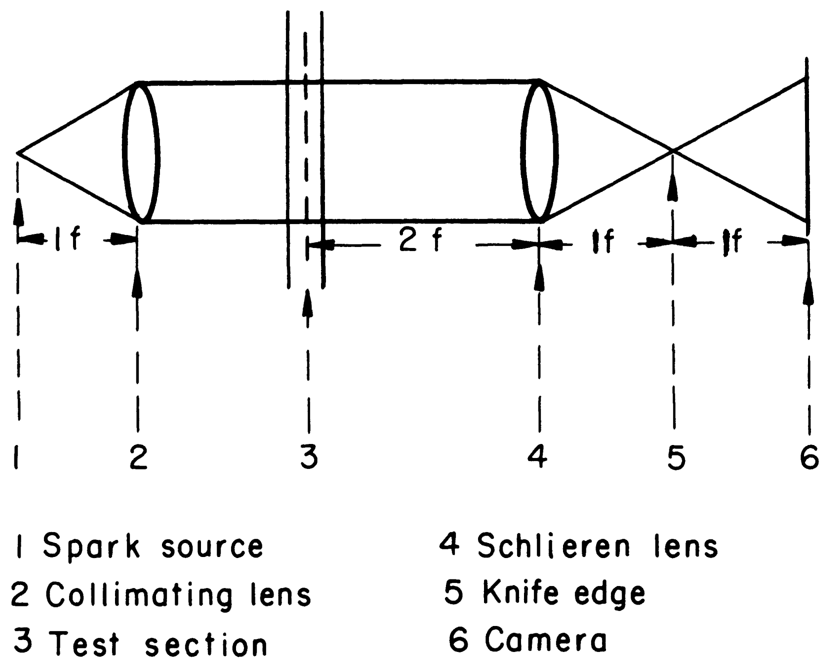

Figure 11. Diagram of the Schlieren Apparatus

Figure 12. Photograph of the Schlieren Apparatus

on the screen. To photograph the detonation wave, a short duration light source and associated electronic time delay equipment were required. The light source used was a short duration (approximately 0.1 microsecond) spark.[4] An ionization probe, located upstream of the test section, activated a variable time delay unit when the hot ionized gases passed over the probe. The time delay was adjusted to energize the spark when the detonation wave was in the test section. Light from the spark was sufficient to obtain a photographic exposure using Royal Pan photographic film.

D. Detonation Tubes

The characteristics of the five detonation tubes used and the detonation coil are shown below in table V.

TABLE V

CHARACTERISTICS OF THE DETONATION TUBES USED IN THE EXPERIMENTAL INVESTIGATION

Tube	Material	ID	Form	Starting Distance(feet from ignition point)	Probe Separation feet	Total Length Feet
A	Stainless Steel	0.125	Straight Tube	7.0	3.0007	11.5
B	"	0.250	"	9.0	2.999	13.50
C	"	0.375	"	7.5	2.0003	12.00
D	"	0.909	"	7.0	3.9944	12.00
E	Carbon Steel	3.250	"		3.000	14.00
F	Stainless Steel	0.250	Coiled Tube	8.0	12.00	24.00

[4] The spark source and time delay unit were on loan from Project Squid under the direction of Dr. Morrison.

E. Temperature Control Equipment

The original objective of the investigation was to obtain the effect of temperature on the detonation velocity. Initially a temperature range between -100 degrees Fahrenheit and 300 degrees Fahrenheit was considered. The attainment of the low temperatures in a straight tube appeared to be unduly difficult and expensive when the design of the equipment was considered in detail. A coil was considered to be the ideal arrangement for the shock tube since it could be immersed directly in a bath. A search of the literature suggested that velocities obtained in a coil might be the same as in a straight tube. Dixon's (14) work was done in a coil and Scorah (49) maintains that the detonation velocity is unaffected by coiling or even zigzaging the tube. Therefore a coil was constructed from twenty-four feet of 1/4 inch ID stainless steel tubing. The probe locations were marked before coiling on a ten inch drum. The characteristics of the coil are given in table V. Some initial measurements were made in the coil and in a straight tube of the same ID to check upon the accuracy of Scorah's statement. The results are shown in Figure 13 plotted as the velocity in the tube versus the velocity in the coil. The coil results appear to be 0.5% lower than the tube results over the range of velocities. This was considered satisfactory for evaluation of the effect of temperature.

A stainless steel tank was fabricated and insulated with two inches of hair felt for use in the low temperature experiments. Five gallons of normal propyl alcohol were used for the bath. Dry ice was used to cool the bath down to -78° centigrade. Liquid nitrogen was added directly to the bath to obtain the lowest temperatures. The high temperatures were obtained by placing the coil in an oven. The

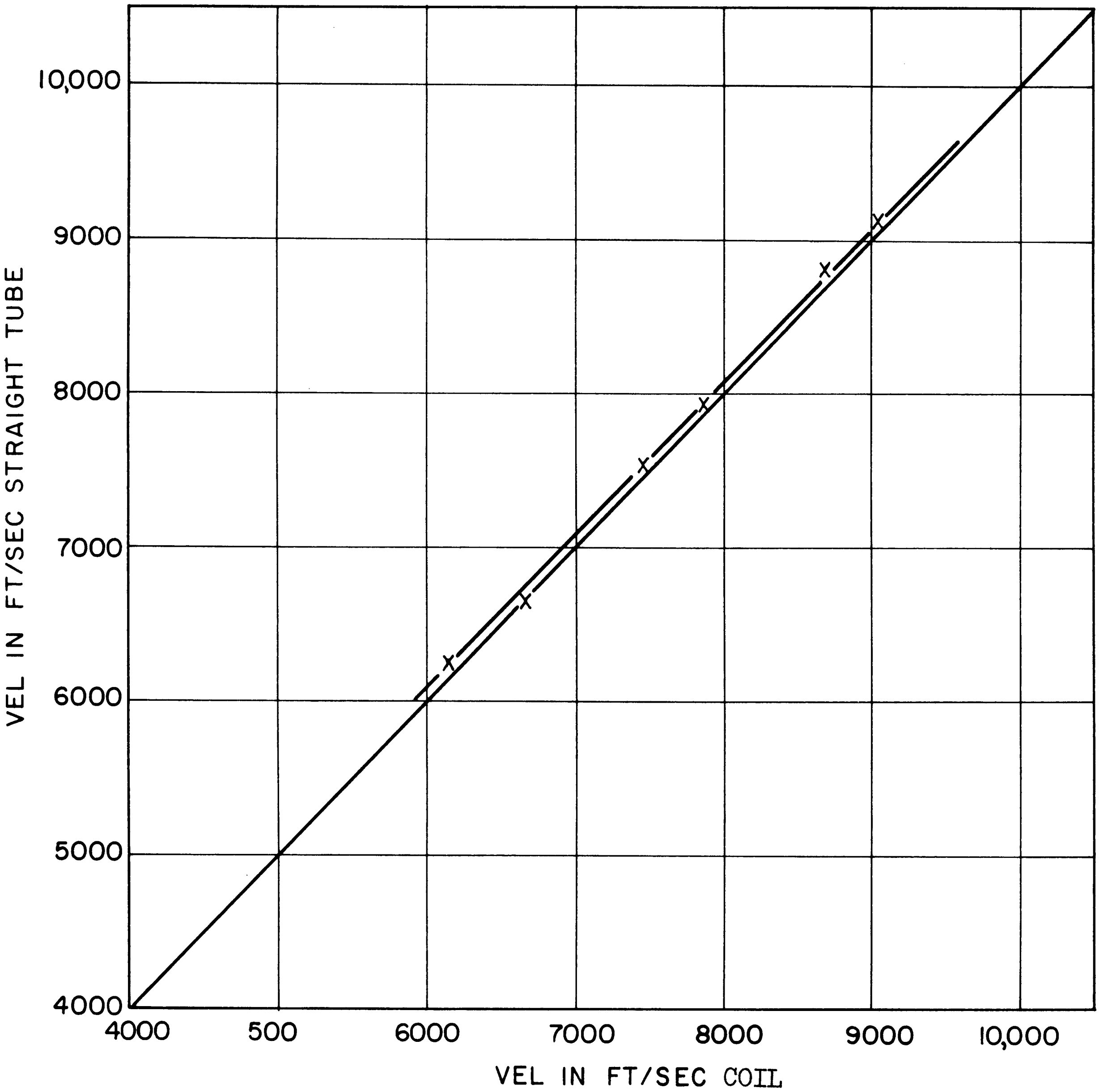

Figure 13. Comparison of Velocity of Detonation in the Coil with Velocity in Straight Tube

temperature range was extended from -176 Fehrenheit to 400 degrees Fahrenheit by using the above techniques.

To obtain data, the coil was evacuated at room temperature and then placed in the bath. Gas was added until the pressure in the tube was slightly above atmospheric pressure. Additional gas was added (or subtracted depending upon the bath temperature) until a constant pressure was obtained. The pressure was considered constant when a mercury U tube connected to the tube remained unchanged for five minutes. Usually fifteen minutes were required for the gas addition. Runs were made using fifteen, twenty, and thirty minute loading intervals. The velocity measurements were identical for all three time intervals.

After a few runs, the probes shorted out due to the solution surrounding them and it was necessary to isolate them from the bath. A piece of 1/16 inch diameter rubber tubing was placed over the probe and carried up and out of the bath. A copper wire was inserted into the tubing and a small wad of steel wool was used for the electrical contact between the probe and conductor.

After a low temperature run was made, it was necessary to lift the coil out of the bath and to allow it to come to room temperature under a vacuum. This procedure was necessary to prevent moisture from freezing on the inner walls of the coil and fouling the probes.

Low temperature runs were made at -78 degrees centigrade and then liquid nitrogen added to lower the temperature further. A temperature of -113 degrees centigrade was ultimately attained. Vigorous stirring was required to obtain a uniform temperature since the alcohol was near the freezing point. The consistency was almost that of a taffy. The temperature variation through the bath was held within $\pm$ 2.0 degrees centigrade. During the fifteen minute loading interval liquid nitrogen had to be added several times to maintain the temperature level. Pictures of the coil, bath and oven used in these experiments are shown in Figures 14, 15, and 16.

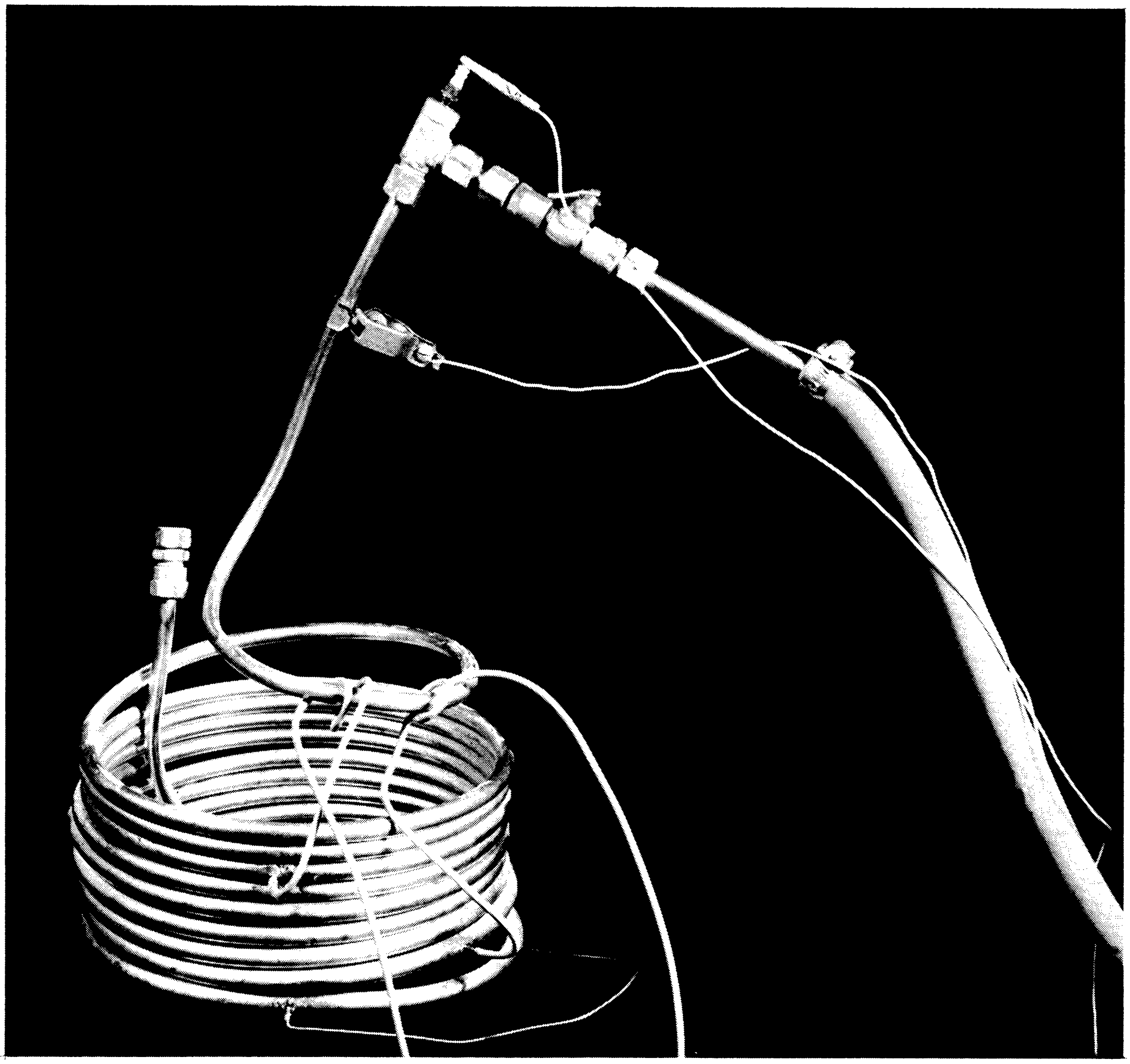

Figure 14. Photograph of the Coil Used to Obtain Experimental Detonation Velocities

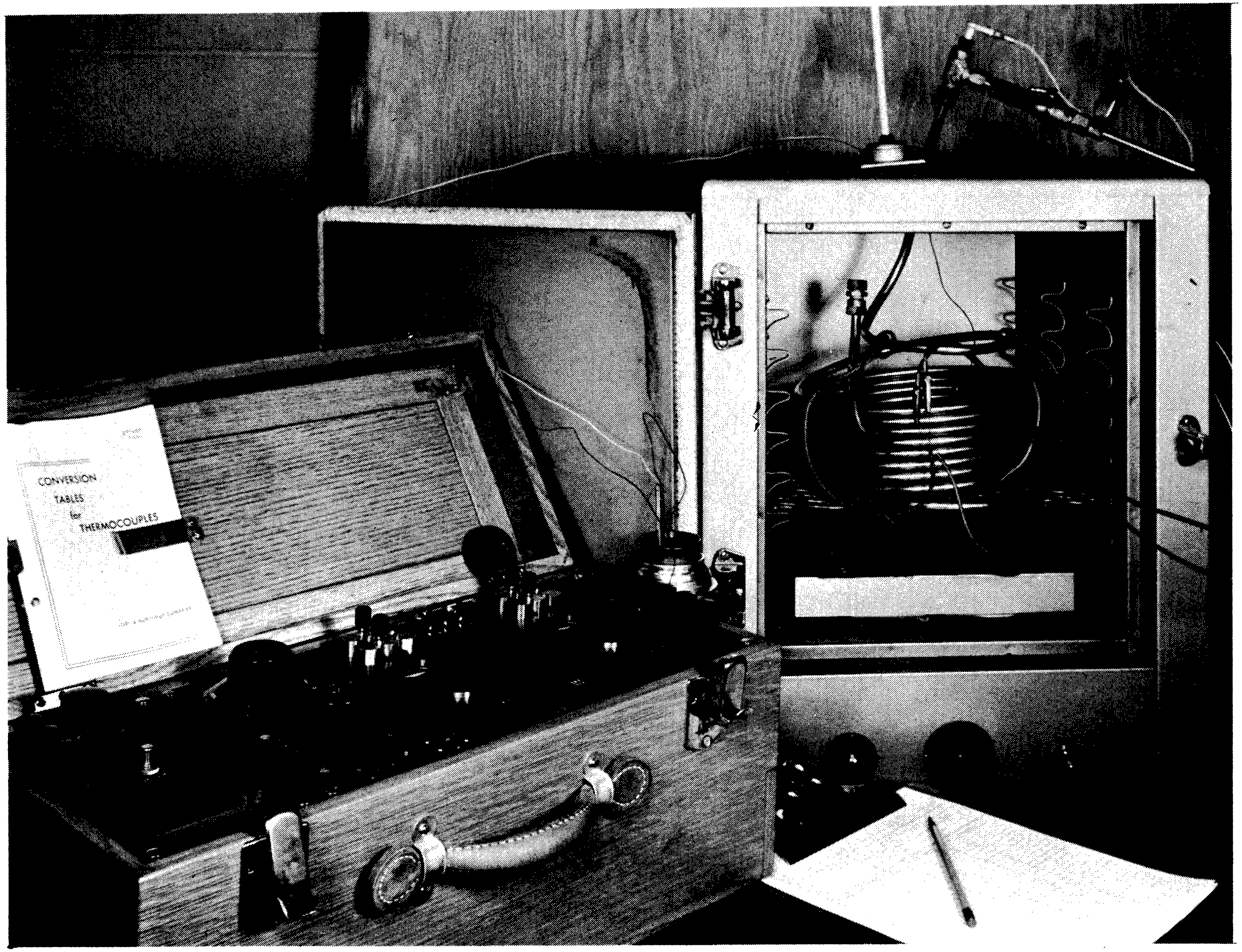

Figure 15. Photograph of Apparatus Used for High Temperature Detonation Velocity Measurement

Figure 16. Photograph of Apparatus Used for Low Temperature Detonation Velocity Measurement

CHAPTER VI

RESULTS

A. Analysis of Detonation Characteristics by Digital Computation.

The method of computation of detonation characteristics using the IBM type 650 digital computor was described in Chapter III. Equilibrium concentrations and detonation characteristics were calculated for various mixtures of hydrogen and oxygen. The effect of temperature and pressure were determined; tabulated results are given in tables VI and VII. Figure 17 shows the variation of the components (H_2, O_2, H_2O, O, H, OH) in the burned gases as a function of the inital gas composition. The variations of the products of reaction with initial temperature are shown in Figures 18 through 23. The variation of the final temperature with the initial temperature is shown in Figure 24 and is almost negligible while the variation of the detonation velocity with initial temperature (Figure 25) decreases with increasing initial temperature and shows a composition effect. Figures 26 through 31 show the effect of initial pressure on the final reaction products. The effect of pressure on the detonation velocity is shown in Figure 32. A slight gradual increase is noted with increasing pressure.

B. Experimental Results

1. Schlieren Photographs of Detonation Waves

TABLE VI.

EQUILIBRIUM COMPOSITIONS BEHIND THE DETONATION WAVE
CALCULATED FOR VARIOUS HYDROGEN-OXYGEN MIXTURES

Run No.	T_1 K	P_1 Atm.	X_{H_2} Mol Frac	X_{H_2O} Mols/gm	X_{H_2} Mols/gm	X_{O_2} Mols/gm	X_H Mols/gm	X_O Mols/gm	X_{OH} Mols/gm
1	200	1.0	0.2500	0.00979	0.00003	0.02524	0.00001	0.00019	0.00073
2	200	1.0	.3333	.01378	.00020	.02188	.00010	.00081	.00223
3	200	1.0	.5000	.02372	.00187	.01299	.00113	.00262	.00645
4	200	1.0	.5504	.02746	.00326	.00994	.00190	.00279	.00772
5	200	1.0	.8000	.04640	.04857	.00011	.00672	.00028	.00302
6	300	1.0	.2500	.00972	.00004	.02518	.00002	.00027	.00086
7	300	1.0	.3333	.01359	.00025	.02177	.00014	.00098	.00248
8	300	1.0	.4000	.01711	.00065	.01852	.00040	.00175	.00406
9	300	1.0	.5000	.02336	.00205	.01295	.00132	.00288	.00663
10	300	1.0	.5504	.02704	.00348	.00995	.00217	.00327	.00783
11	300	1.0	.6000	.03093	.00583	.00702	.00339	.00337	.00873
12	300	1.0	.7601	.04424	.03371	.00051	.00899	.00098	.00551
13	300	1.0	.8000	.04548	.04816	.00017	.00876	.00045	.00363

TABLE VI.(Cont'd.)

14	400	1.0	.2500	.00958	.00006	.02510	.00003	.00035	.00108
15	400	1.0	.3333	.01343	.00029	.02166	.00017	.00115	.00267
16	400	1.0	.5000	.02303	.00221	.01292	.00149	.00310	.00680
17	400	1.0	.5504	.02667	.00367	.00996	.00241	.00350	.00795
18	400	1.0	.8000	.04504	.04799	.00020	.00967	.00054	.00393
19	500	1.0	.2500	.00951	.0007	.02502	.00003	.00045	.00119
20	500	1.0	.3333	.01359	.00025	.02157	.00021	.00131	.00285
21	500	1.0	.5000	.02275	.00234	.01288	.00165	.00332	.00693
22	500	1.0	.5504	.02632	.00385	.00997	.00263	.00371	.00807
23	500	1.0	.8000	.04460	.04788	.00023	.01050	.00063	.00421
24	300	0.5	.3333	.01356	.00026	.02174	.00015	.00106	.00249
25	300	0.5	.5000	.02307	.00023	.01296	.00153	.00313	.00664
26	300	0.5	.7601	.04376	.03364	.00059	.00993	.00114	.00567
27	300	0.5	.8000	.04514	.04786	.00020	.00984	.00054	.00383
28	300	2.0	.3333	.01378	.00019	.02190	.00009	.00075	.00226
29	300	2.0	.5000	.02365	.00188	.02195	.00111	.00261	.00660
30	300	2.0	.7601	.04474	.03379	.00043	.00803	.00083	.00532
31	300	2.0	.8000	.04592	.04836	.00013	.00773	.00036	.00338

TABLE VII.

DETONATION CHARACTERISTIC'S CALCULATED FOR
VARIOUS HYDROGEN-OXYGEN MIXTURES

Run No.	X_{H2} Mol Fract	P_1 Atm.	V_1 L/gm	T_1 K	N_1 Mols/gm	T_2 K	V_1/V_2 Dimensionless	N_2 Mols/gm	D ft/sec
1	0.2500	1.0	0.67000	200	0.04081	2636.6	1.77344	0.03599	5756.9
2	0.3333	1.0	0.74540	200	0.04545	3033.5	1.78426	0.03900	6440.3
3	0.5000	1.0	0.96458	200	0.05878	3510.2	1.79385	0.04878	7761.5
4	0.5504	1.0	1.05942	200	0.06456	3607.2	1.79473	0.05327	8225.2
5	0.8000	1.0	1.2567	200	0.12480	3570.3	1.78899	0.10510	11500.7
6	0.2500	1.0	1.00500	300	0.04081	2670.3	1.75407	0.03609	5738.4
7	0.3333	1.0	1.11810	300	0.04545	3026.7	1.76546	0.03921	6386.4
8	0.4000	1.0	1.23036	300	0.4998	3232.4	1.77117	0.04249	6879.4
9	0.5000	1.0	1.44700	300	0.05878	3463.4	1.77596	0.04919	7672.1
10	0.5504	1.0	1.58914	300	0.06456	3554.0	1.77708	0.05374	8127.8
11	0.6000	1.0	1.75702	300	0.07138	3621.2	1.77747	0.05927	8620.2
12	0.7601	1.0	2.75910	300	0.11209	3557.9	1.77244	0.09394	10758.0
13	0.8000	1.0	3.07700	300	0.12480	3435.8	1.76929	0.10665	11261.7

TABLE VII. (Cont'd.)

14	0.2500	1.0	1.3400	400	0.04081	2691.9	1.73444	0.03620	5706.5
15	0.3333	1.0	1.49170	400	0.04545	3030.1	1.74686	0.03937	6338.1
16	0.5000	1.0	1.92916	400	0.05878	3435.0	1.75795	0.04955	7598.0
17	0.5504	1.0	2.11886	400	0.06456	3519.3	1.75950	0.05416	8046.2
18	0.8000	1.0	4.10268	400	0.12480	3413.9	1.75191	0.10737	11161.9
19	0.2500	1.0	1.67500	500	0.04081	2731.0	1.71534	0.03627	5690.5
20	0.3333	1.0	1.86350	500	0.04545	3037.0	1.72809	0.03955	6340.0
21	0.5000	1.0	2.41145	500	0.05878	3414.4	1.74008	0.04987	7527.8
22	0.5504	1.0	2.64855	500	0.06456	3494.1	1.74181	0.5455	7971.7
23	0.8000	1.0	5.12835	500	0.12480	3399.1	1.73446	0.10805	11070.0
24	0.3333	0.5	1.49080	300	0.04545	3005.0	1.76470	0.03926	6366.5
25	0.5000	0.5	2.89400	300	0.05878	3358.6	1.77281	0.04956	7579.7
26	0.7601	0.5	5.51820	300	0.11209	3440.8	1.76940	0.09473	10618.2
27	0.8000	0.5	6.15400	300	0.12480	3335.3	1.76642	0.10741	11129.3
28	0.3333	2.0	0.37270	300	0.04545	3121.0	1.76879	0.03897	6469.0
29	0.5000	2.0	0.72350	300	0.05878	3570.7	1.77854	0.04880	7763.1
30	0.7601	2.0	1.37955	300	0.11209	3675.7	1.77523	0.09314	10993.7
31	0.8000	2.0	1.53850	300	0.12480	3538.2	1.77207	0.10588	11392.3

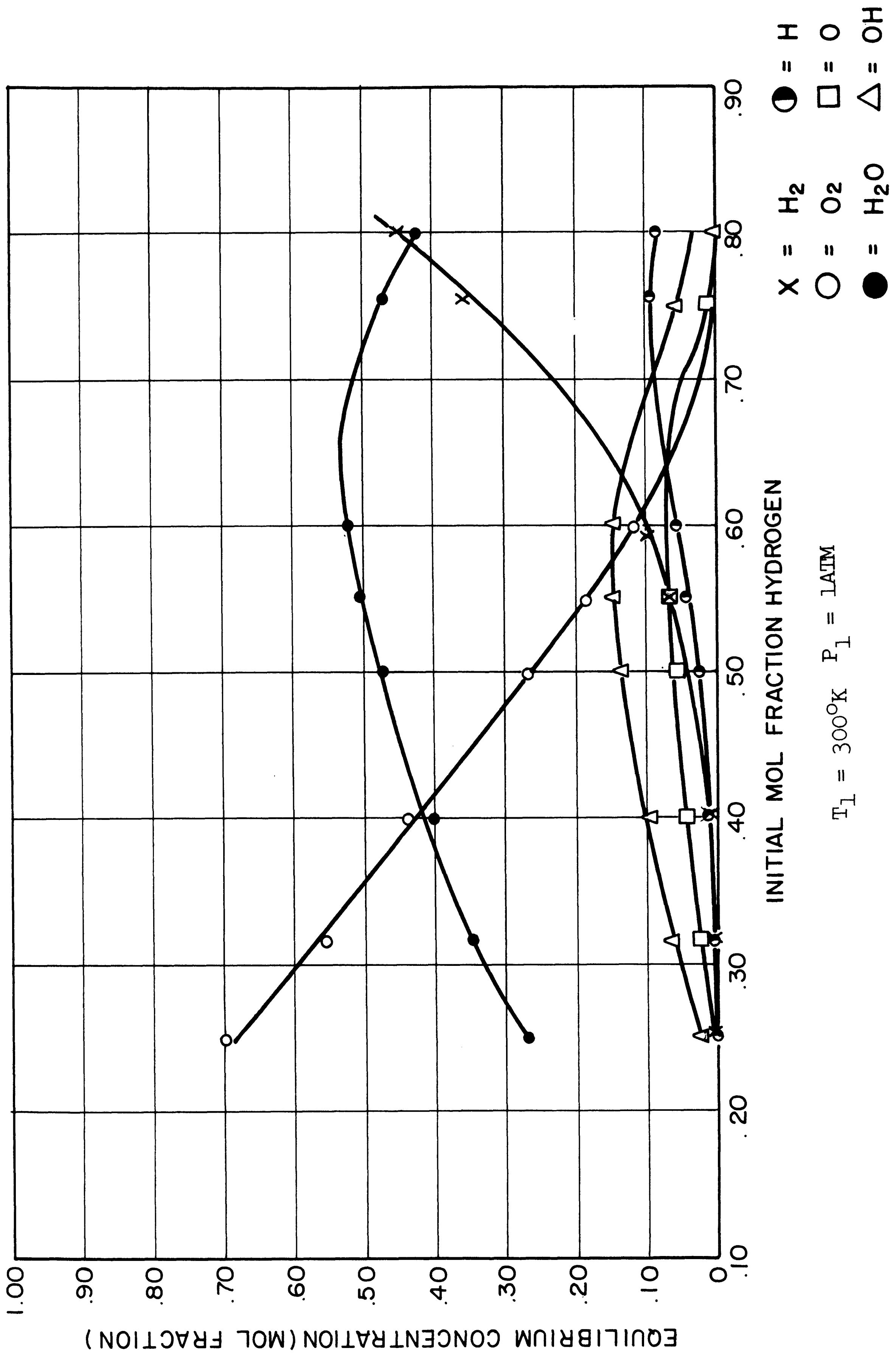

Figure 17. Equilibrium Concentration versus Initial Hydrogen Content

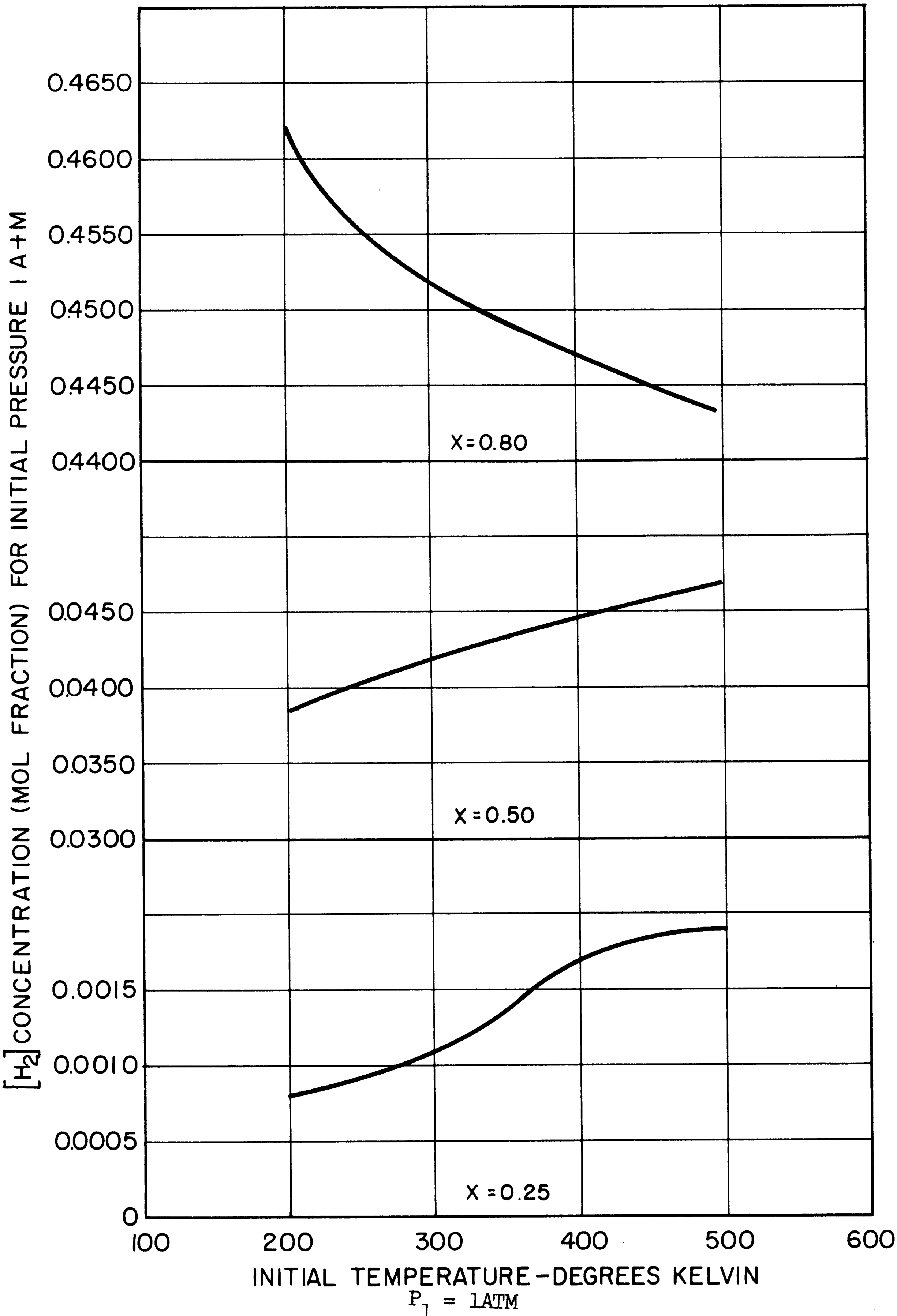

Figure 18. Equilibrium Concentration (H_2) versus Initial Temperature; X = Initial Mol Fraction Hydrogen

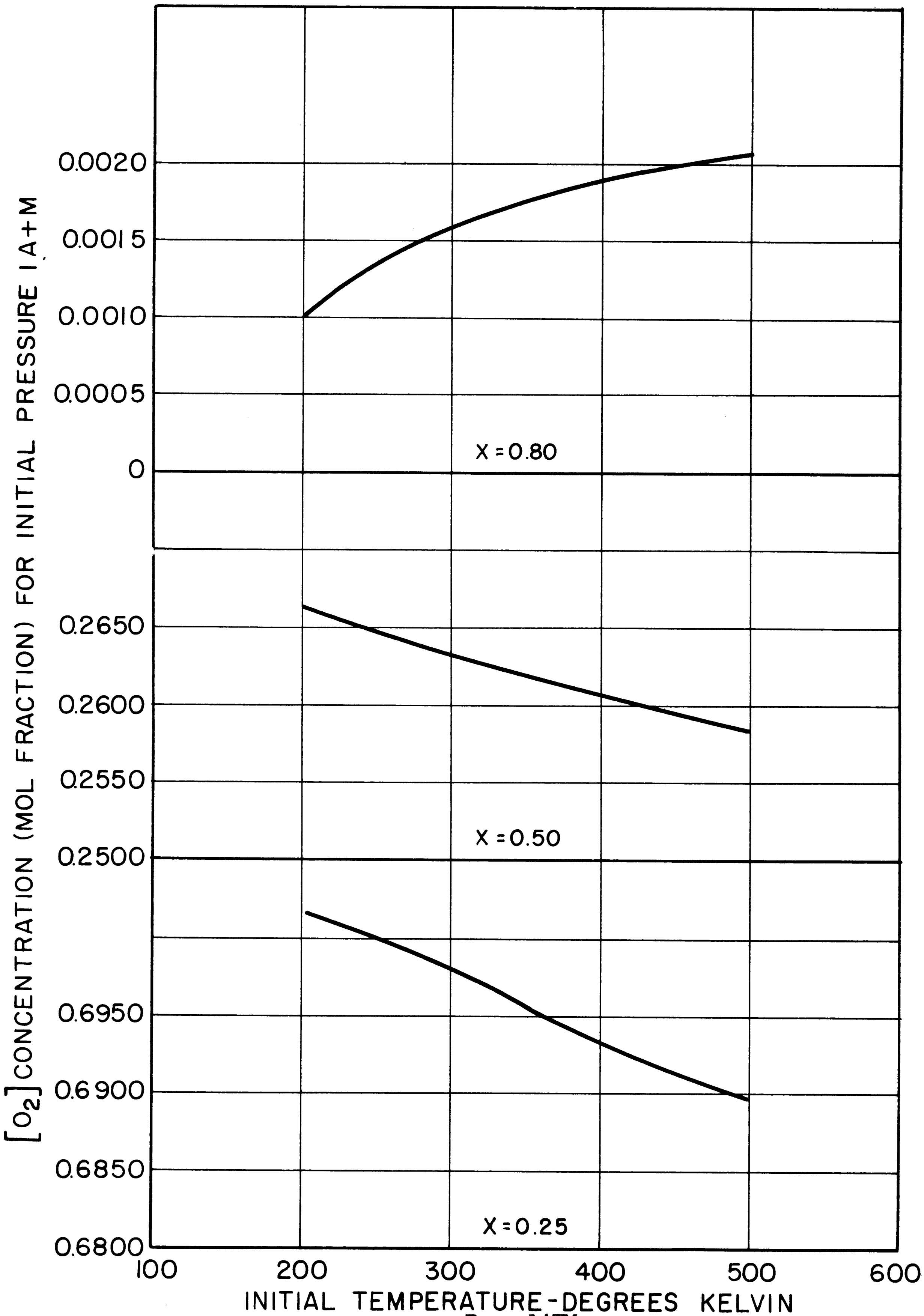

P_1 = 1ATM

Figure 19. Equilibrium Concentration (O_2) versus Initial Temperature; X = Initial Mol Fraction Hydrogen

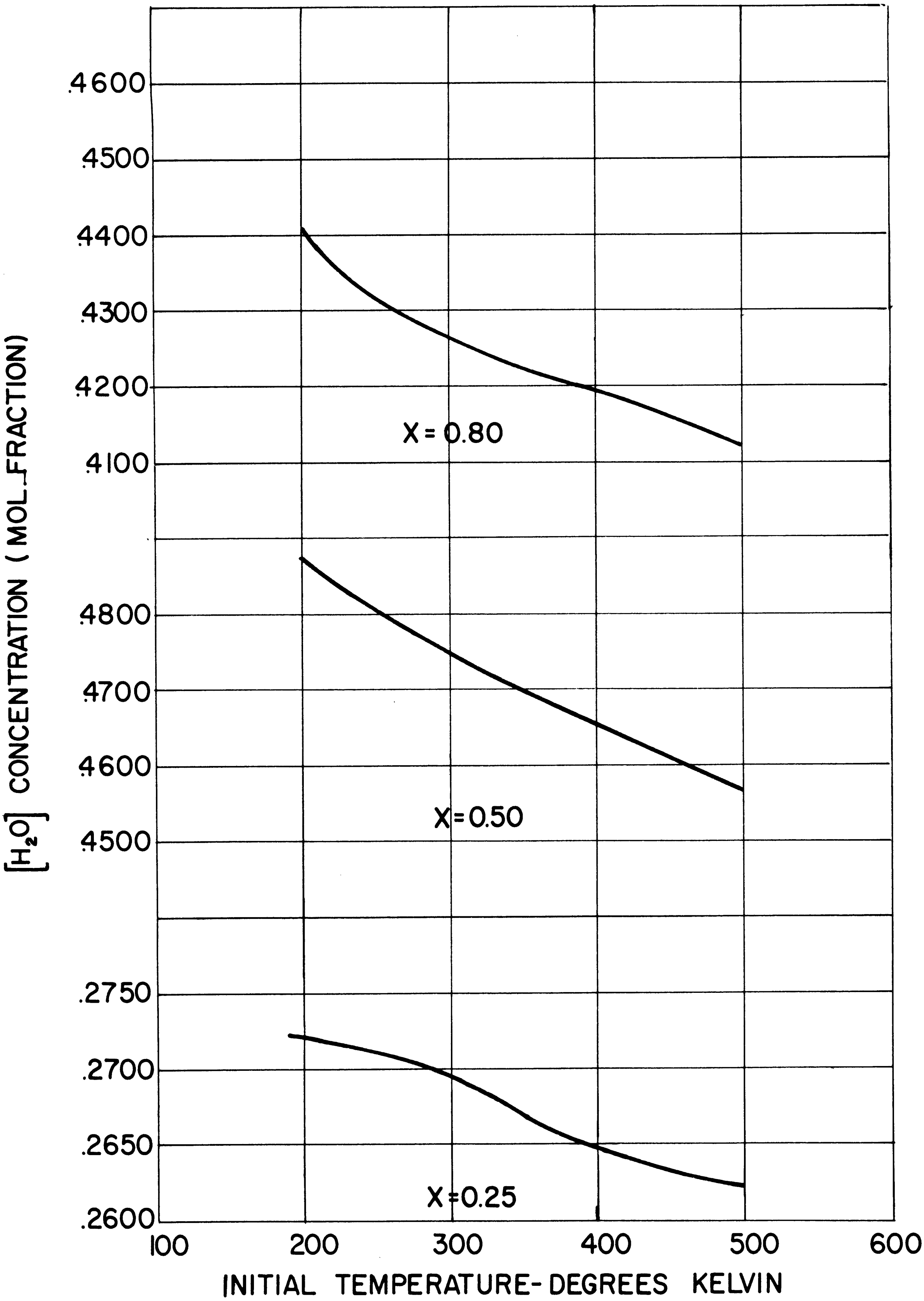

Figure 20. Equilibrium Concentration (H_2O) versus Initial Temperature; X = Initial Mol Fraction Hydrogen

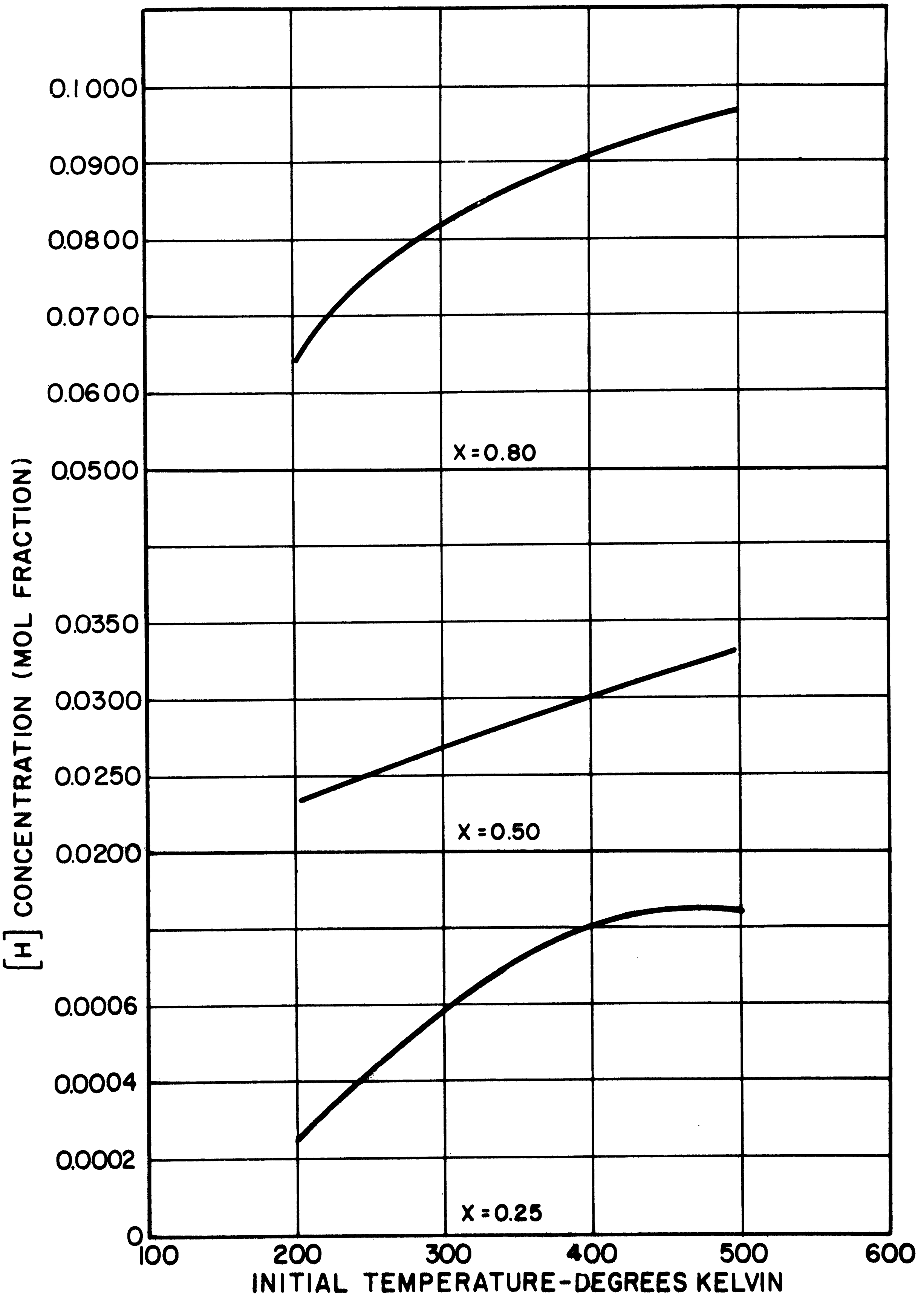

P_1 = 1ATM

Figure 21. Equilibrium Concentration (H) versus Initial Temperature; X=Initial Mol Fraction Hydrogen

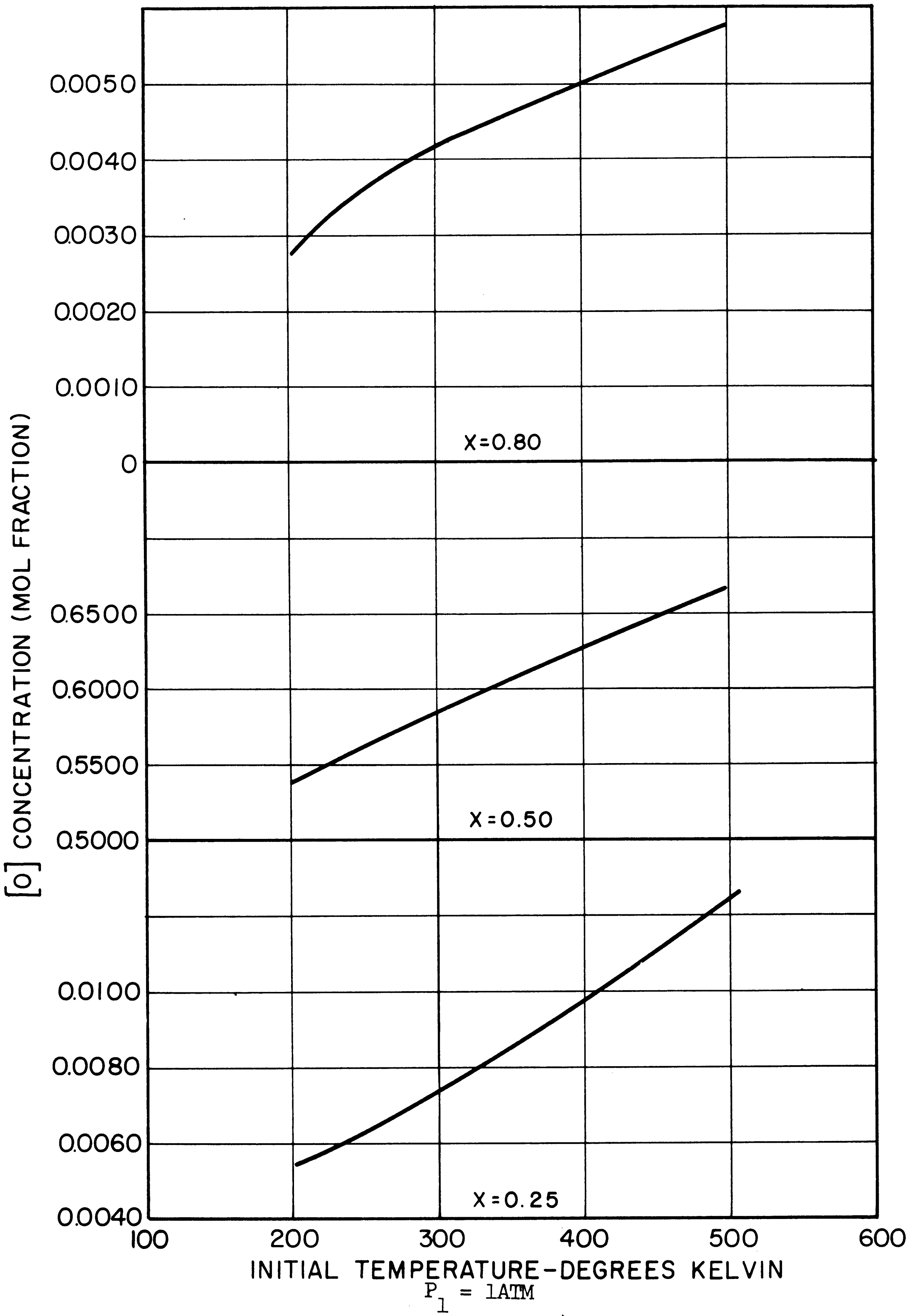

P_1 = 1ATM

Figure 22. Equilibrium Concentration (O) versus Initial Temperature; X = Initial Mol Fraction Hydrogen

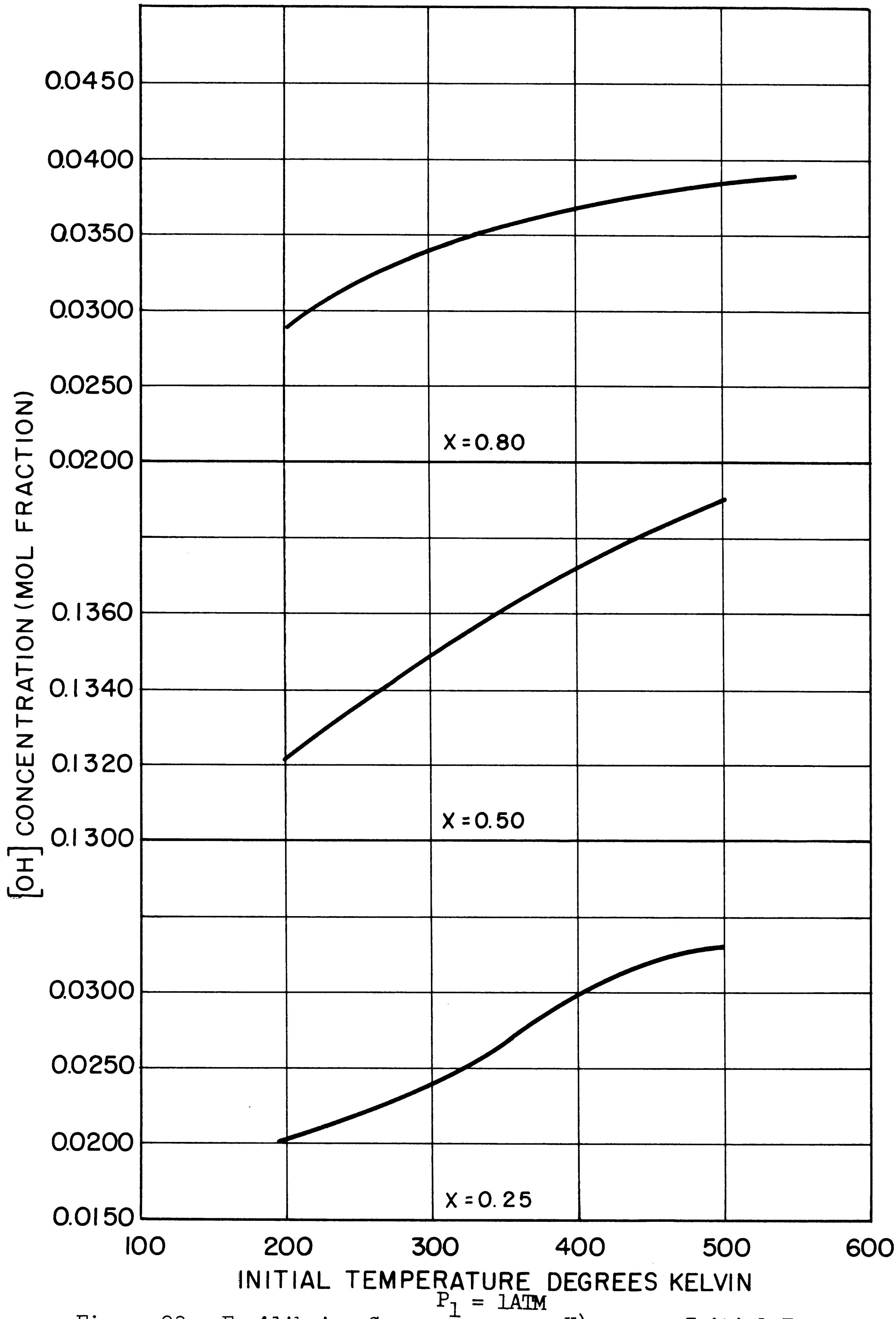

Figure 23. Equilibrium Concentration (OH) versus Initial Temperature; X = Initial Mol Fraction Hydrogen

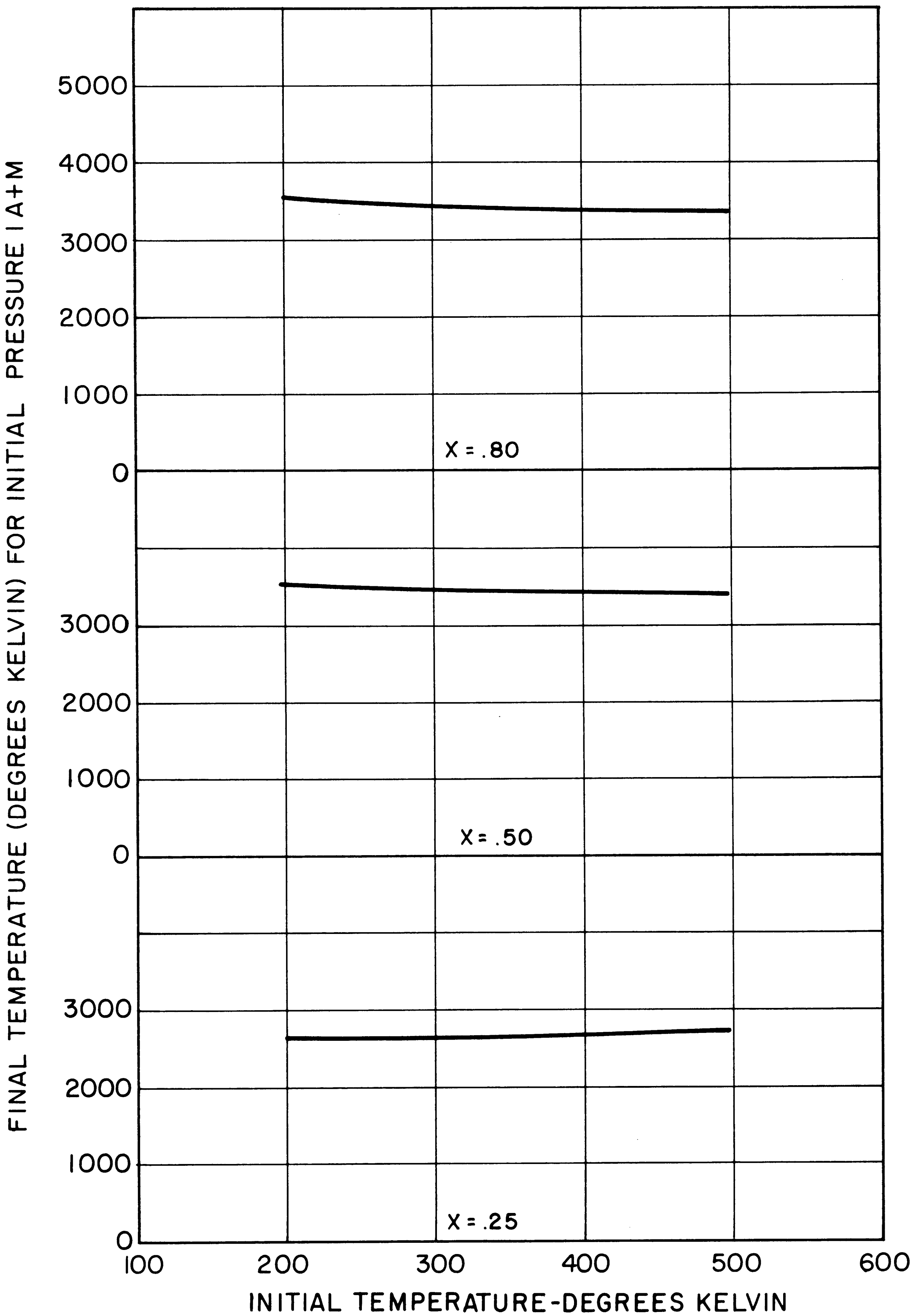

P_1 = 1ATM

Figure 24. Final Temperature versus Initial Temperature

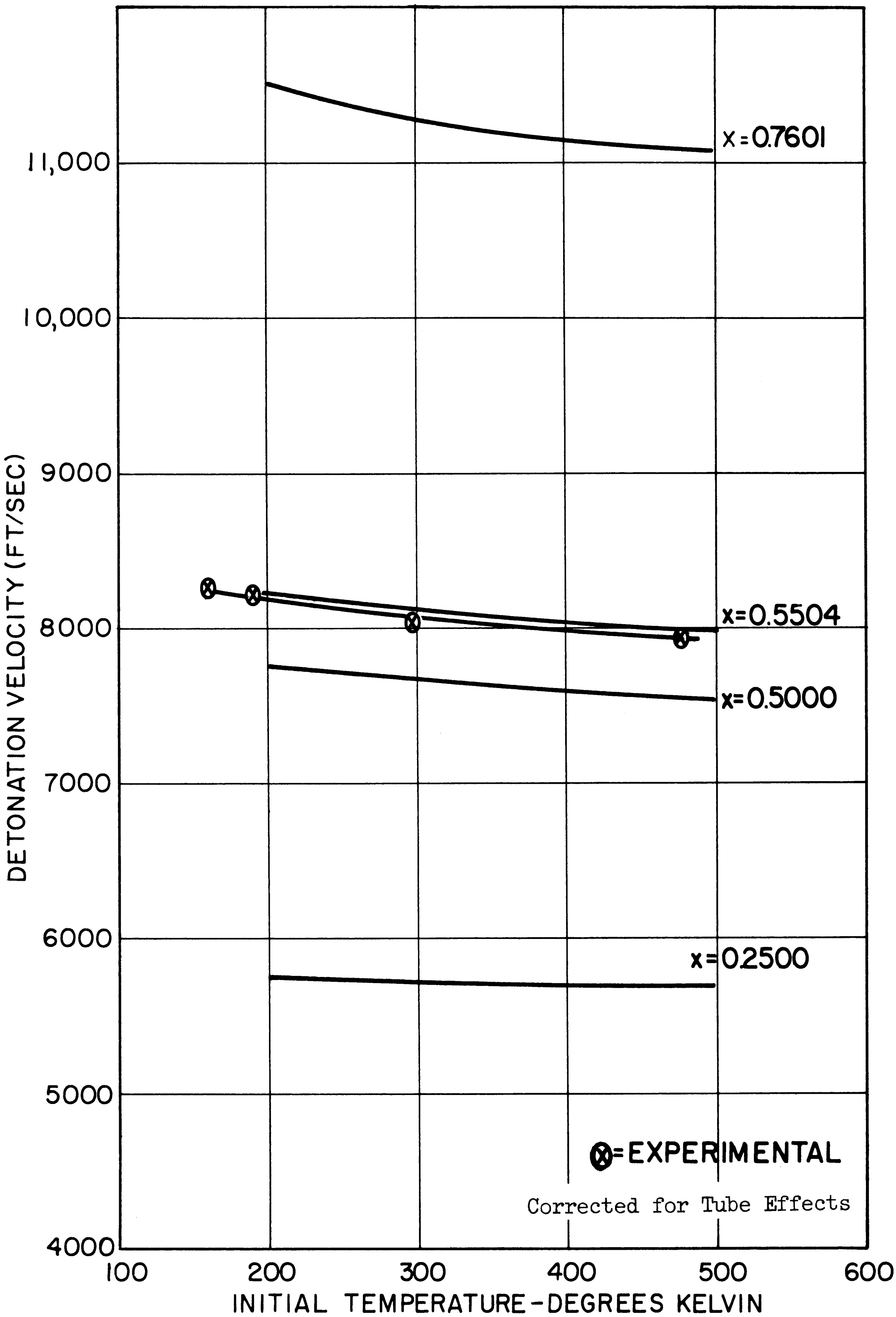

Figure 25. Theoretical Effect of Temperature on the Detonation Velocity

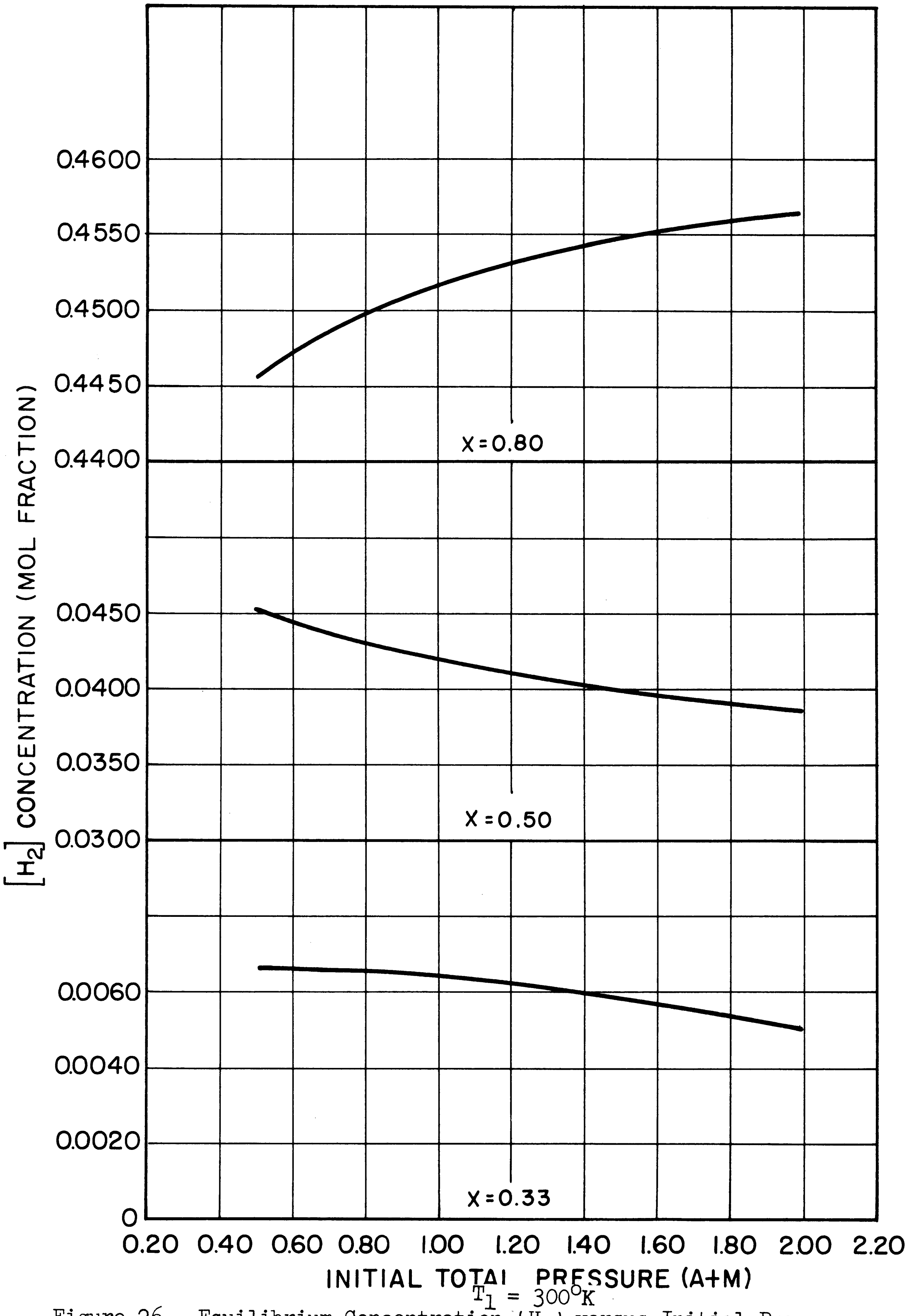

$T_1 = 300^oK$

Figure 26. Equilibrium Concentration (H_2) versus Initial Pressure; X = Initial Mol Fraction Hydrogen

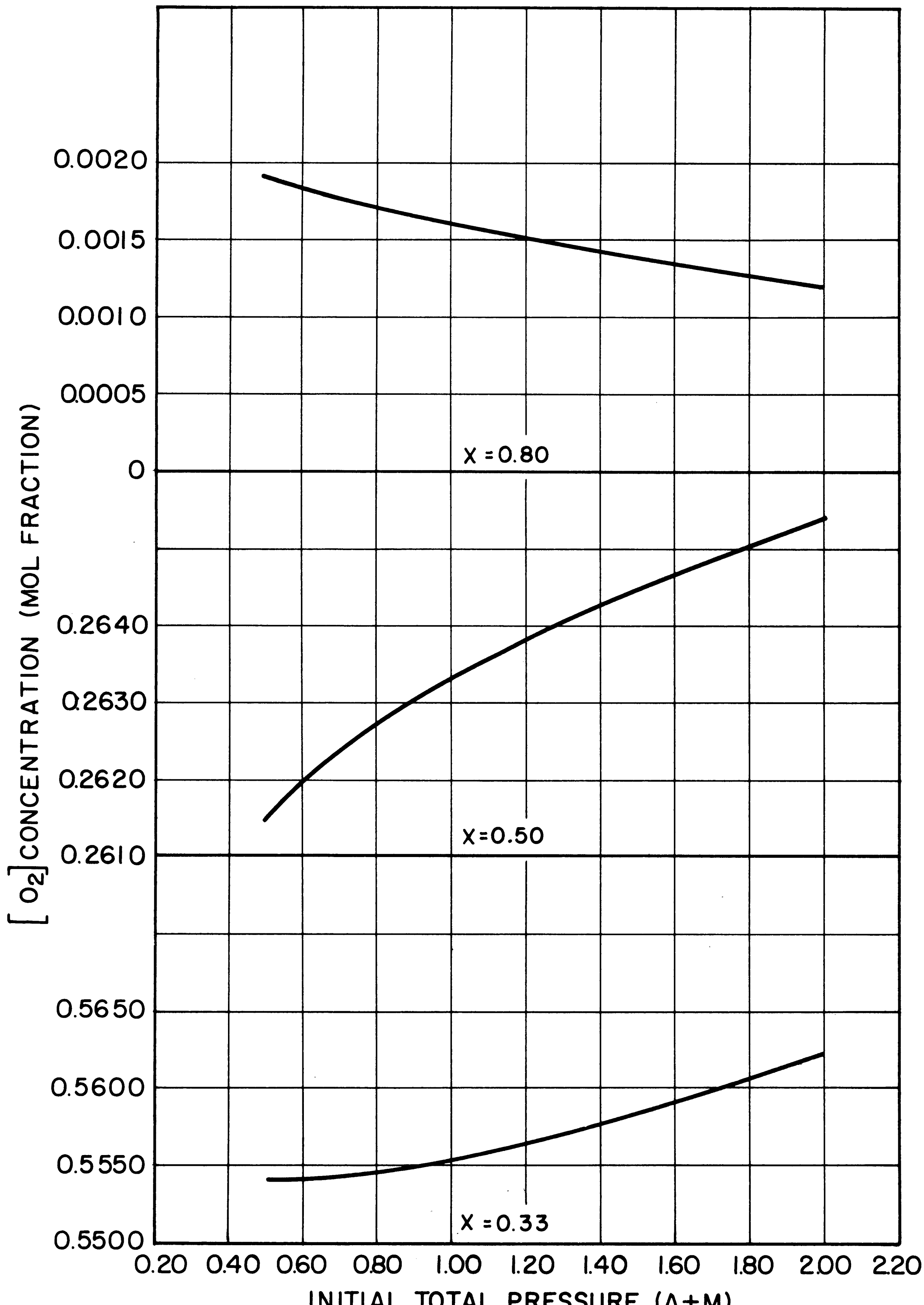

$T_1 = 300°K$

Figure 27. Equilibrium Concentration (O_2) versus Initial Pressure; X = Initial Mol Fraction Hydrogen

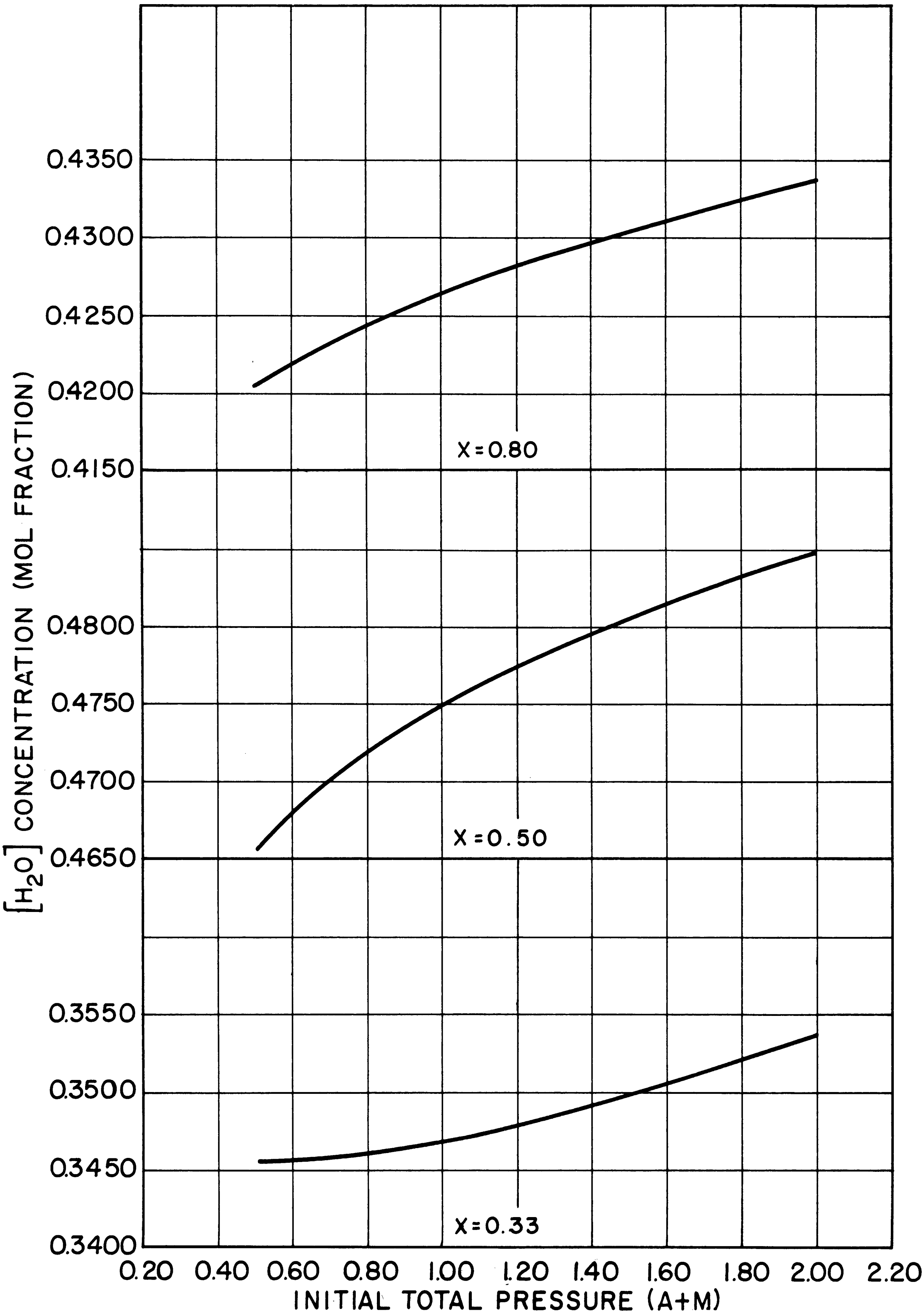

$T_1 = 300^{o}K$

Figure 28. Equilibrium Concentration (H_2O) versus Initial Pressure; X = Initial Mol Fraction Hydrogen

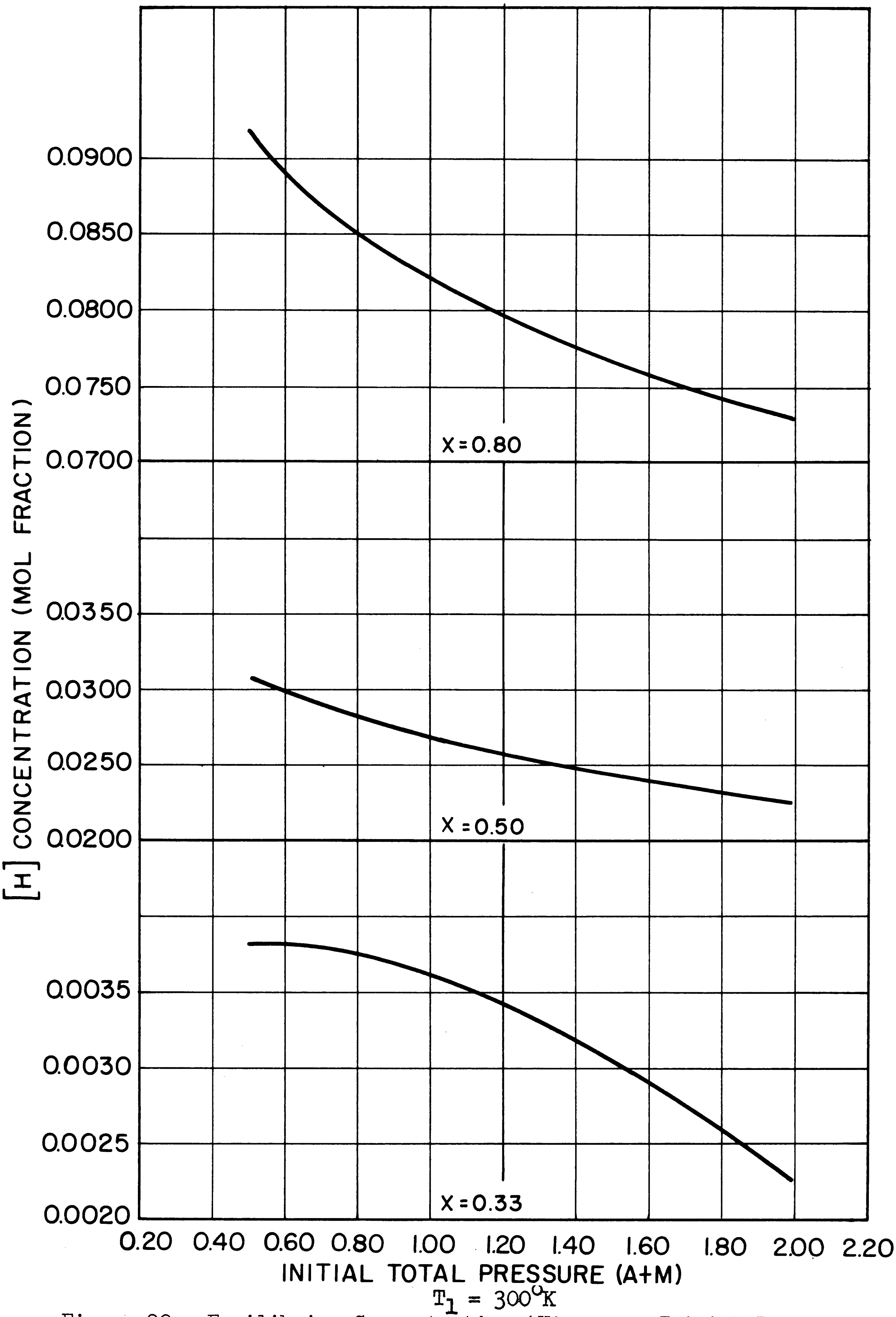

Figure 29. Equilibrium Concentration (H) versus Initial Pressure; X = Initial Mol Fraction Hydrogen

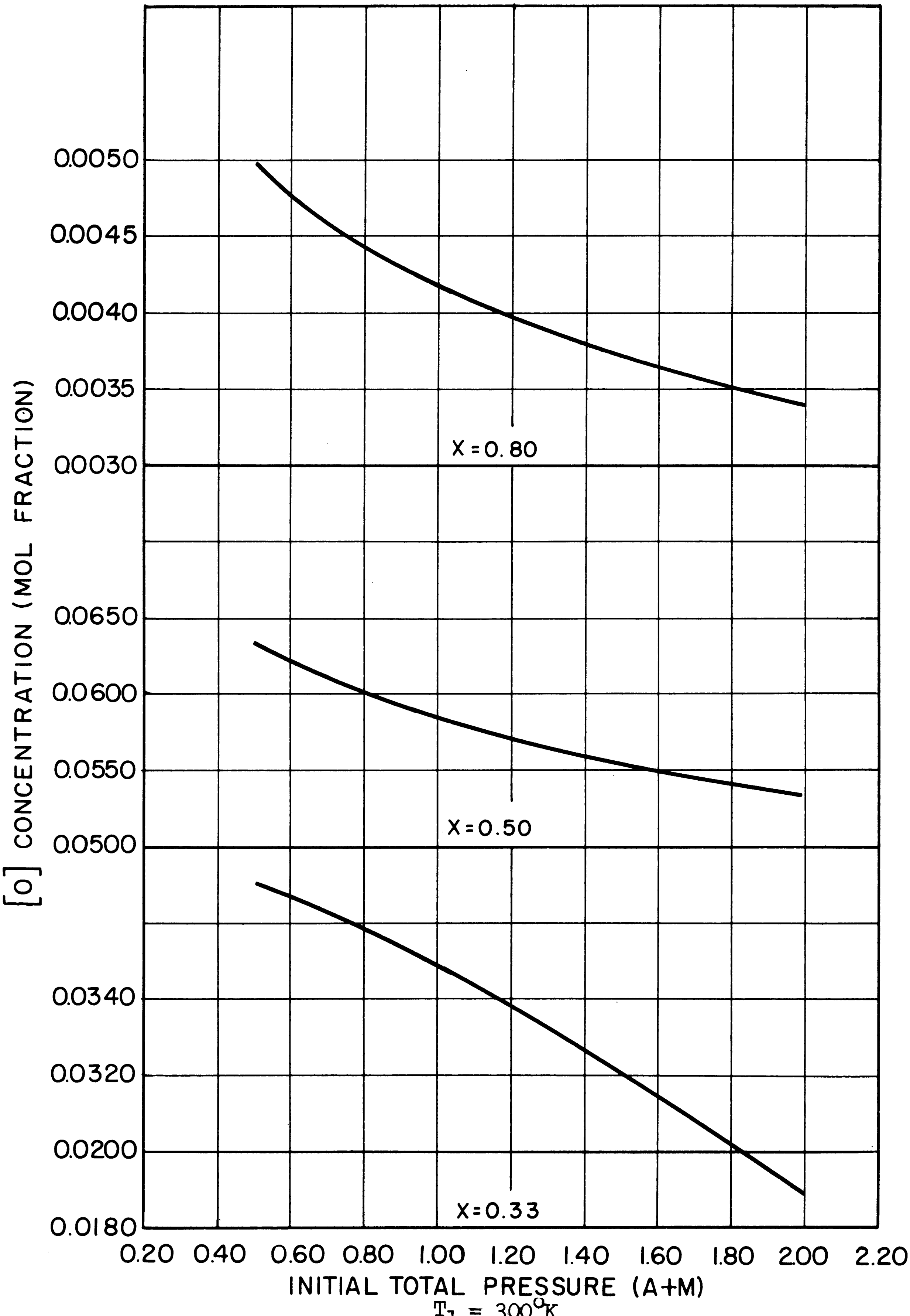

Figure 30. Equilibrium Concentration (O) versus Initial Pressure; X = Initial Mol Fraction Hydrogen

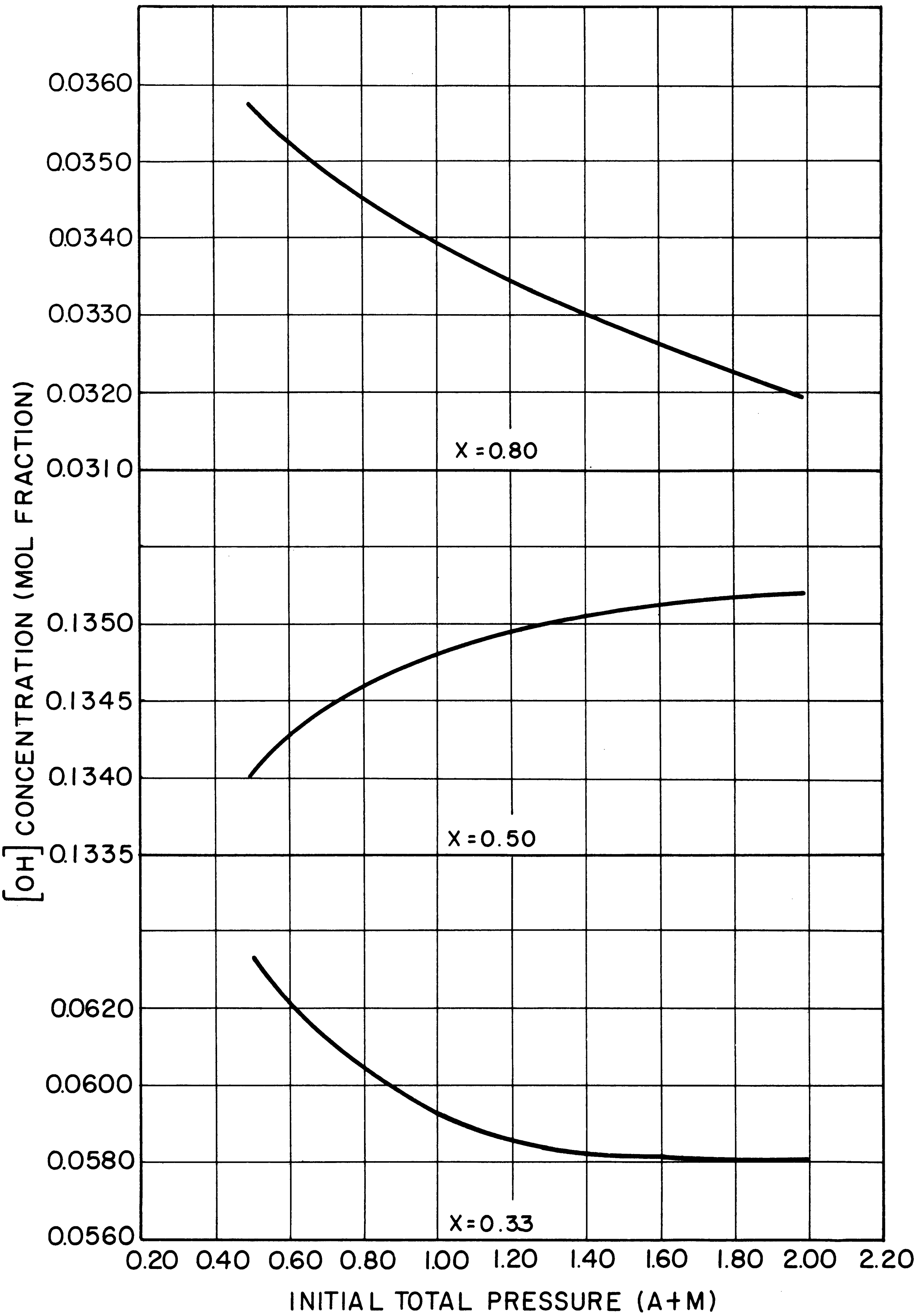

Figure 31. Equilibrium Concentration (OH) versus Initial Pressure; X = Initial Mol Fraction Hydrogen

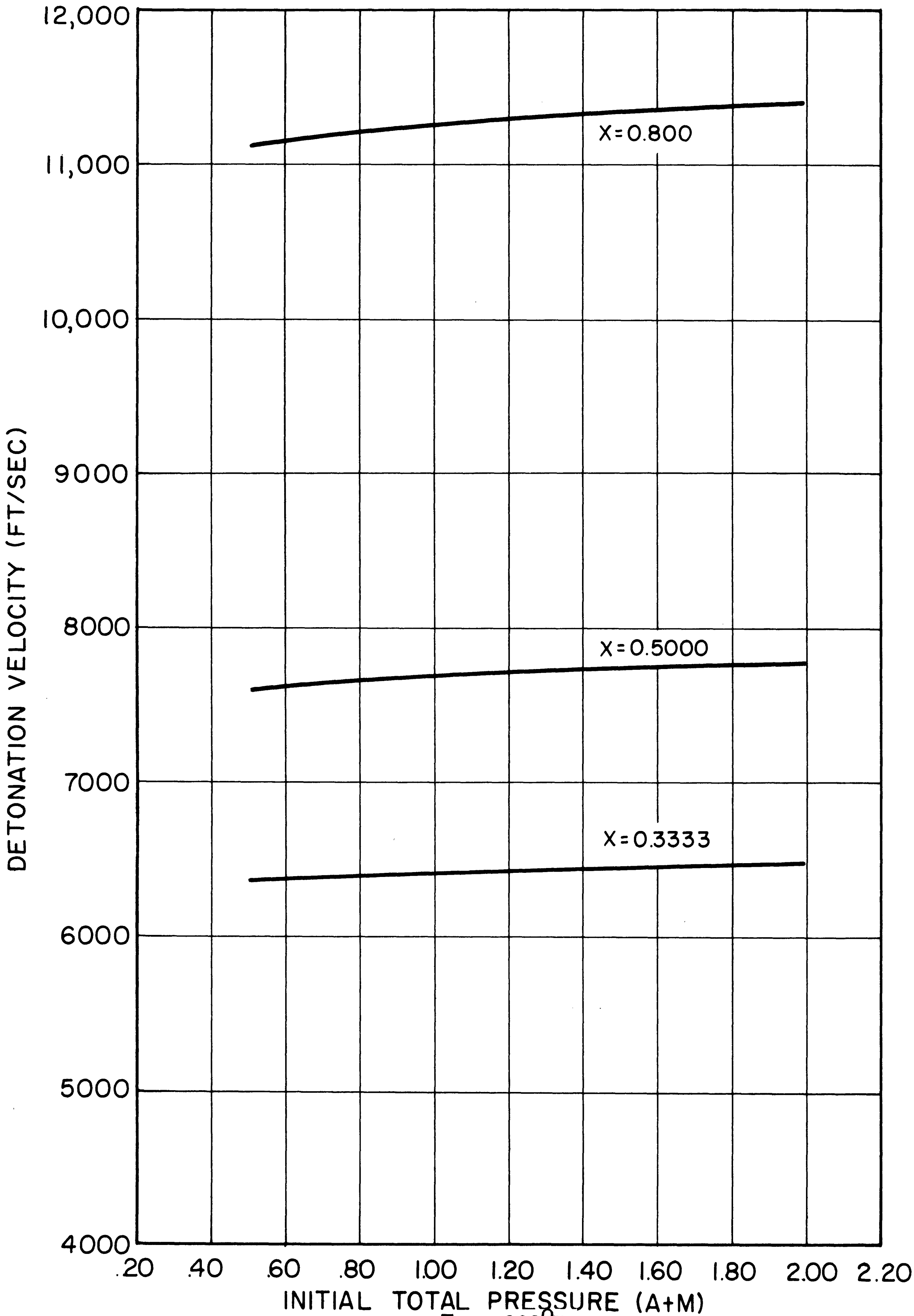

$T_1 = 300^{\circ}K$

Figure 32. Theoretical Effect of Pressure on the Detonation Velocity

Several photographs taken with a vertical knife edge are shown in Figure 33a through f. Figure 33a is a photograph of a 52.50 percent hydrogen 47.50 percent oxygen detonation. The sharp line of demarkation is the detonation wave. Behind the wave a small scale turbulence is noted. Figure 33b is a photograph of a detonation in the same mixture at a slightly shorter time delay. Figure 33c is a photograph of a 39.00 percent hydrogen-oxygen detonation. In this picture the front has begun to thicken. Figure 33d is a photograph of a 28.85 percent hydrogen-oxygen detonation. The front has completely degenerated into a complicated shock pattern followed by an irregular combustion zone. Figures 33e and f are pictures of detonations in the same mixture after the wave has passed out of the test section.

2. Effect of Tube Size on Detonation Velocity

Experimental detonation velocities were obtained at three composition values (34.90 percent hydrogen, 50.00 percent hydrogen, and 66.67 percent hydrogen) in tubes ranging from 0.125 inch to 3.250 inch inside diameter. The experimental data are given in table VIII in Appendix B and are plotted in Figure 34. The characteristics of the tubes are given in table V.

Several sets of data found in the literature were also plotted in Figure 34 for comparison.

3. The Effect of Initial Pressure on Detonation Velocities

During the study of the effect of tube size on the detonation velocity it was noted that the only existing data on the effect of subatmospheric pressure were for stoichiometric mixtures (5, 20). The composition effect was studied by measuring detonation velocities in mixtures over a wide range of composition at pressures between 0.5 and 2.0 atmospheres. The data are included in table VIII

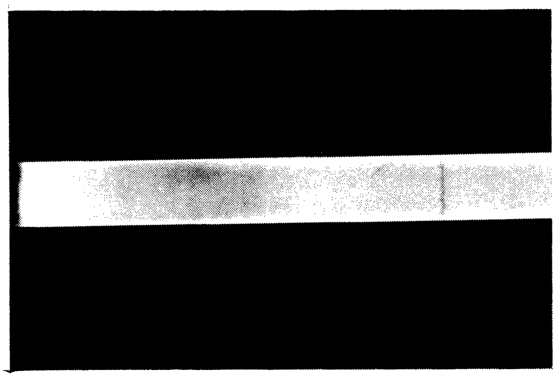

a. 52.50 percent Hydrogen

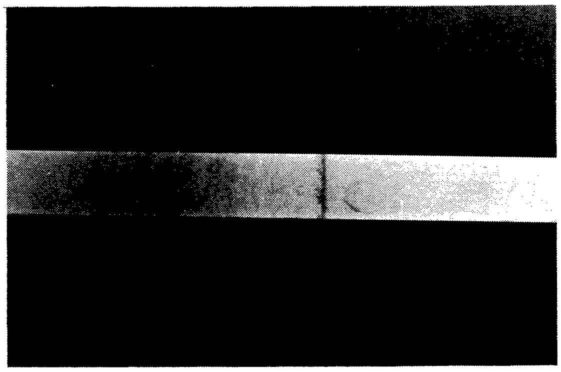

b. 52.50 percent Hydrogen

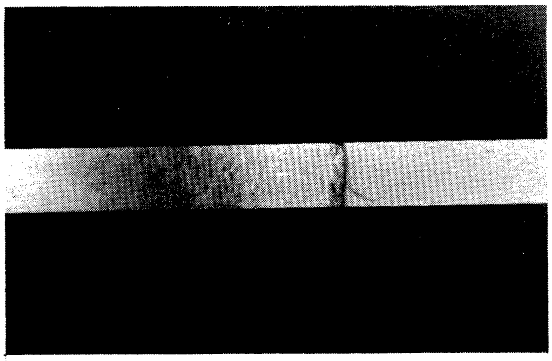

c. 39.00 percent Hydrogen

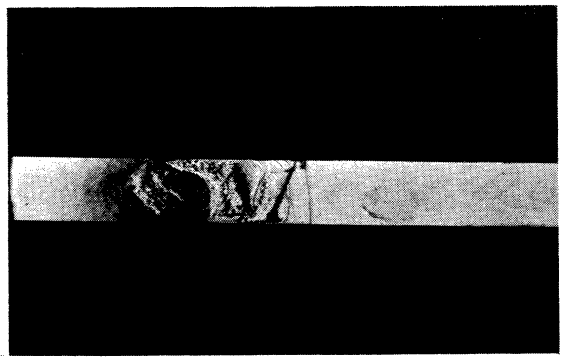

d. 28.75 percent Hydrogen

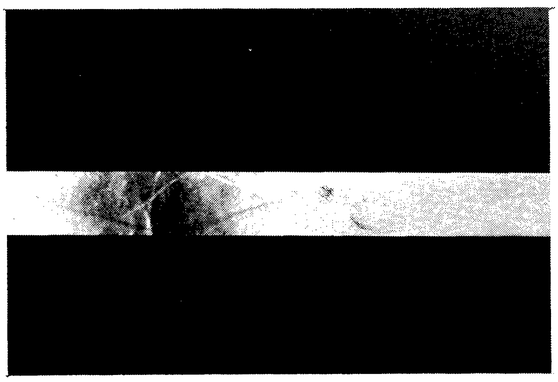

e. 28.75 percent Hydrogen

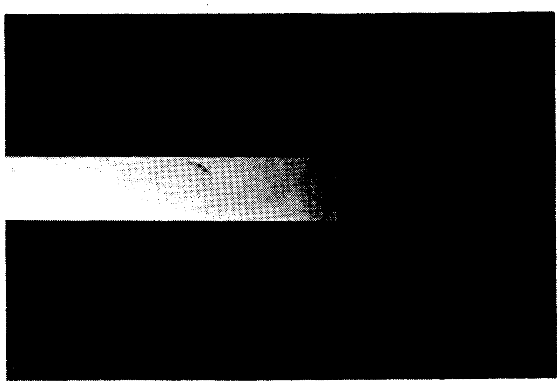

f. 28.75 percent Hydrogen

Figure 33. Spark Schlieren Photograph of the Detonation Wave

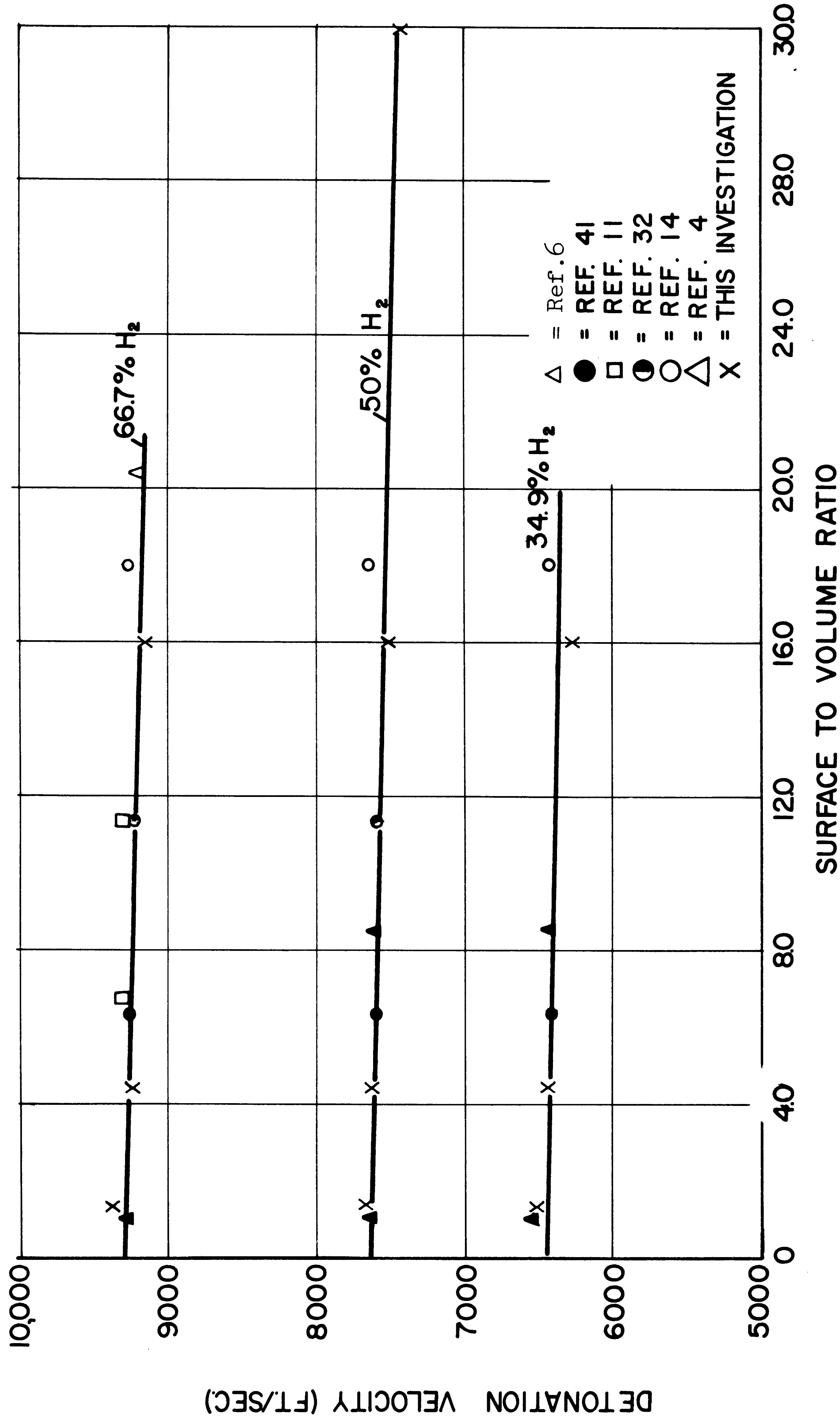

Figure 34. Effect of Tube Size on the Detonation Velocity

in Appendix B and are plotted in Figures 35 and 36. The detonation velocities were measured in the 0.125 inch and the 0.909 inch ID straight tubes.

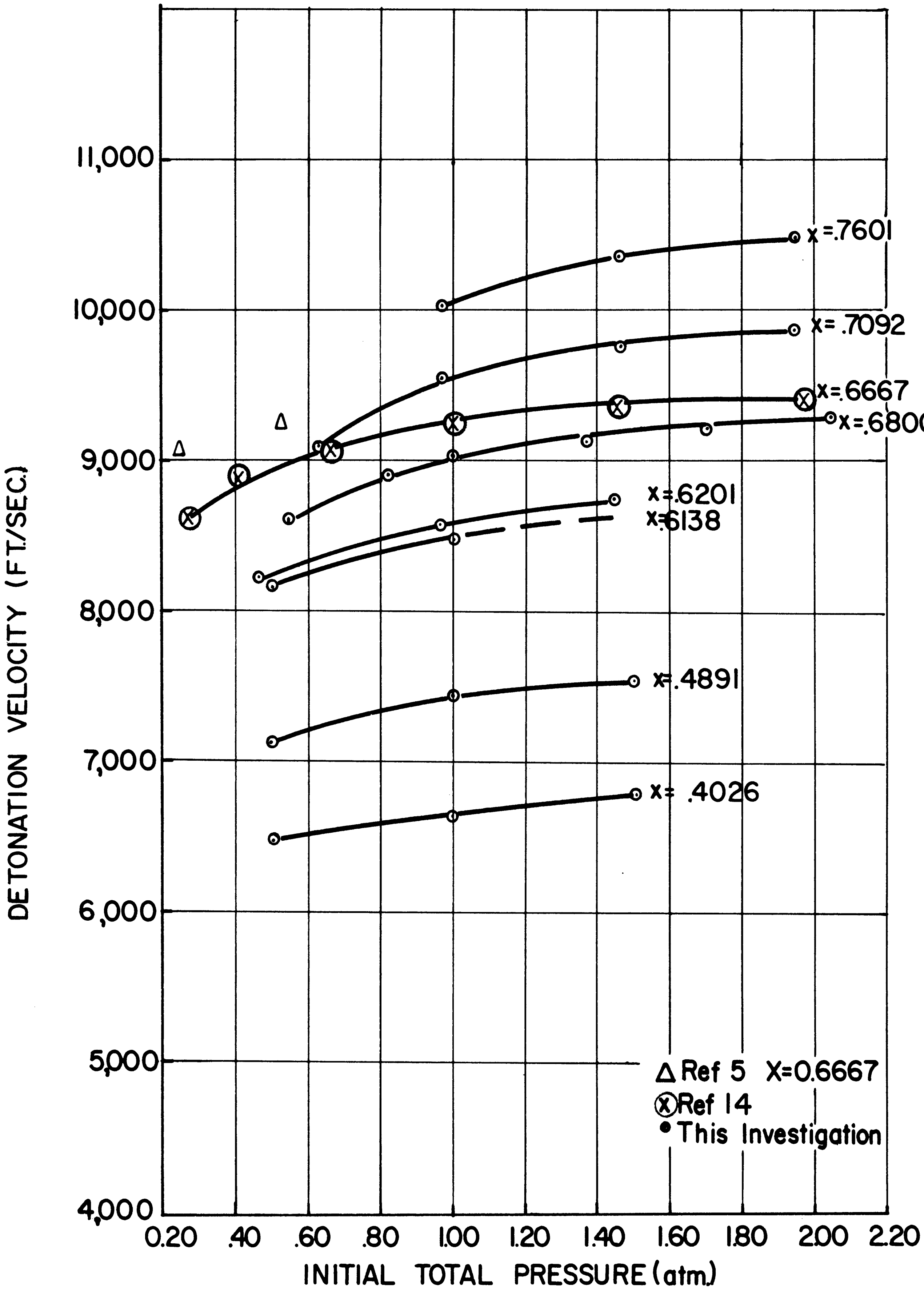

Figure 35. Effect of Initial Pressure on the Detonation Velocity - 0.250 inch Tube

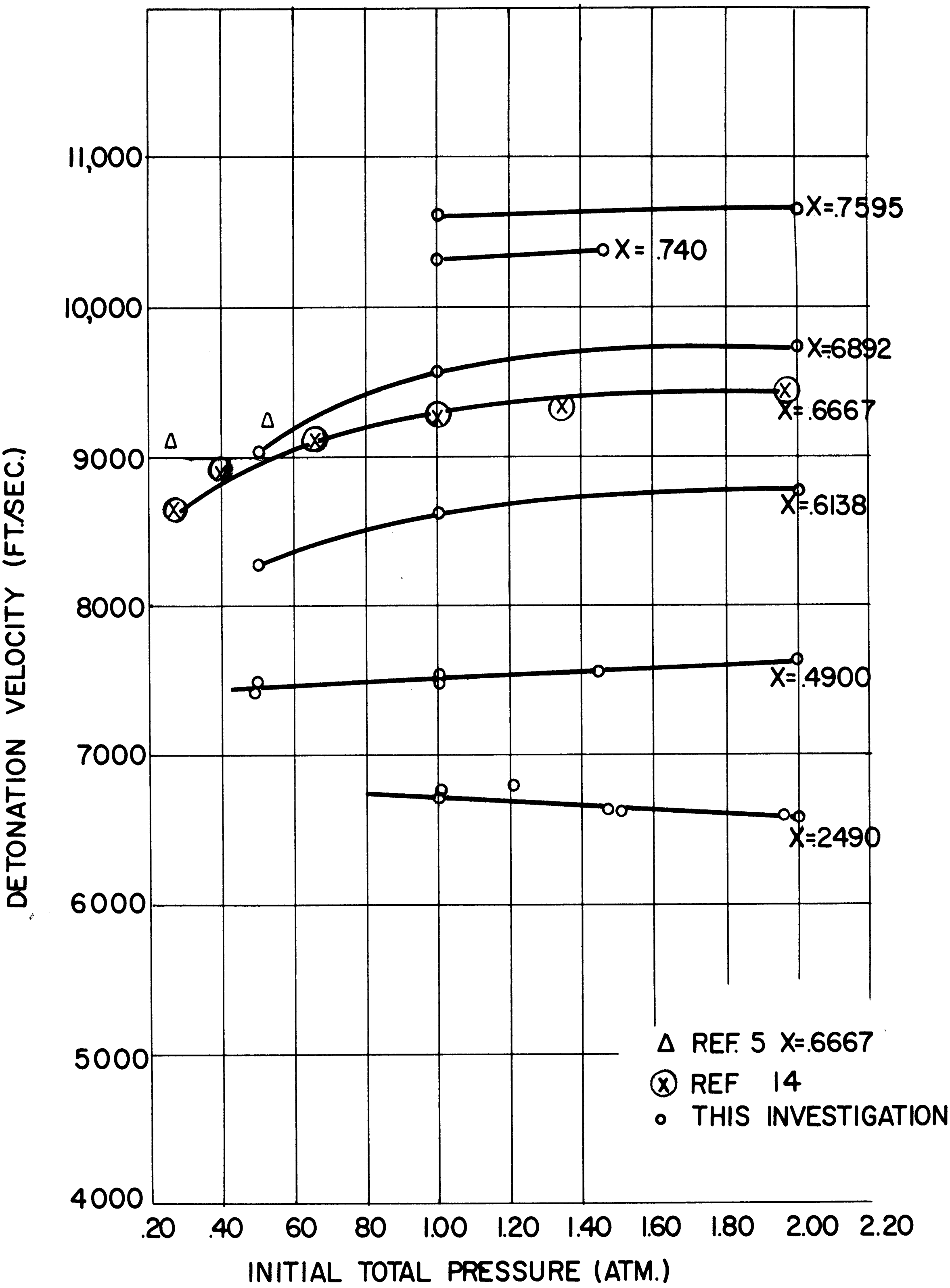

Figure 36. Effect of Initial Pressure Detonation Velocity - 0.909 inch Tube

4. The Effect of Initial Temperature on Detonation Velocity

The main objective of this investigation was the determination of the variation of the detonation velocity with initial temperature. Detonation velocities were measured in mixtures containing 44.70 to 72.06 percent hydrogen over a temperature range from 160 to 480 degrees Kelvin. The experimental data are given in table VIII in Appendix B and are plotted in Figure 37. A slight increase in velocity is noted with decreasing temperature.

5. The Effect of Initial Temperature on Detonation Mach Number

The detonation Mach numbers are plotted versus the initial temperature in Figure 39. The Mach number of a hydrogen-oxygen detonation is not affected appreciably by the hydrogen concentration in the mixture over a large range of composition as shown in Figure 38. Therefore in the plot of Mach number versus temperature, several of the curves for different compositions coincide.

6. The Pressures Developed Behind a Detonation Wave

The pressures developed behind a 55.04 percent hydrogen-oxygen detonation are plotted versus the initial temperature in Figure 40. For an initial pressure of one atmosphere, the pressure developed behind the wave is 470 psia when the initial temperature is maintained at 160 degrees Kelvin while it is 146 psia when the initial temperature is 480 degrees Kelvin.

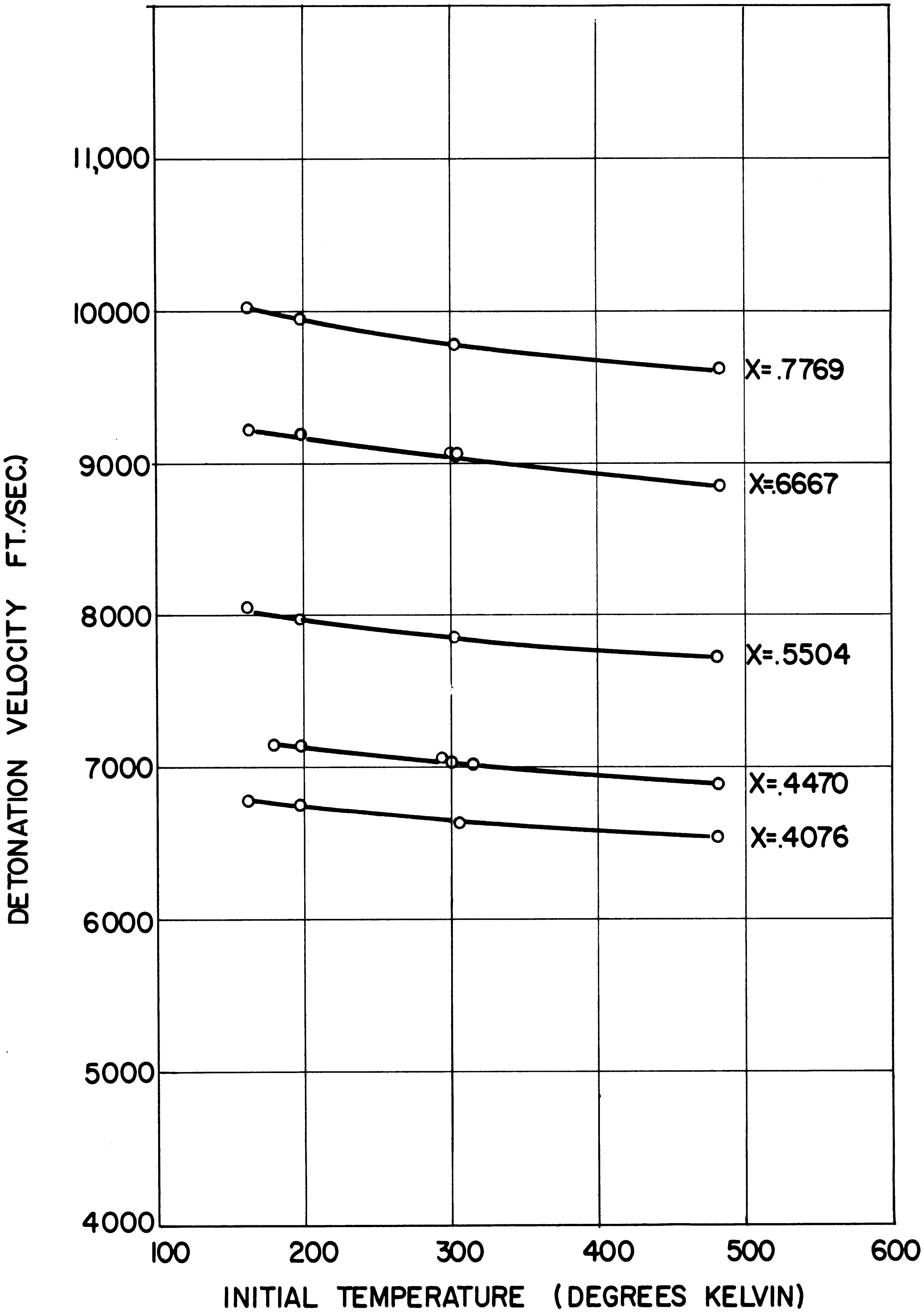

Figure 37. Effect of Initial Temperature on the Detonation Velocity (0.250 inch Coil)

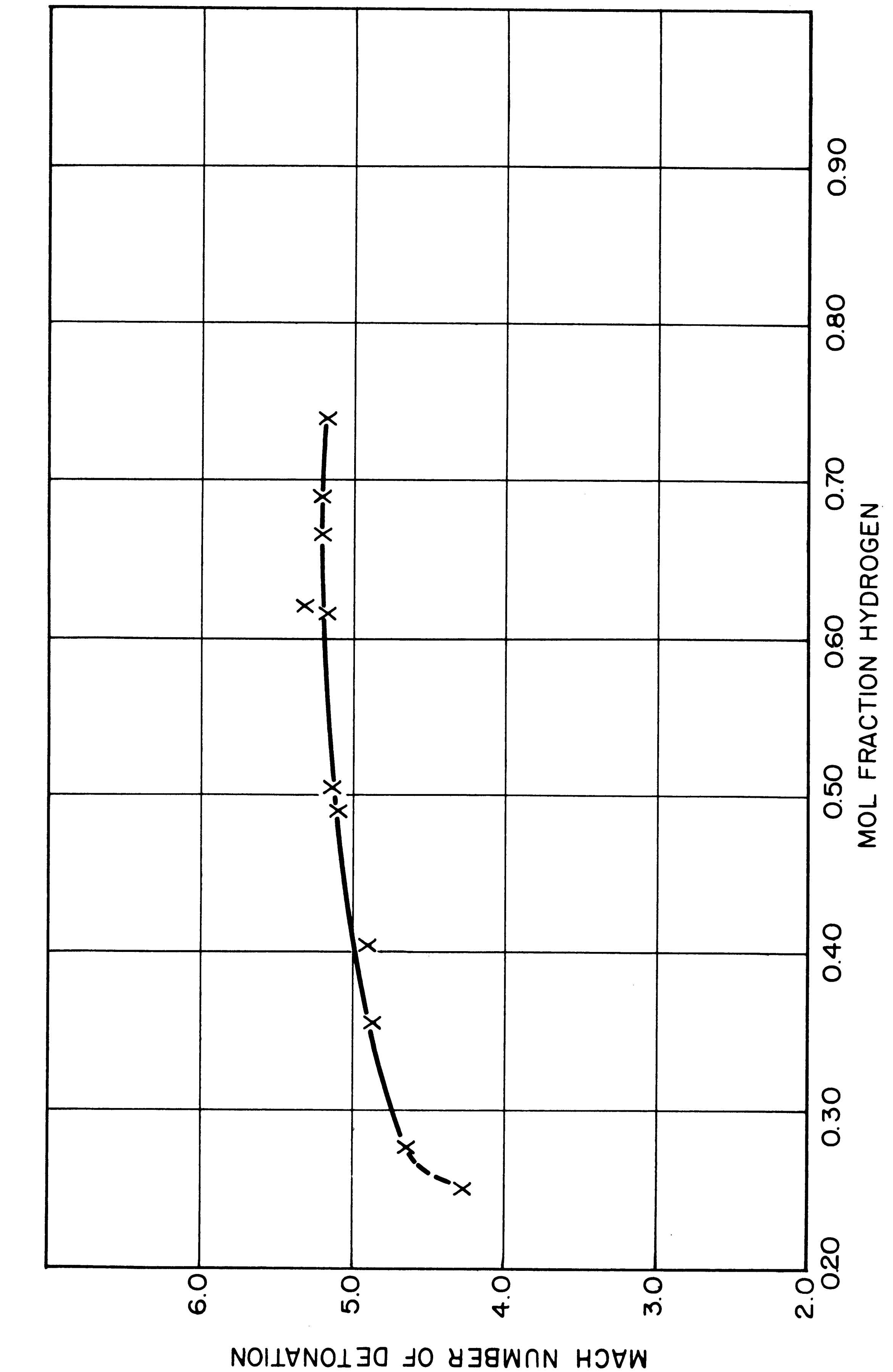

Figure 38. Mach Numbers of Detonation versus Initial Hydrogen Content

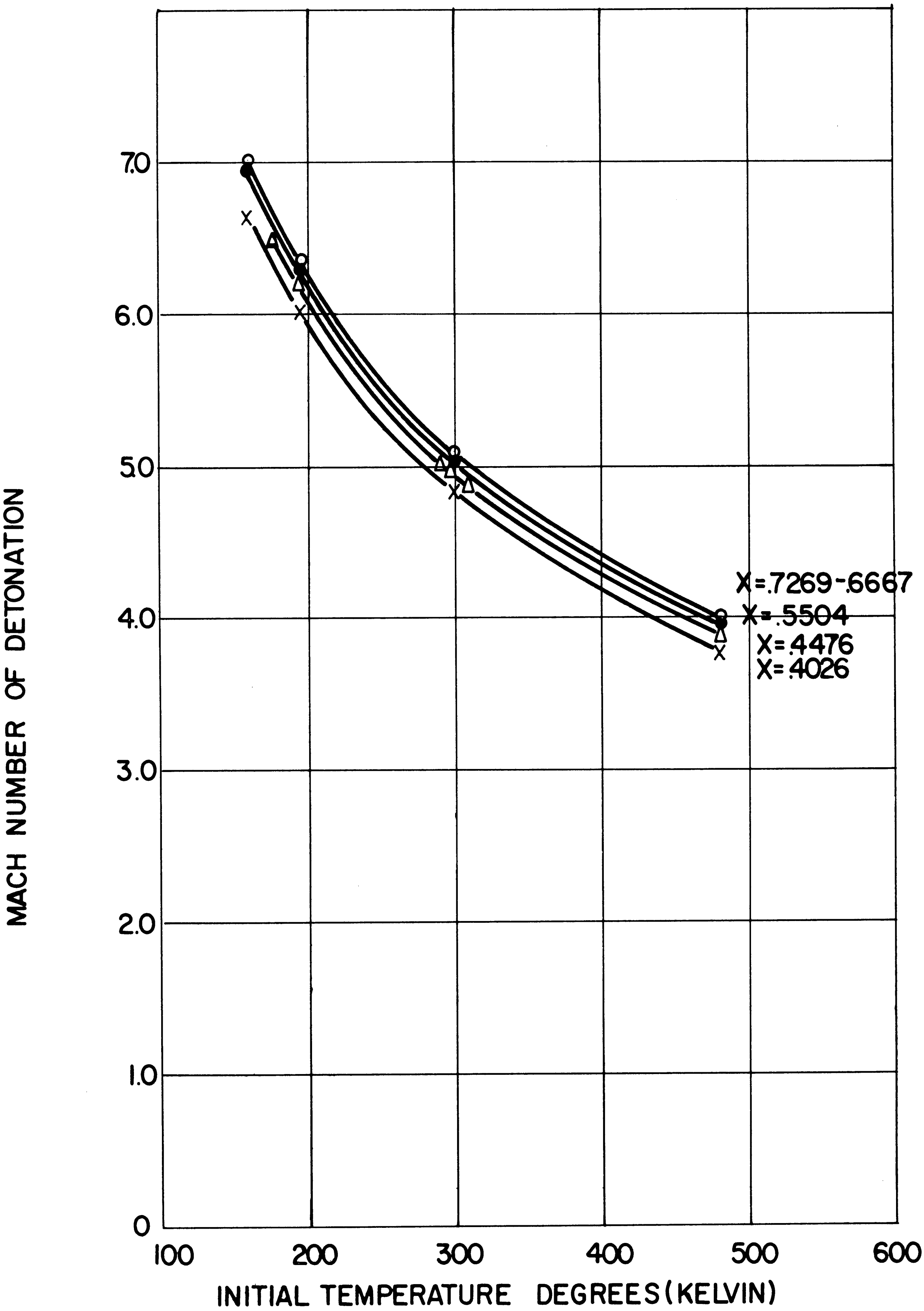

Figure 39. Mach Numbers of Detonation versus Initial Temperature

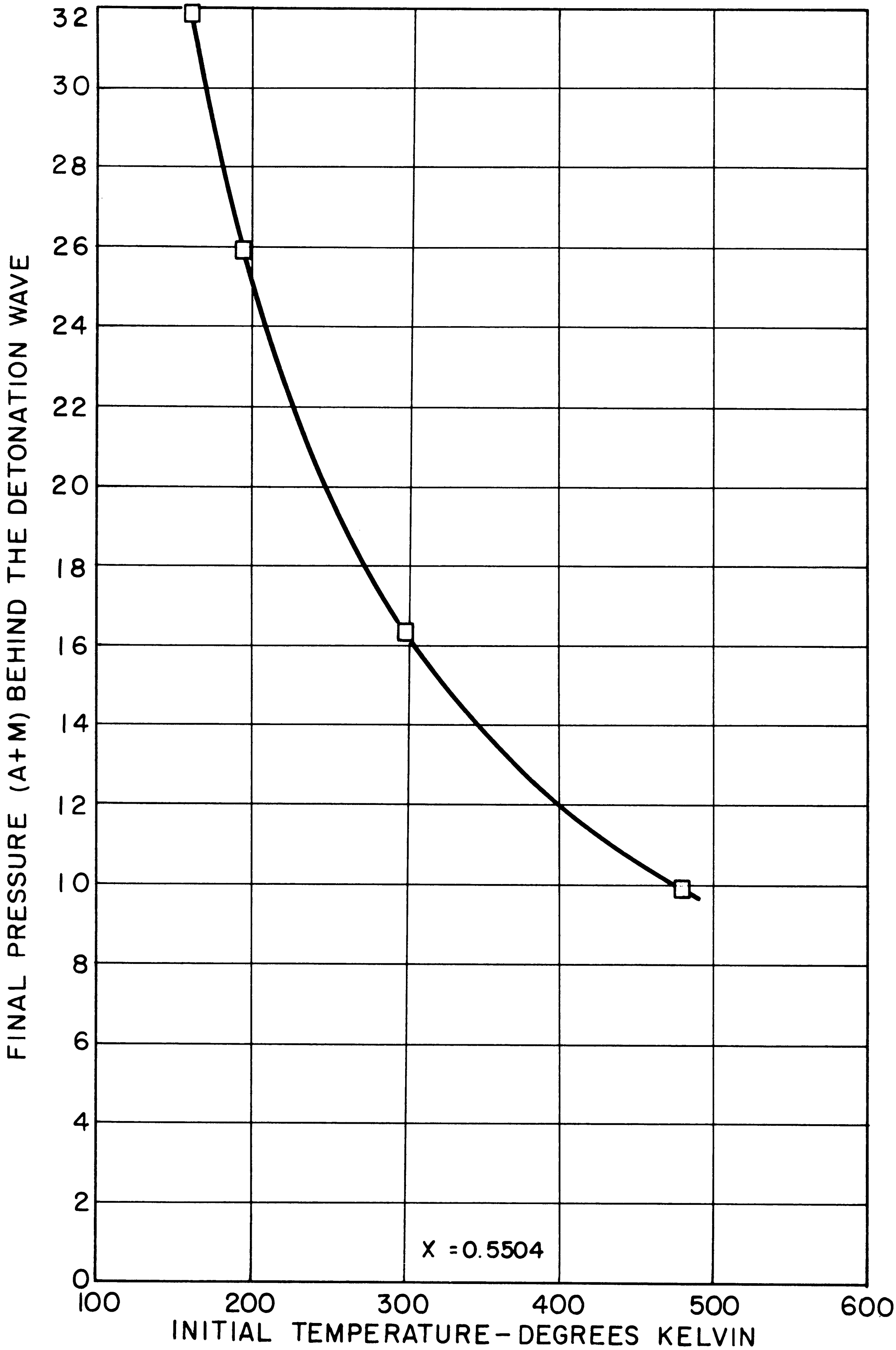

Figure 40. Pressure Developed Behind the Detonation Wave versus Initial Temperature

CHAPTER VII

DISCUSSION

In order to compare the theoretical and experimental values of the detonation velocity, it was necessary to determine the correction for the effect of tube size. Kistiakowsky and Zinman (29) plotted the measured velocity against the reciprocal of the tube diameter and extrapolated linearly to an infinite tube size to obtain the true velocity of detonation. They offer no physical explanation for this extrapolation.

Intuitively, one may conclude that the effect of tube size should diminish as the tube diameter is increased, or conversely, as the surface to volume ratio is decreased. As the surface to volume ratio is decreased the ratio of the energy lost in the degradation processes (heat transfer to the surroundings and skin friction) to the total energy liberated is also decreased. This energy loss is of course responsible for the deficiency in velocity. As the tube diameter approaches infinity, the energy loss per unit volume approaches zero and the measured velocity approaches the true velocity. The functional form of the relationship between tube diameter and velocity of detonation and the interrelation with composition are not known.

For convenience, consider a system in which the detonation wave is stationary and the tube wall moves. The relative magnitudes of the energy losses occurring by heat transfer and skin friction behind the detonation wave can then be evaluated, and insight gained into the functional form of the desired relationship. If the boundary layer developed is assumed to begin directly behind the detonation front and the analysis is restricted to consideration of the plane through the Chapman-Jouguet point, then the detonation velocity moves at a speed of w + a with respect to the fixed tube. If the wave is considered stationary the tube must move at a speed of w + a in the opposite direction i.e. the tube travels at the speed of sound with respect to the gas particles.

The relationship between the heat transfer and the shear stress at the wall is suggested by the analogies proposed by Reynolds, Prandtl and others. The equation recommended by Eckert (16) is for high speed flow.

$$\frac{q_w}{\tau_w} = \frac{\overline{C}_p \ (T_w - T_r)}{U_\infty} \left(\frac{C_p \mu}{k}\right)^{-\frac{2}{3}} \qquad (33)$$

The recovery temperature Tr may be estimated from the relation:

$$T_r = T_\infty + \frac{U_\infty{}^2}{2\ g_c JC_p} \qquad (34)$$

The heat transfer by radiation has been found to be approximately 3% of the total energy liberated and is neglected (9). The velocity which is required in the above equations is the speed of sound with the negative sign. By introducing equation 34 into equation 33 and utilizing the relation $a = (\gamma\ RTg)^{1/2}$ for the speed of sound, equation 33 can be reduced to:

$$q_w = \frac{-C_p T_w P_r{}^{-2/3}}{(\gamma RT_\infty g)^{1/2}} \tau_w + \frac{C_p T_\infty P_r{}^{-2/3}}{(\gamma RT_\infty g)^{1/2}} \tau_w + \frac{(\gamma RT_\infty g)^{1/2} P_r{}^{-2/3}}{2gJ} \tau_w \qquad (35)$$

For the system under investigation, the temperature behind the detonation wave ranged between 2650 and 3650 degrees Kelvin. The maximum value attained by $\overline{C}_p$ was of the order of 1. The Prandtl number is difficult to ascertain since some dissociation products exist in the burned gases. The National Bureau of Standards (37) calculations for the Prandtl number of water indicate a value of approximately 1.0 over the range from 500 to 800 degrees Kelvin. The data given by Drake (16) indicates the Prandtl number approaches 0.8 at 800°K. Using the above values in equation 35 we find that $q_w \approx 0.14\,\tau_w$, or that the heat transfer to the wall is only 14% of the skin friction. This shows that the energy loss due to convection is much less than that due to skin friction. At most the energy loss due to skin friction and heat transfer combined is of the order of $1.2\,\tau_w$. If this energy loss is averaged over the cross section of the tube the expression for the energy loss per unit of cross section is $\frac{1.2\,\tau_w}{R}$, where R is volume of gas per unit area of tube wall. For a round tube R is one quarter of the tube diameter.

The functional relation for the shear stress in turbulent flow over a flat plate is given by Schlicting (47) as

$$\tau_w/\rho u^2 = 0.0296\left[\frac{xu\rho}{\mu}\right]^{-0.2} \qquad (36)$$

τ_w can thus be expressed as a power function of the variables density, viscosity and velocity; but these variables are in turn functions of the hydrogen content or composition of the mixture. The ratio of τ_w minimum to τ_w maximum can be obtained from equation 36:

$$\frac{\tau_w\ \text{min}}{\tau_w\ \text{max}} = \left[\frac{\rho\ \text{min}}{\rho\ \text{max}}\right]^{0.8}\left[\frac{U\ \text{min}}{U\ \text{max}}\right]^{1.8}\left[\frac{\mu\ \text{min}}{\mu\ \text{max}}\right]^{0.8} \qquad (37)$$

By assuming that the viscosity variation with temperature follows the 0.8 power law and introducing maximum and minimum values of the density and velocity in equation, 37, the variation of τ_w is:

$$\tau_w\ \text{min} = 0.71\ \tau_w\ \text{max}.$$

Thus the variation of τ_w over the composition range studied is relatively small.

The variation of the detonation velocity with tube size can be written functionally as:

$$V_D = V_\infty - f(\tau_w/R) \qquad (38)$$

Nothing further can be said concerning the relationship until the data is examined to determine the magnitude of τ_w/R. The experimental velocity values are plotted versus the surface to volume ratio in Figure 34. A number of additional points found in the literature are also plotted in this figure. The experimental results agree quite well except for points taken from Dixon (14). The lower temperature (10°C) of Dixon's data explains this in part.

The effect of tube size is quite small as can be seen by inspection of Figure 34. This means that the magnitude of $\tau w/R$ is small itself and that the variation of τw with composition can be neglected. Thus the curves for the three compositions were drawn parallel. The slope of the curve was found to be 5.7 so that the equation for the detonation velocity becomes:

$$V_D = V_\infty - \frac{22.8}{D} \qquad (39)$$

where D is in inches. The above equation was used to convert the measured detonation velocities to the infinite value.

Although the effect of tube diameter was found to be small, the data of the various investigators were brought into substantially better agreement when the correction was applied.

The experimental detonation velocities, corrected for tube size, are compared with the calculated values in Figure 41. The experimental velocities are generally lower than those computed over the composition range from 20 to 80 percent hydrogen even when the correction was made for tube diameter effects. Beyond these limits the experimental values fall away rapidly from the theoretical curve. The departure from the theoretical curve is not surprising however, in view of the structure of the detonation wave in lean mixtures. Spark schlieren photographs taken of detonation waves (Figure 33) at near stoichiometric mixtures show that the wave form is planar and that combustion takes place in a very narrow region directly behind the front in complete agreement with the model assumed for calculation of detonation characteristics. As the hydrogen concentration is reduced the combustion zone gradually thickens, as shown in the photograph of the 39.00 percent hydrogen detonation. At 28.85 percent hydrogen the wave structure has degenerated into a complicated system of interacting shock waves and turbulent combustion. It is surprising that the theory is valid below 39.00 percent hydrogen where the front begins to broaden.

The theoretical calculations of the detonation characteristics of hydrogen-oxygen mixtures show that the detonation velocity is only slightly affected by variation of either the initial temperature or the initial pressure; they also show that the final temperature behind the detonation wave varies less than five percent when the initial temperature is varied two-hundred fifty percent. This indicates that the variation of the initial energy level of the system was negligible compared with the energy liberated in the reaction and explains why the velocity of detonation is only slightly affected by initial temperature variation.

The theoretical equilibrium concentrations behind the detonation wave were affected slightly by changing the initial pressure and temperature. As the initial hydrogen concentration was increased, at constant pressure and temperature, reaction products containing hydrogen were found to increase to the stoichiometric mixture and then diminish; the oxygen concentration in the product dropped rapidly and approached zero for seventy-five percent hydrogen in the initial mixture. The maximum ion concentration was that of the OH ion which attained a value of 14.50 percent.

The experimental data on the effect of pressure on the detonation velocity indicates that increasing pressure has little effect on detonation velocities above one atmosphere while below one atmosphere there is an appreciable change in velocity with changing pressure. The composition effect is also evident below one atmosphere. Hydrogen rich mixtures show a considerably greater pressure dependence than hydrogen lean mixtures. There appears to be a tube effect associated with the pressure effect however. Velocity measurements obtained in the 0.125 inch tube show a greater pressure dependence than those obtained in the 0.909 inch tube. The experimental data are not sufficiently complete to be conclusive, however, since it was difficult to obtain data below atmospheric pressure in the 0.909 inch tube. The data suggest that a more complete investigation of the effects of initial pressure with different tube sizes is warranted.

The experimental detonation velocity was observed to increase 0.94 ft/sec ^{o}K over the temperature range from 160 to 480 degrees Kelvin. A comparison is made between theoretical and experimental values of the detonation velocity for a 55.04 percent hydrogen mixture in Figure 37; the deviation of the experimental velocities from the theoretical values is less than one percent when corrected for tube effects.

As reported earlier, data obtained in a tube wound into a ten-inch diameter coil were within half of one percent of the data obtained for the same mixtures in a straight tube. The ratio of tube to coil diameter may become a significant parameter (as the ratio becomes large) due to secondary flow phenomena. This problem and the problem of detonation around sharp edged corners of varying angles warrant further investigation.

The detonation Mach numbers plotted in Figure 39 show appreciable variation over the temperature range from 160 to 480 degrees Kelvin. This variation is of considerable interest since the pressure developed behind the detonation wave is directly related to the Mach number as shown by equation A1 in Appendix A. The pressures developed behind a 55.04 percent hydrogen-oxygen detonation are shown in Figure 40. For an initial temperature of 160 degrees Kelvin and initial pressure of 1 atmosphere, the pressure developed is 470 psia. For an initial temperature of 480 degrees Kelvin and an initial pressure of 1 atmosphere it is only 146 psia. It is evident that low initial temperatures promote more violent explosions.

In addition to the pressure developed across the detonation wave, an additional pressure rise occurs when the wave collides with a solid boundary. An analysis of collision phenomena is given in Appendix A. The pressure behind the wave formed in the 160°K mixture would be increased from 470 psia to 1122 psia if it collided with a wall or an elbow in a pipeline.

Although the hydrogen-oxygen system was the subject of this investigation, some of the conclusions are applicable to other combustible gaseous mixtures. Most detonable mixtures, in particular, those containing the hydrocarbons and oxygen are characterized by higher detonation Mach numbers than those containing hydrogen and oxygen, consequently the pressures developed in detonation of these mixtures would be considerably greater than those developed in the hydrogen-oxygen detonation illustrated above.

A knowledge of the pressures developed in detonation are of considerable practical importance to equipment designers as illustrated by the recent disaster at the Standard Oil of Indiana's Fluid Hydroformer Unit at Whiting, Indiana. Other practical utilization of the detonation phenomena include the development of the detonation engine[5] and the determination of thermodynamic properties at elevated temperatures where other techniques are unavailable as suggested by Kistiakowsky[6]. The latter application involves utilization of the experimental detonation velocities in the theoretical equations to back out the thermodynamic properties of the system in the final state. Weir[7] used a similar technique to obtain the equilibrium compositions and temperatures behind the detonation wave. In view of the excellent agreement between theory and experiment found in this investigation, these techniques appear to have considerable justification over a wide range of initial conditions.

---

5 J. Arthur Nicholls, et al. Intermittent Detonation as a Thrust Producing Mechanism. Engineering Research Institute of Univ. of Mich. 1955.

6 George B. Kistiakowsky, Industrial and Engineering News. 33, No. 7 February 14, 1955.

7 Alexander Weir, Jr. and R. B. Morrison, Equilibrium Temperatures and Compositions behind a Detonation Wave, Industrial Engineering Chemistry 46, 1056, 1954.

CHAPTER VIII

CONCLUSION

The velocity of detonation computed by assuming equilibrium and sonic velocity with respect to the burned gases is relatively insensitive to the initial temperature and pressure because the resulting difference in energy is small compared to the heat of reaction. The equilibrium temperature behind a hydrogen-oxygen detonation wave varies only five percent when the initial temperature varies 250 percent. Equilibrium concentrations of OH, H, and H_2O increase and then decrease as the H_2 concentration in the initial mixture is increased to the stoichimetric mixtures and beyond. The maximum ion concentration is that of the OH ion which attains a value of 14.5 percent.

Spark schlieren photographs taken of the detonation wave at near stoichiometric mixtures show that the wave form is planar and combustion takes place in a very narrow region behind the front. As the hydrogen concentration in the mixture is reduced the combustion zone gradually thickens as shown in the photograph of the 39.00 percent hydrogen-oxygen detonation. A photograph of a 28.85 percent hydrogen detonation shows that the wave form has degenerated to a complicated system of interacting shock waves and the combustion zone is spread out over a very non-homogeneous region.

The effect of tube diameter on the detonation velocity was found to be small. However the data of this investigation and that of previous investigators was brought into substantially better agreement when the correction was applied. The effect of tube diameter was found to be invariant with composition; therefore, an expression could be written for the velocity of detonation in terms of the velocity in an infinite tube

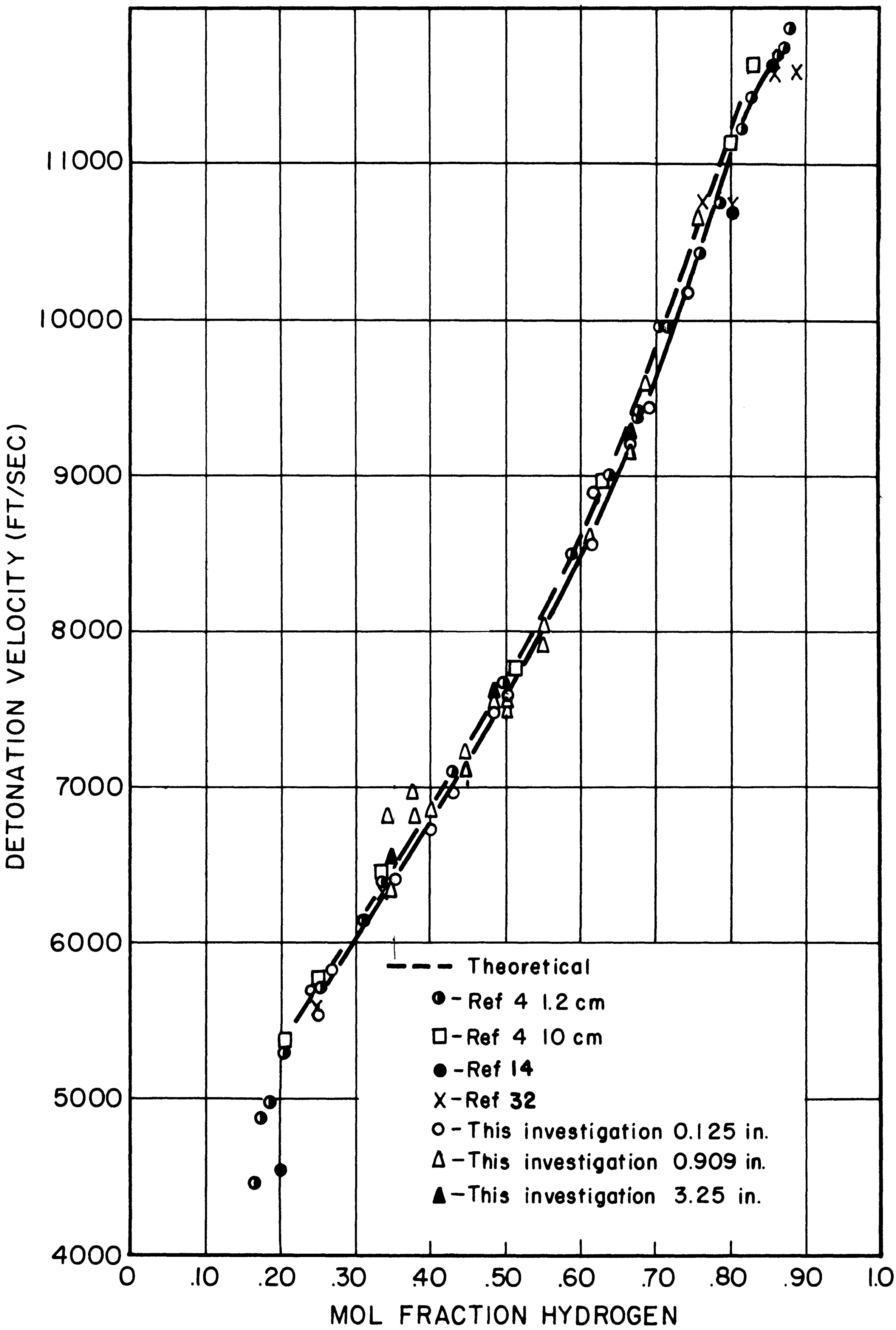

Figure 41. Detonation Velocity versus Hydrogen Content Corrected to Infinite Diameter Tube

and the reciprocal of the tube diameter.

Experimental detonation velocities in hydrogen-oxygen mixtures are slightly lower than theoretical values over the composition range from 20 to 80 percent hydrogen even when corrected for tube diameter effects. Beyond these composition limits the experimental values fall away rapidly from the theoretical curve as shown in Figure 41.

The effect of initial pressure on detonation velocities above one atmosphere was found to be negligible while below one atmosphere an appreciable change in velocity with changing pressure was observed. A composition effect is also evident below one atmosphere. Hydrogen rich mixtures show a considerably greater pressure dependence than hydrogen lean mixtures. As noted above the theoretical pressure dependence was found to be slight at all pressures and the agreement between theoretical and experimental results was therefore poor below one atmosphere pressure. The effect of initial composition was greater than the predicted effect.

The detonation velocity was observed to increase 0.94 ft./sec.$^{\circ}$K. over the temperature range from 160 to 480 degrees Kelvin. The deviation of these velocities from the theoretical values was less than one percent when corrections were applied for tube size.

Mach numbers computed from the measured velocities showed an appreciable change with temperature due to the change of the velocity of sound in the unburned mixture. The pressures computed from the measured velocities were considerably higher for low initial temperatures than for high initial temperatures. Over the temperature range from 160 to 480 degrees Kelvin, the pressure varied approximately three fold- a consideration which should be taken into account in the design of low temperature equipment.

The experimental results and theoretical conclusions thus indicate the range of temperatures, pressures, and compositions over which the hydrodynamic theory of detonation is applicable.

APPENDIX A

DEVELOPMENT OF THE EQUATIONS FOR COLLISION PHENOMENA

DEVELOPMENT OF THE EQUATIONS FOR COLLISION PHENOMENA

There are many types of collision phenomena which have been analyzed (13, 52). The head on collision of a detonation wave with a solid boundary is most interesting from a practical viewpoint. Figure 42 is the characteristic diagram showing the incident detonation wave and the reflected shock wave. The state 0 is the undisturbed gas ahead of the detonation wave and is

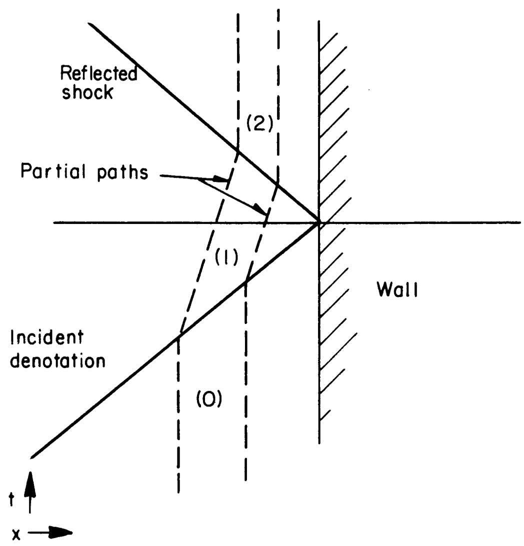

Figure 42. Characteristic Diagram for the Collision of a Wave with a Solid Boundary

characterized by the quantities, $U_o = 0$, ρ_o, P_o, and a_o. State 1 behind the detonation wave is characterized by $U = U_1$, ρ_1, P_1, and a_1 while state behind the reflected shock is characterized by $U = U_2 = 0$, ρ_2, P_2 and a_2. The state values behind the detonation wave may be solved for directly. The pressure ratio is given by:

$$\frac{P_1}{P_o} = \frac{1 + \gamma_2 M_D^2}{1 + \gamma_2} \qquad \text{(A-1)}$$

The pressure ratio across the reflected shock wave may be obtained from the momentum equation for a moving wave:

$$P_2 - P_1 = \rho_1 (U_{rw} - U_1)(U_2 - U_1) \tag{A-2}$$

By factoring P_1 and noting that :

$$a^2 = \frac{\gamma P}{\rho} \tag{A-3}$$

the pressure ratio across the reflect shock becomes:

$$P_2/P_1 = 1 + \left(\frac{U_{rw} - U_1}{a_1}\right)\left(\frac{U_2 - U_1}{a_1}\right) \tag{A-4}$$

or in terms of Mach numbers:

$$P_2/P_1 = 1 + M_{rw} M_{21} \tag{A-5}$$

One of the boundary conditions was that $U_2 = 0$, therefore $M_{21} = -M_1$ and equation A-5 becomes

$$P_2/P_1 = 1 - M_{rw} M_1 \tag{A-6}$$

Equation A-6 may be combined with the equation for the pressure ratio across a shock wave:

$$P_2/P_1 = \frac{2\gamma M_{rw}^2}{\gamma+1} - \frac{\gamma-1}{\gamma+1} \tag{A-7}$$

to yield a solution of M_{rw}:

$$M_{rw} = \frac{\gamma+1}{4} M_1 - \left[1 + \left(\frac{\gamma+1}{4}\right)^2 M_1^{\,2}\right]^{1/2} \tag{A-8}$$

Morrison (52) has solved equation A-8 for the interaction both of shock and detonation waves using the ratio of specific heats as a parameter.

APPENDIX B

EXPERIMENTAL DETONATION VELOCITIES

TABLE VIII.

EXPERIMENTAL DETONATION VELOCITIES

Tube	ID	Type	Tube	ID	Type
A	0.125	Straight	D	0.909	Straight
B	0.250	Straight	E	3.250	Straight
C	0.375	Straight	F	0.125	Coil

Run No.	Mol Fraction Hydrogen	Tube	Total Pressure MM Hg	Temperature °C	Time Micro seconds	Velocity ft/sec
1	0.5165	B	760.0	26.0	403	7441.7
2	0.5165	B	760.0	26.0	403	7441.7
3	0.5160	B	760.0	26.0	403	7441.7
4	0.5160	B	760.0	26.0	403	7441.7
5	0.5160	B	760.0	26.0	404	7423.3
6	0.5160	C	760.0	26.0	265	7548.3
7	0.5160	C	760.0	26.0	268	7463.8
8	0.5160	C	760.0	26.0	266	7519.9
9	0.5160	C	760.0	26.0	266	7519.9
10	0.5160	C	760.0	26.0	266	7519.9
11	0.5160	C	760.0	26.0	266	7519.9

TABLE VIII. (Cont'd.)

12	0.5160	A	760.0	26.0	404	7427.5
13	0.5160	A	760.0	26.0	404	7427.5
14	0.5160	A	760.0	26.0	403	7445.9
15	0.5160	A	760.0	26.0	404	7427.5
16	0.5160	A	760.0	26.0	404	7427.5
17	0.5160	A	760.0	26.0	406	7390.9
18	0.5160	A	760.0	26.0	407	7372.7
19	0.5160	A	760.0	26.0	405	7409.1
20	0.5160	A	760.0	26.0	405	7409.1
21	0.5160	A	760.0	26.0	405	7409.1
22	0.5160	A	760.0	26.0	405	7409.1
23	0.5160	A	760.0	26.0	404	7427.5
24	0.5160	A	760.0	26.0	404	7427.5
25	0.2516	B	760.0	26.0	554	5413.4
26	0.2516	B	760.0	26.0	551	5442.8
27	0.2516	B	760.0	26.0	556	5393.9
28	0.2516	B	760.0	26.0	547	5482.6

TABLE VIII.(Cont'd.)

29	0.2516	B	760.0	26.0	547	5482.6
30	0.4337	B	760.4	24.9	430	6974.4
31	0.4337	B	760.4	24.9	430	6974.4
32	0.4337	B	760.4	24.9	431	6958.2
33	0.4337	B	760.4	24.9	432	6942.1
34	0.4337	B	760.4	24.9	432	6942.1
35	0.4337	B	760.4	24.9	433	6926.1
36	0.4337	B	760.4	24.9	431	6958.2
37	0.4337	B	760.4	24.9	429	6990.7
38	0.4337	B	760.4	24.9	430	6974.4
39	0.4337	B	1110.5	24.9	426	7039.9
40	0.4337	B	1110.5	24.9	426	7039.9
41	0.4337	B	1110.5	24.9	425	7056.5
42	0.4337	B	1110.5	24.9	426	7039.9
43	0.4337	B	370.1	24.9	440	6815.9
44	0.4337	B	370.1	24.9	439	7039.9
45	0.4337	B	370.1	24.9	442	6785.1

TABLE VIII. (Cont'd.)

46	0.4337	B	370.1	24.9	441	6800.4
47	0.4337	B	370.1	24.9	442	6785.1
48	0.6201	B	735.1	24.9	350	8568.6
49	0.6201	B	735.1	24.9	350	8568.6
50	0.6201	B	735.1	23.9	350	8568.6
51	0.6201	B	735.1	24.9	350	8568.6
52	0.6201	B	735.1	24.9	348	8617.8
53	0.6201	B	735.1	24.9	350	8568.6
54	0.6201	B	735.1	24.9	350	8568.6
55	0.6201	B	735.1	24.9	350	8568.6
56	0.6201	B	1104.7	24.9	343	8743.4
57	0.6201	B	1104.7	24.9	343	8743.4
58	0.6201	B	1104.7	24.9	341	8794.7
59	0.6201	B	1104.7	24.9	343	8743.4
60	0.6201	B	1104.7	24.9	342	8769.0
61	0.6201	B	1104.7	24.9	343	8743.4
62	0.6201	B	1104.7	24.9	343	8743.4

TABLE. VIII. (Cont'd.)

63	0.6201	B	351.0	24.9	361	8307.5
64	0.6201	B	351.0	24.9	365	8216.4
65	0.6201	B	351.0	24.9	365	8216.4
66	0.6201	B	351.0	24.9	364	8239.0
67	0.6201	B	351.0	24.9	365	8216.4
68	0.7092	B	738.4	24.9	313	9581.4
69	0.7092	B	738.4	24.9	314	9551.0
70	0.7092	B	738.4	24.9	314	9551.0
71	0.7092	B	738.4	24.9	314	9551.0
72	0.7092	B	738.4	24.9	315	9520.6
73	0.7092	B	1476.8	24.9	304	9865.1
74	0.7092	B	1476.8	24.9	304	9865.1
75	0.7092	B	1476.8	24.9	304	9865.1
76	0.7092	B	1476.8	24.9	302	9930.5
77	0.7092	B	1476.8	24.9	303	9897.8
78	0.7092	B	1107.5	24.9	307	9768.7
79	0.7092	B	1107.5	24.9	308	9737.0
80	0.7092	B	1107.5	24.9	308	9737.0

TABLE VIII.(Cont'd.)

81	0.7092	B	1107.5	24.9	307	9768.7
82	0.7092	B	1107.5	24.9	307	9768.7
83	0.7092	B	1107.5	24.9	308	9737.0
84	0.7092	B	474.2	24.9	328	9143.3
85	0.7092	B	474.2	24.9	324	9256.2
86	0.7092	B	474.2	24.9	327	9171.3
87	0.7092	B	474.2	24.9	330	9088.9
88	0.7092	B	474.2	24.9	333	9006.0
89	0.7092	B	474.2	24.9	333	
90	0.7601	B	1475.8	26.0	286	10486.0
91	0.7601	B	1475.8	26.0	285	10522.8
92	0.7601	B	1475.8	26.0	286	10486.0
93	0.7601	B	1475.8	26.0	286	10486.0
94	0.7601	B	1475.8	26.0	286	10486.0
95	0.7601	B	1475.8	26.0	285	10522.8
96	0.7601	B	1108.0	26.0	289	10377.2
97	0.7601	B	1108.0	26.0	289	10377.2

TABLE VIII.(Cont'd.)

98	0.7601	B	1108.0	26.0	289	10377.2
99	0.7601	B	1108.0	26.0	289	10377.2
100	0.7601	B	1108.0	26.0	289	10377.2
101	0.7601	B	1108.0	26.0	290	10341.4
102	0.7601	B	1108.0	26.0	290	10341.4
103	0.7601	B	1108.0	26.0	290	10341.4
104	0.7601	B	737.9	26.0	299	10030.1
105	0.7601	B	737.9	26.0	298	10063.8
106	0.7601	B	737.9	26.0	301	9963.5
107	0.7601	B	737.9	26.0	297	10097.6
108	0.7601	B	737.9	26.0	301	9963.5
109	0.7601	B	737.9	26.0	298	10063.8
110	0.7601	B	737.9	26.0	301	9963.5
111	0.4888	D	760.0	24.9	534	7480.1
112	0.4888	D	760.0	24.9	533	7494.2
113	0.4888	D	760.0	24.9	533	7494.2
114	0.4888	D	760.0	24.9	534	7480.1

TABLE VIII. (Cont'd.)

115	0.4888	D	760.0	24.9	535	7466.2
116	0.4888	D	1101.6	24.9	528	7565.2
117	0.4888	D	1101.6	24.9	528	7565.2
118	0.4888	D	1101.6	24.9	528	7565.2
119	0.4888	D	1101.6	24.9	528	7565.2
120	0.4888	D	1101.6	24.9	528	7565.2
121	0.4888	D	1101.6	24.9	527	7579.5
122	0.4888	D	1101.6	24.9	400	9986.0
123	0.4888	D	1101.6	24.9	400	9986.0
124	0.4888	D	1101.6	24.9	400	9986.0
125	0.4888	D	1101.6	24.9	400	9986.0
126	0.4888	D	1101.6	24.9	400	9986.0
127	0.4888	B	760.0	24.9	405	7404.9
128	0.4888	B	760.0	24.9	405	7404.9
129	0.4888	B	760.0	24.9	404	7423.3
130	0.4888	B	760.0	24.9	404	7423.3
131	0.4888	B	760.0	24.9	404	7423.3

TABLE VIII.(Cont'd.)

132	0.4888	B	760.0	24.9	406	7386.7
133	0.4888	D	760.0	24.9	-	--
134	0.4888	D	380.0	24.9	559	7145.6
135	0.4888	D	380.0	24.9	549	7275.8
136	0.4888	D	380.0	24.9	-	--
137	0.4888	D	380.0	24.9	-	--
138	0.4888	D	380.0	24.9	544	7342.6
139	0.4888	D	380.0	24.9	503	7941.2
140	0.4888	D	380.0	24.9	534	7480.1
141	0.4888	D	380.0	24.9	537	7438.4
142	0.4888	D	380.0	24.9	554	7210.1
143	0.4888	D	380.0	24.9	508	7863.0
144	0.4888	D	380.0	24.9	542	7369.7
145	0.4888	D	380.0	24.9	553	7223.1
146	0.3553	D	1489.8	24.9	602	6635.2
147	0.3553	D	1489.8	24.9	606	6591.4
148	0.3553	D	1489.8	24.9	608	6569.7

TABLE VIII.(Cont'd.)

149	0.3553	D	1113.8	24.9	606	6591.4
150	0.3553	D	1113.8	24.9	608	6569.7
151	0.3553	D	1113.8	24.9	602	6635.2
152	0.3553	D	1113.8	24.9	603	6624.2
153	0.3553	D	1113.8	24.9	599	6668.4
154	0.3553	B	760.0	24.9	472	6353.8
155	0.3553	B	760.0	24.9	472	6353.8
156	0.3553	B	760.0	24.9	476	6300.4
157	0.3553	B	760.0	24.9	473	6340.4
158	0.3553	B	760.0	24.9	475	6313.7
159	0.3553	B	760.0	24.9	476	6300.4
160	0.3553	D	760.0	24.9	589	6781.7
161	0.3553	D	760.0	24.9	594	6724.6
162	0.3553	D	760.0	24.9	589	6781.7
163	0.3553	D	760.0	24.9	-	--
164	0.3553	D	760.0	24.9	588	6793.2
165	0.7428	D	760.0	24.9	385	10375.1

TABLE VIII. (Cont'd.)

166	0.7428	D	1111.8	24.9	384	10402.1
167	0.7428	D	1111.8	24.9	-	--
168	0.7428	D	1111.8	24.9	-	--
169	0.7428	D	1111.8	24.9	384	10402.1
170	0.7428	D	1111.8	24.9	384	10402.1
171	0.7428	D	760.0	24.9	388	10294.8
172	0.7428	D	760.0	24.9	386	10348.2
173	0.7428	D	760.0	24.9	386	10348.2
174	0.7428	D	760.0	24.9	386	10348.2
175	0.7428	D	760.0	24.9	387	10321.4
176	0.7428	B	760.0	24.9	297	10097.6
177	0.7428	B	760.0	24.9	297	10097.6
178	0.7428	B	760.0	24.9	297	10097.6
179	0.7428	D	380.0	24.9	-	--
180	0.7428	D	380.0	24.9	-	--
181	0.7428	D	704.1	24.9	385	10348.2
182	0.7428	D	704.1	24.9	386	10348.2

TABLE VIII.(Cont'd.)

183	0.4891	D	1520.0	24.9	523	7637.5
184	0.4891	D	1520.0	24.9	523	7637.5
185	0.4891	D	1520.0	24.9	523	7637.5
186	0.4891	D	760.0	24.9	530	7536.6
187	0.4891	D	760.0	24.9	530	7536.6
188	0.4891	D	760.0	24.9	531	7522.4
189	0.4891	D	760.0	24.9	530	7536.6
190	0.4891	D	380.0	24.9	533	7494.2
191	0.4891	D	380.0	24.9	529	7550.9
192	0.4891	D	380.0	24.9	532	7508.3
193	0.4891	D	380.0	24.9	534	7480.1
194	0.4891	D	380.0	24.9	534	7480.1
195	0.4891	B	1140.0	24.9	399	7516.3
196	0.4891	B	1140.0	24.9	-	--
197	0.4891	B	1140.0	24.9	398	7535.2
198	0.4891	B	1140.0	24.9	398	7535.2
199	0.4891	B	1140.0	24.9	398	7535.2

TABLE VIII. (Cont'd.)

200	0.4891	B	1140.0	24.9	398	7535.2
201	0.4891	B	760.0	24.9	403	7441.7
202	0.4891	B	760.0	24.9	403	7441.7
203	0.4891	B	760.0	24.9	404	7423.3
204	0.4891	B	760.0	24.9	403	7441.7
205	0.4891	B	760.0	24.9	403	7441.7
206	0.4891	B	380.0	24.9	422	7106.7
207	0.4891	B	380.0	24.9	422	7106.7
208	0.4891	B	380.0	24.9	421	7123.5
209	0.4891	B	380.0	24.9	420	7140.5
210	0.6138	D	1520.0	24.9	456	8759.6
211	0.6138	D	1520.0	24.9	456	8759.6
212	0.6138	D	1520.0	24.9	-	--
213	0.6138	D	760.0	24.9	463	8627.2
214	0.6138	D	760.0	24.9	464	8608.6
215	0.6138	D	760.0	24.9	465	8590.1
216	0.6138	D	760.0	24.9	464	8608.6

TABLE VIII.(Cont'd.)

217	0.6138	D	760.0	24.9	464	8608.6
218	0.6138	D	380.0	24.9	481	8304.4
219	0.6138	D	380.0	24.9	498	8020.9
220	0.6138	D	380.0	24.9	476	8391.6
221	0.6138	D	380.0	24.9	482	8287.1
222	0.6138	D	380.0	24.9	487	8202.1
223	0.6138	D	380.0	24.9	475	8409.3
224	0.6138	D	380.0	24.9	482	8287.1
225	0.6138	D	380.0	24.9	479	8339.0
226	0.6138	B	760.0	24.9	352	8519.9
227	0.6138	B	760.0	24.9	352	8519.9
228	0.6138	B	760.0	24.9	353	8495.8
229	0.6138	B	760.0	24.9	353	8495.8
230	0.6138	B	760.0	24.9	353	8495.8
231	0.6138	B	760.0	24.9	353	8495.8
232	0.6138	B	380.0	24.9	366	8194.0
233	0.6138	B	380.0	24.9	368	8149.5

TABLE VIII.(Cont'd.)

233	0.6138	B	380.0	24.9	368	8149.5
234	0.6138	B	380.0	24.9	369	8127.4
235	0.6138	B	380.0	24.9	366	8194.0
236	0.6138	B	380.0	24.9	368	8149.5
237	0.6903	D	1520.0	24.9	411	9718.7
238	0.6903	D	1520.0	24.9	411	9718.7
239	0.6903	D	1520.0	24.9	410	9742.4
240	0.6903	D	760.0	24.9	418	9556.0
241	0.6903	D	760.0	24.9	418	9556.0
242	0.6903	D	760.0	24.9	418	9556.0
243	0.6903	D	380.0	24.9	447	8936.0
244	0.6903	D	380.0	24.9	435	9182.5
245	0.6903	D	380.0	24.9	442	9037.1
246	0.6903	D	380.0	24.9	444	8996.4
247	0.6903	D	380.0	24.9	445	8976.2
248	0.6903	D	380.0	24.9	445	8976.2
249	0.6903	D	380.0	24.9	434	9203.7

TABLE VIII. (Cont'd.)

250	0.6903	D	380.0	24.9	448	8916.1
251	0.6903	B	760.0	24.9	327	9171.3
252	0.6903	B	760.0	24.9	323	9284.8
253	0.6903	B	760.0	24.9	323	9284.8
254	0.6903	B	760.0	24.9	320	9371.9
255	0.6903	B	760.0	24.9	320	9371.9
256	0.6903	B	760.0	24.9	321	9342.7
257	0.6903	B	760.0	24.9	320	9371.9
258	0.6903	B	760.0	24.9	320	9371.9
259	0.6903	B	380.0	24.9	334	8979.0
260	0.6903	B	380.0	24.9	342	8769.0
261	0.6903	B	380.0	24.9	333	9006.0
262	0.6903	B	380.0	24.9	334	8979.0
263	0.6903	B	380.0	24.9	335	8952.2
264	0.6903	B	380.0	24.9	334	8979.0
265	0.7840	D	1520.0	24.9	-	--
266	0.7840	D	1520.0	24.9	-	--

TABLE VIII.(Cont'd.)

267	0.3785	D	1520.0	24.9	580	6886.7
268	0.3785	D	1520.0	24.9	578	6910.7
269	0.3785	D	1520.0	24.9	578	6910.7
270	0.3785	D	1520.0	24.9	578	6910.7
271	0.3785	D	760.0	24.9	574	6958.9
272	0.3785	D	760.0	24.9	572	6983.2
273	0.3785	D	760.0	24.9	575	6946.8
274	0.3785	D	760.0	24.9	577	6922.7
275	0.3785	D	760.0	24.9	576	6934.7
276	0.3785	D	760.0	24.9	575	6946.8
277	0.3785	B	1126.0	24.9	439	6831.4
278	0.3785	B	1126.0	24.9	439	6831.4
279	0.3785	B	1126.0	24.9	440	6815.9
280	0.3785	B	1126.0	24.9	439	6831.4
281	0.3785	D	380.3	24.9	-	-
282	0.3785	D	380.3	24.9	577	6922.7
283	0.3785	D	380.3	24.9	559	7145.6

TABLE VIII (Cont'd.)

284	0.3785	D	1519.7	24.9	541	7383.4
285	0.7595	D	1519.7	24.9	-	-
286	0.7595	D	1519.7	24.9	375	10651.7
287	0.7595	D	1519.7	24.9	375	10651.7
288	0.7595	D	1519.7	24.9	375	10651.7
289	0.7595	D	760.0	24.9	378	10651.2
290	0.7595	D	760.0	24.9	370	10795.7
291	0.7595	D	760.0	24.9	-	-
292	0.7595	D	760.0	24.9	371	10766.6
293	0.7595	D	760.0	24.9	374	10680.2
294	0.7595	D	760.0	24.9	380	10511.6
295	0.7595	D	760.0	24.9	390	10011.3
296	0.7595	D	760.0	24.9	381	10484.0
297	0.7595	D	760.0	24.9	372	10737.6
298	0.7595	D	760.0	24.9	372	10737.6
299	0.7595	D	760.0	24.9	371	10766.6
300	0.4026	D	1520.5	24.9	582	6863.2

TABLE VIII.(Cont'd.)

301	0.4026	D	1520.5	24.9	581	6875.0
302	0.4026	D	1520.5	24.9	580	6886.9
303	0.4026	D	1520.5	24.9	581	6875.0
304	0.4026	D	760.3	24.9	573	6971.0
305	0.4026	D	760.3	24.9	579	6898.8
306	0.4026	D	760.3	24.9	586	6816.4
307	0.4026	D	760.3	24.9	593	6735.9
308	0.4026	D	760.3	24.9	583	6851.5
309	0.4026	D	760.3	24.9	596	6702.0
310	0.4026	D	760.3	24.9	-	-
311	0.4026	D	760.3	24.9	-	-
312	0.4026	B	1140.0	24.9	441	6800.5
313	0.4026	B	1140.0	24.9	441	6800.5
314	0.4026	B	1140.0	24.9	442	6785.1
315	0.4026	B	1140.0	24.9	441	6800.5
316	0.4026	B	1140.0	24.9	-	-
317	0.4026	B	1140.0	24.9	442	6785.1

TABLE VIII.(Cont'd.)

318	0.4026	B	734.3	24.9	449	6679.3
319	0.4026	B	734.3	24.9	450	6664.4
320	0.4026	B	734.3	24.9	451	6649.7
321	0.4026	B	734.3	24.9	452	6635.0
322	0.4026	B	734.3	24.9	453	6620.3
323	0.4026	B	734.3	24.9	453	6620.3
324	0.4026	B	734.3	24.9	450	6664.4
325	0.4026	B	734.3	24.9	453	6620.3
326	0.4026	B	734.3	24.9	453	6620.3
327	0.4026	B	380.3	24.9	-	-
328	0.4026	B	380.3	24.9	-	-
329	0.4026	B	380.3	24.9	-	-
330	0.4026	B	380.3	24.9	-	-
331	0.4026	B	380.3	24.9	456	6676.8
332	0.4026	B	380.3	24.9	468	6408.1
333	0.4026	B	380.3	24.9	460	6519.6
334	0.4026	B	380.3	24.9	460	6519.6

TABLE VIII.(Cont'd.)

335	0.4026	B	380.3	24.9	461	6505.4
336	0.4026	B	380.3	24.9	463	6477.3
337	0.4026	B	380.3	24.9	466	6435.6
338	0.4026	B	380.3	24.9	466	6435.6
339	0.4026	B	380.3	24.9	464	6463.4
340	0.4026	B	380.3	24.9	464	6463.4
341	0.4026	F	760.0	24.9	1801	6663.0
342	0.4026	F	760.0	24.9	1802	6659.3
343	0.4026	F	760.0	24.9	1801	6663.0
344	0.4026	F	760.0	24.9	1801	6663.0
345	0.4026	B	760.0	24.9	440	6815.9
346	0.4026	B	759.7	24.9	445	6739.3
347	0.6195	B	760.0	24.9	340	8820.6
348	0.6195	B	760.0	24.9	340	8820.6
349	0.6195	B	760.0	24.9	340	8820.6
350	0.6195	B	760.0	24.9	340	8820.6

TABLE VIII. (Cont'd.)

351	0.6195	B	760.0	24.3	340	8820.6
352	0.6195	F	760.0	24.3	1382	8683.1
353	0.6195	F	760.0	24.3	1381	8689.4
354	0.6195	F	760.0	24.3	1381	8689.4
355	0.6195	F	760.0	24.3	1381	8689.4
356	0.6195	F	760.0	24.3	1381	8689.4
357	0.6195	D	761.0	24.3	448	8916.1
358	0.6195	D	761.0	24.3	449	8896.2
359	0.2711	B	1519.5	26.0	528	5679.9
360	0.2711	B	1519.5	26.0	528	5679.9
361	0.2711	B	1519.5	26.0	530	5658.5
362	0.2711	B	1519.5	26.0	528	5679.9
363	0.2711	B	1519.5	26.0	528	5679.9
364	0.2711	B	760.0	26.0	521	5756.2
365	0.2711	B	760.0	26.0	521	5756.2
366	0.2711	B	760.0	26.0	521	5756.2
367	0.2711	D	760.0	26.0	-	-

TABLE VIII. (Cont'd.)

368	0.6678	F	758.0	24.3	1326	9049.8
369	0.6678	F	758.0	24.3	1326	9049.8
370	0.6678	F	758.0	24.3	1326	9049.8
371	0.6678	B	758.0	24.3	327	9171.3
372	0.6678	B	758.0	24.3	328	9143.3
373	0.6678	B	758.0	24.3	328	9143.3
374	0.6678	B	758.0	24.3	329	9143.3
375	0.6678	B	758.0	24.3	328	9115.6
376	0.5026	F	760.5	24.3	1608	7462.7
377	0.5026	F	760.5	24.3	1609	7458.0
378	0.5026	F	760.5	24.3	1607	7467.3
379	0.5026	F	760.5	24.3	1608	7462.7
380	0.5026	B	760.5	24.3	397	7554.2
381	0.5026	B	760.5	24.3	398	7535.2
382	0.5026	B	760.5	24.3	399	7516.3
383	0.5026	B	760.5	24.3	399	7516.3
384	0.5026	B	760.5	24.3	399	7516.3

TABLE VIII. (Cont'd.)

385	0.4470	F	760.0	35.0	1712	7009.3
386	0.4470	F	760.0	35.0	1712	7009.3
387	0.4470	F	760.0	35.0	1712	7009.3
388	0.4470	F	760.0	35.0	1712	7009.3
389	0.4470	F	374.8	35.0	1768	6787.3
390	0.4470	F	374.8	35.0	1782	6734.0
391	0.4470	F	379.6	35.0	1765	6798.9
392	0.4470	F	379.6	35.0	1764	6802.7
393	0.4470	F	379.6	35.0	1753	6845.4
394	0.4470	F	379.6	35.0	1763	6806.6
395	0.4470	F	379.6	35.0	1749	6861.1
396	0.4470	F	379.6	35.0	1765	6798.9
397	0.4470	F	379.6	35.0	1754	6841.5
398	0.4470	F	1520.4	35.0	1676	7159.9
399	0.4470	F	1520.4	35.0	1676	7159.9
400	0.4470	F	1520.4	35.0	1676	7159.9
401	0.4470	F	760.0	180.0	1743	6884.7

TABLE VIII. (Cont'd.)

402	0.4470	F	760.0	180.0	1735	6916.4
403	0.4470	F	760.0	180.0	1735	6916.4
404	0.4470	F	760.0	180.0	1736	6912.4
405	0.4470	F	760.0	180.0	1735	6916.4
406	0.4470	F	760.0	18.89	1698	7067.1
407	0.4470	F	760.0	18.89	1694	7083.8
408	0.4470	F	760.0	18.89	1712	7009.3
409	0.4470	F	760.0	18.89	1710	7017.5
410	0.4470	F	760.0	-98.0	-	-
411	0.4470	F	760.0	-98.0	-	-
412	0.4470	F	760.0	-98.0	1722	6968.6
413	0.4470	F	760.0	18.89	1703	7046.4
414	0.4470	F	760.0	18.89	1701	7054.7
415	0.4470	F	760.0	18.89	1697	7071.3
416	0.4470	F	760.0	18.89	1696	7075.5
417	0.4470	F	760.0	-87.0	1674	7168.5
418	0.6667	F	759.0	24.9	1323	8070.3

TABLE VIII. (Cont'd.)

419	0.6667	F	759.0	24.9	1323	9070.3
420	0.6667	F	759.0	24.9	1318	9104.7
421	0.6667	F	759.0	24.9	1325	9056.6
422	0.6667	F	759.0	24.9	1320	9090.9
423	0.6667	F	759.0	24.9	1326	9049.8
424	0.6667	F	759.0	24.9	1324	9063.4
425	0.6667	F	759.0	24.9	1324	9063.4
426	0.6667	F	760.0	204.0	1351	8882.3
427	0.6667	F	760.0	204.0	1355	8856.1
428	0.6667	F	760.0	204.0	1353	8869.2
429	0.6667	F	760.0	204.0	1354	8862.6
430	0.6667	F	760.0	204.0	1353	8869.2
431	0.6667	F	484.0	204.0	1423	8432.9
432	0.6667	F	484.0	204.0	1409	8516.7
433	0.7507	F	759.5	204.0	1211	9908.3
434	0.7507	F	759.5	204.0	1209	9925.6
435	0.7507	F	759.5	204.0	1208	9933.7

TABLE VIII. (Cont'd.)

436	0.7507	F	759.5	204.0	1207	9942.0
437	0.7507	F	759.5	204.0	1208	9933.8
438	0.5501	F	759.8	204.0	1550	7741.9
439	0.5501	F	759.8	204.0	1553	7727.0
440	0.5501	F	759.8	204.0	1552	7732.0
441	0.5501	F	759.8	204.0	1554	7722.0
442	0.5501	F	759.8	204.0	1554	7722.0
443	0.4521	F	760.1	204.0	1738	6904.5
444	0.4521	F	760.1	204.0	1738	6904.5
445	0.4521	F	760.1	204.0	1742	6888.6
446	0.4521	F	760.1	204.0	1737	6908.4
447	0.4521	F	760.1	204.0	1740	6896.6
448	0.4521	F	760.1	24.9	1712	7009.3
449	0.4521	F	760.1	24.9	1711	7013.4
450	0.4521	F	760.1	24.9	1712	7009.3
451	0.4521	F	706.1	24.9	1712	7009.3
452	0.4521	F	760.1	24.9	1713	7005.6

TABLE VIII. (Cont'd.)

453	0.4521	F	760.1	24.9	1712	7009.3
454	0.4521	F	760.1	24.9	1714	7001.2
455	0.4521	F	760.1	24.9	1712	7009.3
456	0.4521	F	760.1	26.0	1712	7009.3
457	0.3558	F	760.0	26.0	1963	6113.1
458	0.3558	F	760.0	26.0	1977	6069.8
459	0.3558	F	760.0	26.0	2024	5928.9
460	0.3495	F	759.5	25.8	1952	6147.5
461	0.3495	F	759.5	25.8	1948	6160.2
462	0.3495	F	759.5	25.8	1955	6138.1
463	0.3495	F	759.5	25.8	1957	6131.8
464	0.3495	F	759.5	25.8	1955	6138.1
465	0.3495	F	759.5	25.8	1957	6131.8
466	0.3495	F	759.6	22.8	1924	6237.0
467	0.3495	F	759.6	22.8	1924	6237.0
468	0.3495	F	759.6	22.8	1923	6240.2
469	0.3495	F	759.6	22.8	1924	6237.0

TABLE VIII. (Cont'd.)

470	0.3495	F	759.6	22.8	1927	6227.3
471	0.3495	F	759.6	22.8	1925	6233.8
472	0.3495	F	759.6	22.8	1924	6237.0
473	0.4483	F	760.0	26.7	1708	7025.8
474	0.4483	F	760.0	26.7	1709	7021.6
475	0.4483	F	760.0	26.7	1709	7021.6
476	0.4483	F	760.0	26.7	1708	7025.8
477	0.4483	F	760.0	26.7	1709	7021.6
478	0.4483	F	760.0	26.7	1708	7025.8
479	0.4483	F	760.0	27.0	1614	7434.9
480	0.4483	F	760.0	27.0	1613	7439.5
481	0.4483	F	760.0	27.0	1613	7439.5
482	0.4483	F	760.0	27.0	1613	7439.5
483	0.4483	F	760.0	27.0	1612	7444.2
484	0.4483	F	760.0	27.0	1614	7434.9
485	0.4483	F	760.0	27.0	1614	7434.9
486	0.5488	F	760.0	27.0	1535	7817.6

TABLE VIII. (Cont'd.)

487	0.5488	F	760.0	27.0	1535	7817.6
488	0.5488	F	760.0	27.0	1533	7827.8
489	0.5488	F	760.0	27.0	1534	7822.7
490	0.5488	F	760.0	27.0	1535	7817.6
491	0.5488	F	760.0	27.0	1535	7817.6
492	0.3511	F	760.0	27.0	1916	6263.0
493	0.3511	F	760.0	27.0	1905	6299.2
494	0.3511	F	760.0	27.0	1913	6272.9
495	0.3511	F	760.0	27.0	1894	6335.8
496	0.3511	F	760.0	27.0	1901	6312.5
497	0.3511	F	760.0	27.0	1908	6289.3
498	0.3511	F	760.0	27.0	1911	6279.4
499	0.3511	F	760.0	27.0	1903	6305.8
500	0.3511	F	760.0	27.0	1911	6279.4
501	0.3511	F	760.0	27.0	1917	6259.8
502	0.3511	F	760.0	27.0	1903	6305.8
503	0.3511	F	760.0	27.0	1909	6286.0

TABLE VIII. (Cont'd.)

504	0.3511	F	760.0	27.0	1898	6322.4
505	0.3511	F	760.0	27.0	1920	6250.0
506	0.3511	F	760.0	27.0	1923	6240.4
507	0.3511	F	760.0	27.0	1926	6230.5
508	0.6678	F	760.0	27.0	1332	9009.0
509	0.6678	F	760.0	26.7	1333	9002.3
510	0.6678	F	760.0	26.7	1332	9009.0
511	0.6678	F	760.0	26.7	1333	9002.3
512	0.6678	F	760.0	26.7	1333	9002.3
513	0.6678	F	760.0	-74.3	1309	9167.3
514	0.6678	F	760.0	-75.5	1308	9174.3
515	0.6678	F	760.0	-78.0	1306	9188.3
516	0.6678	F	760.0	-78.0	1304	9202.5
517	0.6678	F	760.0	-78.0	1304	9202.5
518	0.6678	F	760.0	-111.5 - 113.2	1300	9230.8
519	0.6678	F	760.0	25.0	1300	9230.8
520	0.6678	F	760.0	25.0	1300	9230.8

TABLE VIII. (Cont'd.)

521	0.5504	F	760.0	25.0	1529	7848.3
522	0.5504	F	760.0	25.0	1527	7858.5
523	0.5504	F	760.0	25.0	1526	7863.7
524	0.5504	F	760.0	25.0	1526	7863.7
525	0.5504	F	760.0	25.0	1526	7863.7
526	0.5504	F	760.0	25.0	1526	7863.7
527	0.5504	F	760.0	-78.0	1501	7994.7
528	0.5504	F	760.0	-78.0	1502	7989.3
529	0.5504	F	760.0	-78.0	1500	8000.0
530	0.5504	F	760.0	-78.0	1501	7994.7
531	0.5504	F	760.0	-103.0	1495	8026.8
532	0.5504	F	760.0	-112.0	1488	8064.5
533	0.5504	F	760.0	-112.0	1489	8059.1
534	0.5504	F	760.0	-112.0	1488	8064.5
535	0.4988	F	760.0	26.7	1609	7458.0
536	0.4988	F	760.0	26.7	1609	7458.0
537	0.4988	F	760.0	26.7	1609	7458.0

TABLE VIII.(Cont'd.)

538	0.4076	F	760.0	27.0	1798	.6674.0
539	0.4076	F	760.0	27.0	1799	6670.4
540	0.4076	F	760.0	27.0	1801	6663.0
541	0.4076	F	760.0	27.0	1806	6644.5
542	0.4076	F	760.0	27.0	1806	6644.5
543	0.4076	F	760.0	27.0	1806	6644.5
544	0.4076	F	760.0	-78.0	1778	6749.2
545	0.4076	F	760.0	-78.0	1776	6756.8
546	0.4076	F	760.0	-78.0	1778	6749.2
547	0.4076	F	760.0	-113.0	1764	6802.7
548	0.4076	F	760.0	-113.0	1770	6779.7
549	0.4076	F	760.0	-113.0	1769	6783.5
550	0.7269	F	760.0	25.6	1228	9772.0
551	0.7269	F	760.0	25.6	1227	9780.0
552	0.7269	F	760.0	25.6	1229	9764.0
553	0.7269	F	760.0	25.6	1230	9756.1
554	0.7269	F	760.0	25.6	1231	9748.2

TABLE VIII. (Cont'd.)

555	0.7269	F	760.0	25.6	1231	9748.2
556	0.7269	F	760.0	25.6	1229	9764.0
557	0.7269	F	760.0	-78.0	1207	9942.0
558	0.7269	F	760.0	-78.0	1206	9950.2
559	0.7269	F	760.0	-78.0	1203	9975.1
560	0.7269	F	760.0	-78.0	1204	9966.8
561	0.7269	F	760.0	26.7	1227	9780.0
562	0.7269	F	760.0	26.7	1227	9780.0
563	0.7269	F	760.0	26.7	1224	9803.9
564	0.7269	F	760.0	26.7	1228	9772.0
565	0.7269	F	760.0	26.7	1228	9772.0
566	0.7269	F	760.0	26.7	1197	10025.0
567	0.6681	F	760.0	26.0	1323	9070.3
568	0.6681	F	760.0	26.0	1324	9063.4
569	0.6681	F	760.0	26.0	1324	9063.4
570	0.6681	F	760.0	26.0	1325	9056.6
571	0.6681	F	760.0	26.0	1325	9056.6

TABLE VIII. (Cont'd.)

572	0.6681	F	760.0	26.0	1325	9056.6
573	0.6681	F	1501.0	26.0	1290	9302.3
574	0.6681	F	1501.0	26.0	1290	9302.3
575	0.6681	F	1501.0	26.0	-	-
576	0.6681	F	1501.0	26.0	1290	9302.3
577	0.6681	F	1501.0	26.0	1291	9295.1
578	0.6681	F	1501.0	26.0	1290	9302.3
579	0.6681	F	1251.0	26.0	1300	9230.8
580	0.6681	F	1251.0	26.0	1300	9230.8
581	0.6681	F	1251.0	26.0	1300	9230.8
582	0.6681	F	1251.0	26.0	1300	9230.8
583	0.6681	F	1251.0	26.0	1299	9237.9
584	0.6681	F	1001.0	26.0	1313	9139.4
585	0.6681	F	1001.0	26.0	1314	9132.4
586	0.6681	F	1001.0	26.0	1314	9132.4
587	0.6681	F	1001.0	26.0	1314	9132.4
588	0.6681	F	1001.0	26.0	1316	9132.4

TABLE VIII.(Cont'd.)

589	0.6681	F	601.0	26.0	1342	9118.5
590	0.6681	F	601.0	26.0	-	8941.9
591	0.6681	F	601.0	26.0	1343	-
592	0.6681	F	601.0	26.0	1345	8921.9
593	0.6681	F	601.0	26.0	1345	8921.9
594	0.6681	F	401.0	26.0	1406	8535.9
595	0.6681	F	401.0	26.0	1387	8651.7
596	0.6681	F	401.0	26.0	1388	8645.5
597	0.6681	F	401.0	26.0	-	-
598	0.6681	F	401.0	26.0	1389	8639.3
599	0.6681	F	401.0	26.0	-	-
600	0.6681	F	401.0	26.0	-	-
601	0.6681	F	401.0	26.0	-	-
602	0.6681	F	401.0	26.0	1386	8658.0
603	0.3490	D	760.0	24.9	572	6983.2
604	0.3490	D	760.0	24.9	567	7044.8
605	0.3490	D	760.0	24.9	-	-

TABLE VIII. (Cont'd.)

606	0.3490	D	760.0	24.9	570	7007.7
607	0.3490	D	760.0	24.9	567	7044.8
608	0.3490	D	1180.0	24.9	602	6635.2
609	0.3490	D	1180.0	24.9	605	6602.3
610	0.3490	D	1180.0	24.9	602	6635.2
611	0.3490	D	1180.0	24.9	601	6646.3
612	0.3490	D	940.0	24.9	-	-
613	0.3490	D	940.0	24.9	589	6781.7
614	0.3490	D	940.0	24.9	585	6828.0
615	0.3490	D	940.0	24.9	588	6793.2
616	0.5501	D	760.4	24.9	497	8037.0
617	0.5501	D	760.4	24.9	497	8037.0
618	0.5501	D	760.4	24.9	498	8020.9
619	0.5501	D	760.4	24.9	498	7171.3
620	0.4483	D	760.0	26.7	557	7171.3
621	0.4483	D	760.0	26.7	556	7184.2
622	0.4483	D	760.0	26.7	554	7210.1

TABLE VIII. (Cont'd.)

623	0.4483	D	760.0	26.7	554	7210.1
624	0.4483	D	760.0	26.7	553	7223.3
625	0.4483	D	760.0	26.7	553	7223.3
626	0.4483	D	760.0	26.7	553	7223.3
627	0.3800	D	760.0	26.7	586	6816.4
628	0.3800	D	760.0	26.7	591	6758.7
629	0.3800	D	760.0	26.7	586	6816.4
630	0.3800	D	760.0	26.7	591	6758.7
631	0.3800	D	760.0	26.7	585	6828.0
632	0.3800	D	760.0	26.7	584	6839.7
633	0.3484	D	760.0	26.7	588	6793.2
634	0.3484	D	760.0	26.7	587	6804.8
635	0.3484	D	760.0	26.7	570	7007.7
636	0.3484	D	760.0	26.7	581	6875.0
637	0.3484	D	760.0	26.7	585	6828.0
638	0.3484	D	760.0	26.7	592	6747.3
639	0.3484	D	1024.0	26.7	593	6735.9

TABLE VIII. (Cont'd.)

640	0.4895	E	760.0	26.7	535	7515.9
641	0.4895	E	760.0	26.7	522	7703.1
642	0.4895	E	760.0	26.7	530	7586.7
643	0.4895	E	760.0	26.7	524	7673.7
644	0.5000	E	760.0	24.8	421	9551.1
645	0.5000	E	760.0	24.8	444	9056.3
646	0.5000	E	760.0	24.8	438	9180.3
647	0.5000	E	760.0	24.8	422	9528.4
648	0.3490	E	760.0	24.8	632	6362.3
649	0.3490	E	760.0	24.8	594	6769.4
650	0.3490	E	760.0	24.8	629	6392.7
651	0.3490	E	760.0	24.8	625	6433.6
652	0.3490	E	760.0	24.8	624	6443.9
653	0.3490	E	760.0	24.8	590	6815.3

APPENDIX C

CALIBRATION DATA

CALIBRATION DATA

A. Temperature Measurements:

Temperatures were determined by using a 24 gauge iron constantan thermocouple with a Leeds and Northrop portable potentiometer model 8662 serial number 119787. An ice bath was used for the cold junction. The thermocouple emf relationship was checked at a number of fixed points:

Standard	EMF (International Scale)	EMF (Measured)
Dry Ice - 78.5°C	-3.715 MV.	-3.690 MV.
Water - 100.0°C	5.270 MV.	5.279 MV.
Naphalene - 217.96°C	11.778 MV.	11.833 MV

B. Time Interval Measurements:

The time intervals were measured with a Berkley time Interval Meter Model 5120. A laboratory oscillator was tuned to 100 kilocycles by beating against National Bureau of Standards station WWV until a zero beat was obtained. The 100 kilocycle signal was applied to the horizontal axis of an oscilloscope at the same time the one megacycle signal from the timer oscillator output was applied to the vertical axis. The Lissajois pattern formed appeared to be stable with negligible tuning of the timer oscillator circuit. Further calibration was not attempted.

The consistency of the time measurements, probe operation and mixing operation was checked periodically by measuring the velocity of detonation of a 50 percent hydrogen-oxygen mixture in the 0.125 inch ID tube. A reading of 7500 $\pm$ 50 ft/sec was considered satisfactory. If the reading was outside this range, the system was examined for possible sources of error.

C. Pressure Measurements:

Pressures were measured with a mercury U tube attached to a fibre board. A paper scale, graduated in millimeters, was glued to the fibre board. Calibration of this manometer was considered unnecessary.

BIBLIOGRAPHY

BIBLIOGRAPHY

1. Beams, J. W., Physical Measurements in Gas Dynamics and Combustion, 26-46, Princeton, (1954).

2. Becker, R., "Stosswelle und Detonation," Z. S. F. Phys., Vol. 8 (1922).

3. Becker, R., "Impact Waves and Detonation, Part I." NACA-TM 505, (1929), Part II, NACA TM 506 (1929).

4. Berets, D. J., Greene, E. F., and Kistiakowsky, G. B., J. Am. Chem. Soc., 72, 1080 (1950).

5. Bennett, A. L., and Wedaa, H. W., "Detonation in Gases at Low Pressure," Second symposium on Detonation, Feb. 9-11, 1955, Washington, D. C.

6. Berthelot, M., and Vielle, Plk Compt. rend 93, 18 (1881).

7. Berthelot, M., and Vielle, P., Ann De Phys et chim. 28 Serv (1881).

8. Bolle, E., "Explosion und Explosionswellen," Handbuch Der phys. und techn. Mechanik, ed. by Auerbach and Hart, Vol. VI, Leipzig, (1927).

9. Bone, W. A., and Townend, D. T. A., "Flame and Combustion in Gases," pp. 48, 49, 103-163, 167-180, 186, 165, 516, Longman, Green and Co., London (1927).

10. Brown, G. G., Ph.D. Thesis, University of Michigan (1924).

11. Campbell, C., J. Chem. Soc. 2483 (1922).

12. Chapman, D. L., Phil. Magazine, 47, 90 (1889).

13. Courant, R., and Friedrichs, K. O., Supersonic Flow and Shock Waves, Interscience Publisher, Inc., New York, (1948).

14. Dixon, H. B., Pil. Trans. Roy., Soc. A184, 97, 1893, A200, 315 (1903).

15. Doering, W., Ann Physik 43, 431 (1943).

16. Eckert, E. R. G., Introduction to the Transfer of Heat and Mass, McGraw-Hill Book Co., New York (1950).

17. Eyring, H., Powell, R. E., Duffey, G. H., and Parlin, R. B., OSRD Rept. 2026 (1942).

18. Eyring, H., Powell, R., Duffey, G., and Parlin, R., Chem. Revs., 45, 69 (1949).

19. Gordon, W. E., "Third Symposium on Combustion and Flame and Explosion Phenomena," Wilkins and Wilkins Co., Baltimore (1949).

20. Greene, E. F., Ph.D. Thesis, Harvard University, 1949.

21. Hirshfelder, J. O. Curtiss, C. F., and Bird, R. Byron, Molecular Theory of Gases and Liquids, John Wiley and Sons, Inc., New York (1954).

22. Hoelzer, C. A., and Stobaugh, W. K., "Influence of Initial Pressure on Detonation Parameters in Combustible Gases." Thesis Air University Command USAF Inst. Tech. WADC, March, (1954).

23. Hugoniot, H., "Sur la Propagation du Movement dans les corps et specialement dans les gag parfaits," Journal de l'ecole polylecthnique 58, 1-125 (1889).

24. Jost, W., "Explosions-und Verbrennungsvorgange in Gasen," Springer, Berlin (1939) (Reprinted: Edwards Brothers, Ann Arbor (1943).

25. Jouguet, E., Mathematique, 347, (1905).

26. Jouguet, E., Mecanique des Explosifs, O. Doin, Paris (1917).

27. Jouguet, E., La Theorie Thermodynamique de la Propagation des Explosions," Du Deuxier Congres International de Mechanique Appliquee. (Translation by R.J.Dean, UM 898-2 Univerity of Michigan (1952).

28. Kistiakowsky, G. B., Industrial and Engineering News. 33, No. 7 February (1955).

29. Kistiakowsky, G. B., and Zinman, W. G., "The Attainment of Thermodynamic Equilibrium in Detonation Waves," Second ONR Symposium on Detonation, February 9-11, (1955) Washington, D.C.

30. Knight, H. T., and Duff, R. E., "Precision Measurement of Detonation and Strong Shock Velocity in Gases," The Review of Scientific Instruments 26, March, 1955.

31. Laffitte, P. and Dumanois, P., Compt. rend. 183, 284 (1926).

32. Lewis, B. and Friauf, J. B., J. Am. Chem. Soc. 52, 3905 (1930).

33. Lewis, B. and van Elbe, G., "Combustion, Flames and Explosions of Gases," pp. 579-631, Academic Press Inc., New York (1951).

34. Mallard, E., and Le Chatelier, H. L., Comte rend 93, 145 (1881).

35. Mallard, E., and Le Chaletier, H. L., Annales des Mines 8, Ser. IV (1883).

36. Morrison R. B., University of Michigan Report UMM 97 (Jan. 1952).

37. National Bureau of Standards, Selected Values of Chemical Thermodynamic Properties (1947, 1948).

38. Newman, J. von, OSRD Rept. 549 (1942).

39. Nicholls, J. A., et al., Intermittent Detonation as a Thrust Producing Mechanism. Engineering Research Institute of Univ. of Mich., (1955).

40. Nicholls, J. A., Morrison, R. B., and Cullen, R. E., "Measurements of Gaseous Detonation Waves," Second ONR Symposium on Detonation, February 9-11 (1955) Washington, D. C.

41. Payman, W., and Walls, J., J. Chem. Soc. 123, 420 (1923).

42. Peek, H. M. and Thrap, R. G., "High Temperature Thermodynamic and Gaseous Detonations in Mixtures of Cyanogen, Oxygen and Nitrogen," Second ONR Symposium on Detonation, February 9-11, Washington, D. C.

43. Rankine, W. J. M., "On the Thermodynamic Theory of Waves of Finite Longitudinal Disturbance," Transactions of the Royal Society of London 160, pp. 277-288 (1870).

44. Resler, E. L. Lin, S. C., and Kantrowitz, A, J. Appl. Phys. 23, 1390 (1952).

45. Riemann, B., "Uber die Fortpftangung ebener Luftwellen von endlicher Schwingungsweite," Abhandlungen der Gesellschaft der Wissenschaften Zu Gottingen, Mathematisch physikalische Klasse 8, 43 (1860).

46. Schardin, H., Die Schlierenverfahren und irhe anwendung, Ergeb. exact Nature, 20, 303-439 (1942).

47. Schlicting, H., Boundary Layer Theory, McGraw-Hill Book Co., New York, 1955.

48. Schmidt, A., "Die Theorie des verdichtungs-stresses in Gasen und der Delonationswelle," ZSF ges Schiess und Sprengstoffwesen, Vol. 27,(1932) pp. 145, 184, 225, 264, 299.

49. Scorah, R. L., Chem. Phys. 3, 425 (1935).

50. Temperature, Its Measurement and Control in Science and Industry, Vol. 2, pp. 416-419, Reinhold Publishing Co., New York (1955).

51. Thomas, L. H., Note on Becker's Theory of the Shock Front, J. Chem. Phys. 12, 499 (1944).

52. Weir, A. Jr., Morrison, R. B., and Adamson, T. C., "Combustion," College of Engineering, University of Michigan, Ann Arbor, Mich. (1956).

53. Weir, Alexander Jr., and Morrison, R. B., "Equilibrium Temperatures and Compositions Behind a Detonation Wave," Industrial Engineering Chemistry 46, 1056 (1954).

54. Weyl, F. J.,"Analytical Methods in Optical Examination of Supersonic Flow," Nav. Ord. Rept. 211-45, 1945.

55. Zeldovich, Y. B., "On the Theory of the Propagation of Detonation in Gaseous Systems," NACA TM 1261, 1950. (Translation-K Teorrir Rasprobanenia Detonatsii V Gasobraznykh Sistenakh, Thurnel Experimetalnoi i Teoreticheskoi Fiziki, T. 10, (1940).

56. Zeldovich, Y. B., "Theory of Combustion and Detonation in Gases," Technical Report No. R-Ts-1226-IH (Translation from Russian prepared by Brown University.